

# Nobel prize for Eugene P. Wigner



## Nobelprize in Physics 1963

"for his contributions to the theory of the atomic nucleus and the elementary particles, particularly through the discovery and application of **fundamental symmetry principles**"

together with Maria Göppert-Maier and J. Hans D. Jensen

Eugene P. Wigner

\*17.11.1902, Budapest

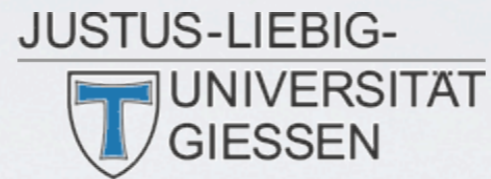
† 1.1.1995, Princeton

# Symmetries and in-medium effects

breaking and restoration of chiral symmetry and  
in-medium modifications of hadrons

Volker Metag\*

II. Physikalisches Institut

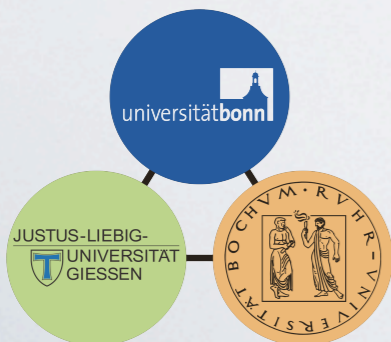


\*and University of Bonn

## Outline

- chiral symmetry breaking and restoration
- experimental approaches for studying in-medium properties of hadrons
- in-medium properties of the  $\eta'$  meson
- summary and outlook

\*funded by the DFG within SFB/TR16

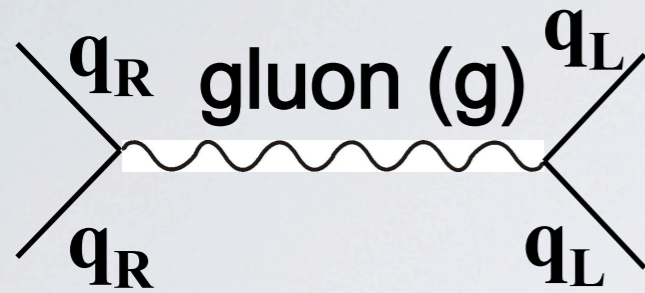


Wigner III symposium  
Nov. 11-14. 2013, Budapest, Hungary



# Chiral symmetry

- Chiral symmetry = fundamental symmetry of QCD for  $m_q = 0$



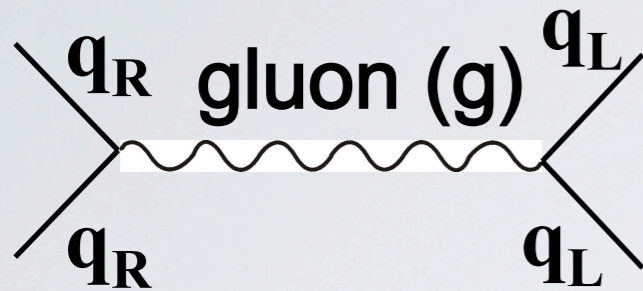
in interaction by gluon exchange

$q_R$  stays  $q_R$ ;  $q_L$  stays  $q_L$

chirality is conserved

# Chiral symmetry

- Chiral symmetry = fundamental symmetry of QCD for  $m_q = 0$



in interaction by gluon exchange

$q_R$  stays  $q_R$ ;  $q_L$  stays  $q_L$

**chirality is conserved**

- QCD Lagrangian for  $m_q=0$  :

$$L_{QCD}^{m=0} = \bar{\psi}(i\gamma_\mu D^\mu) \psi - \frac{1}{4} G_{\mu\nu}^a G_a^{\mu\nu}$$

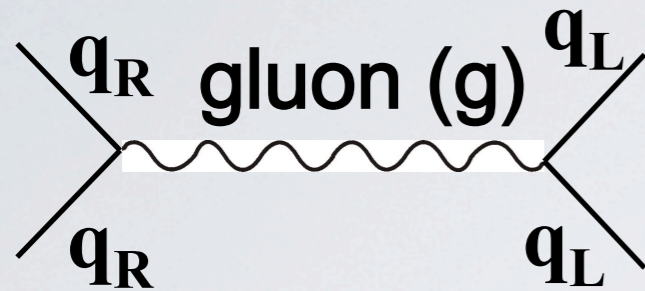
invariant under  $SU(3)_L \otimes SU(3)_R$

chiral transformation

$$\psi_{L,R} \rightarrow \exp(i\theta_{L,R}^a \frac{\lambda_a}{2}) \psi_{L,R}$$

# Chiral symmetry

- Chiral symmetry = fundamental symmetry of QCD for  $m_q = 0$



in interaction by gluon exchange

$q_R$  stays  $q_R$ ;  $q_L$  stays  $q_L$

chirality is conserved

- QCD Lagrangian for  $m_q=0$  :

$$L_{QCD}^{m=0} = \bar{\psi}(i\gamma_\mu D^\mu) \psi - \frac{1}{4} G_{\mu\nu}^a G_a^{\mu\nu}$$

invariant under  $SU(3)_L \otimes SU(3)_R$

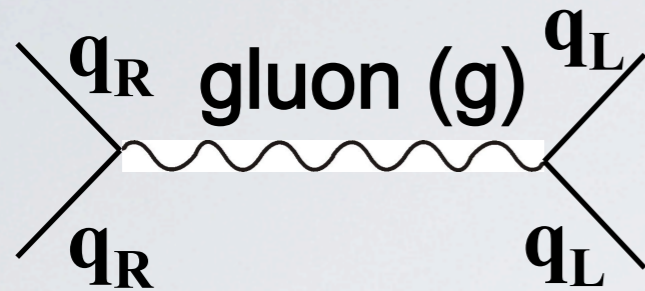
chiral transformation

$$\psi_{L,R} \rightarrow \exp(i\theta_{L,R}^a \frac{\lambda_a}{2}) \psi_{L,R}$$

- QCD ground state does not share  $\chi$  symmetry
- QCD vacuum populated by  $q\bar{q}$  pairs in  ${}^3P_0$  states:  $J^\pi=0^+$
- $\chi$  condensate  $\langle 0|q\bar{q}|0\rangle$

# Chiral symmetry

- Chiral symmetry = fundamental symmetry of QCD for  $m_q = 0$



in interaction by gluon exchange

$q_R$  stays  $q_R$ ;  $q_L$  stays  $q_L$   
**chirality is conserved**

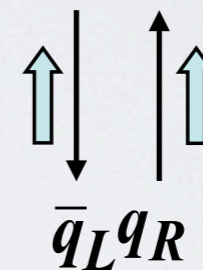
- QCD Lagrangian for  $m_q=0$  :

$$L_{QCD}^{m=0} = \bar{\psi}(i\gamma_\mu D^\mu) \psi - \frac{1}{4} G_{\mu\nu}^a G_a^{\mu\nu}$$

invariant under  $SU(3)_L \otimes SU(3)_R$   
 chiral transformation

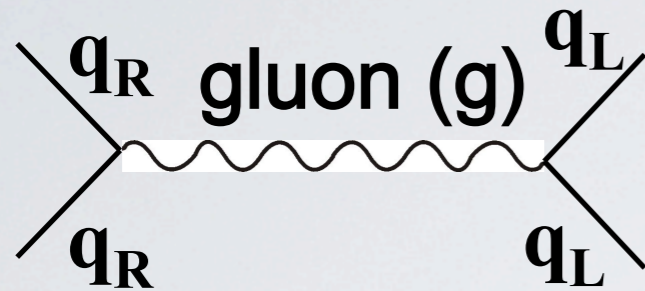
$$\psi_{L,R} \rightarrow \exp(i\theta_{L,R}^a \frac{\lambda_a}{2}) \psi_{L,R}$$

- QCD ground state does not share  $\chi$  symmetry  
 QCD vacuum populated by  $q\bar{q}$  pairs  
 in  ${}^3P_0$  states:  $J^\pi=0^+$ :  
 $\chi$  condensate  $\langle 0|q\bar{q}|0\rangle$



# Chiral symmetry

- Chiral symmetry = fundamental symmetry of QCD for  $m_q = 0$



in interaction by gluon exchange

$q_R$  stays  $q_R$ ;  $q_L$  stays  $q_L$

chirality is conserved

- QCD Lagrangian for  $m_q=0$  :

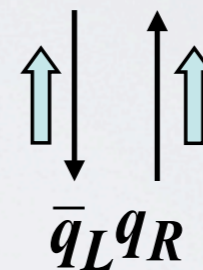
$$L_{QCD}^{m=0} = \bar{\psi}(i\gamma_\mu D^\mu) \psi - \frac{1}{4} G_{\mu\nu}^a G_a^{\mu\nu}$$

invariant under  $SU(3)_L \otimes SU(3)_R$

chiral transformation

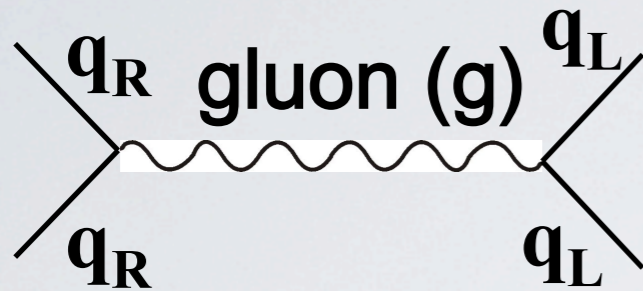
$$\psi_{L,R} \rightarrow \exp(i\theta_{L,R}^a \frac{\lambda_a}{2}) \psi_{L,R}$$

- QCD ground state does not share  $\chi$  symmetry
- QCD vacuum populated by  $q\bar{q}$  pairs in  ${}^3P_0$  states:  $J^\pi=0^+$ :  
 $\chi$  condensate  $\langle 0|q\bar{q}|0\rangle$
- chiral symmetry breaking:



# Chiral symmetry

- Chiral symmetry = fundamental symmetry of QCD for  $m_q = 0$



in interaction by gluon exchange

$q_R$  stays  $q_R$ ;  $q_L$  stays  $q_L$   
**chirality is conserved**

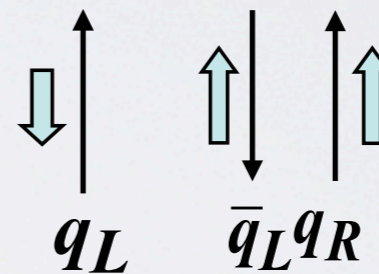
- QCD Lagrangian for  $m_q=0$  :

$$L_{QCD}^{m=0} = \bar{\psi}(i\gamma_\mu D^\mu) \psi - \frac{1}{4} G_{\mu\nu}^a G_a^{\mu\nu}$$

invariant under  $SU(3)_L \otimes SU(3)_R$   
 chiral transformation

$$\psi_{L,R} \rightarrow \exp(i\theta_{L,R}^a \frac{\lambda_a}{2}) \psi_{L,R}$$

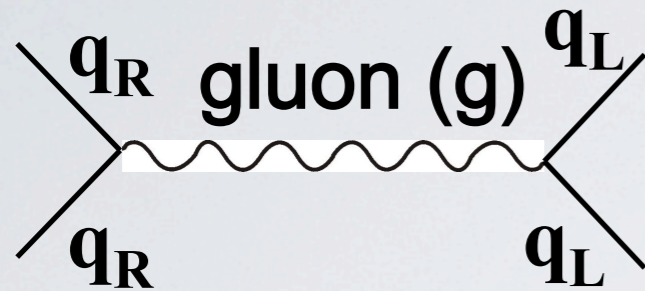
- QCD ground state does not share  $\chi$  symmetry  
 QCD vacuum populated by  $q\bar{q}$  pairs in  ${}^3P_0$  states:  $J^\pi=0^+$ :  
 $\chi$  condensate  $\langle 0|q\bar{q}|0\rangle$
- chiral symmetry breaking:





# Chiral symmetry

- Chiral symmetry = fundamental symmetry of QCD for  $m_q = 0$



in interaction by gluon exchange

$q_R$  stays  $q_R$ ;  $q_L$  stays  $q_L$   
**chirality is conserved**

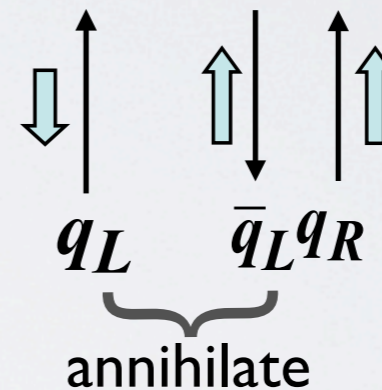
- QCD Lagrangian for  $m_q=0$  :

$$L_{QCD}^{m=0} = \bar{\psi}(i\gamma_\mu D^\mu) \psi - \frac{1}{4} G_{\mu\nu}^a G_a^{\mu\nu}$$

invariant under  $SU(3)_L \otimes SU(3)_R$   
 chiral transformation

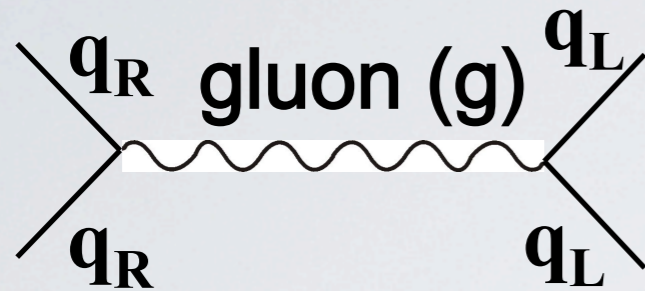
$$\psi_{L,R} \rightarrow \exp(i\theta_{L,R}^a \frac{\lambda_a}{2}) \psi_{L,R}$$

- QCD ground state does not share  $\chi$  symmetry  
 QCD vacuum populated by  $q\bar{q}$  pairs in  $^3P_0$  states:  $J^\pi=0^+$ :  
 $\chi$  condensate  $\langle 0|q\bar{q}|0\rangle$
- chiral symmetry breaking:



# Chiral symmetry

- Chiral symmetry = fundamental symmetry of QCD for  $m_q = 0$



in interaction by gluon exchange

$q_R$  stays  $q_R$ ;  $q_L$  stays  $q_L$   
**chirality is conserved**

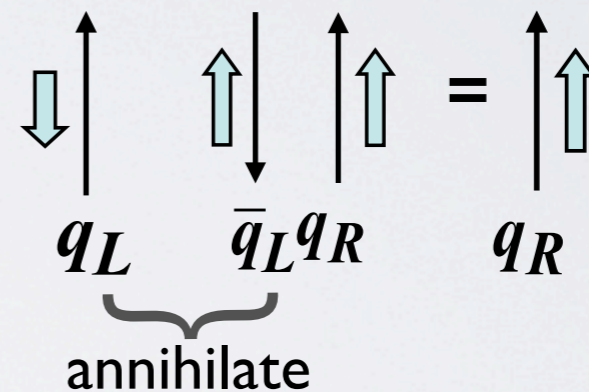
- QCD Lagrangian for  $m_q=0$  :

$$L_{QCD}^{m=0} = \bar{\psi}(i\gamma_\mu D^\mu) \psi - \frac{1}{4} G_{\mu\nu}^a G_a^{\mu\nu}$$

invariant under  $SU(3)_L \otimes SU(3)_R$   
 chiral transformation

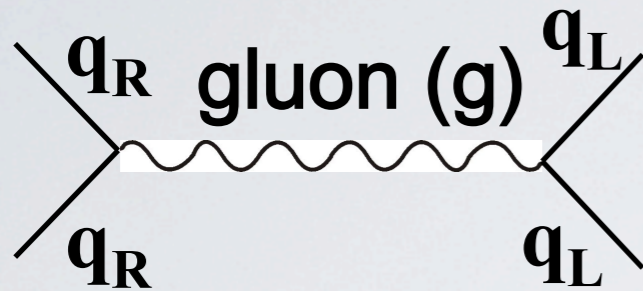
$$\psi_{L,R} \rightarrow \exp(i\theta_{L,R}^a \frac{\lambda_a}{2}) \psi_{L,R}$$

- QCD ground state does not share  $\chi$  symmetry  
 QCD vacuum populated by  $q\bar{q}$  pairs in  ${}^3P_0$  states:  $J^\pi=0^+$ :  
 $\chi$  condensate  $\langle 0|q\bar{q}|0\rangle$
- chiral symmetry breaking:



# Chiral symmetry

- Chiral symmetry = fundamental symmetry of QCD for  $m_q = 0$



in interaction by gluon exchange

$q_R$  stays  $q_R$ ;  $q_L$  stays  $q_L$   
**chirality is conserved**

- QCD Lagrangian for  $m_q=0$  :

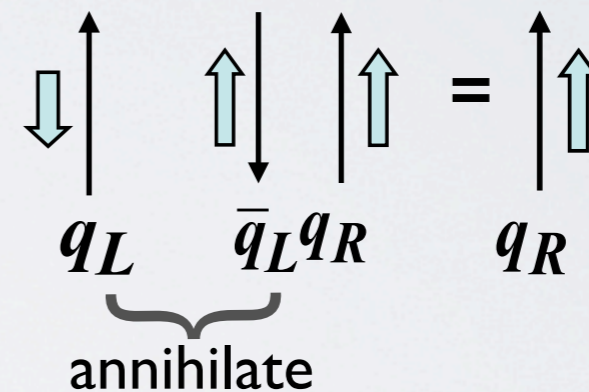
$$L_{QCD}^{m=0} = \bar{\psi}(i\gamma_\mu D^\mu) \psi - \frac{1}{4} G_{\mu\nu}^a G_a^{\mu\nu}$$

invariant under  $SU(3)_L \otimes SU(3)_R$   
 chiral transformation

$$\psi_{L,R} \rightarrow \exp(i\theta_{L,R}^a \frac{\lambda_a}{2}) \psi_{L,R}$$

- QCD ground state does not share  $\chi$  symmetry  
 QCD vacuum populated by  $q\bar{q}$  pairs in  ${}^3P_0$  states:  $J^\pi=0^+$ :  
 $\chi$  condensate  $\langle 0|q\bar{q}|0\rangle$

- chiral symmetry breaking:



- $q_L \Rightarrow q_R$ ;  $\chi$  symmetry broken  
 in presence of a chiral condensate

$\langle 0|q\bar{q}|0\rangle$  is order parameter for  $\chi$ -symmetry

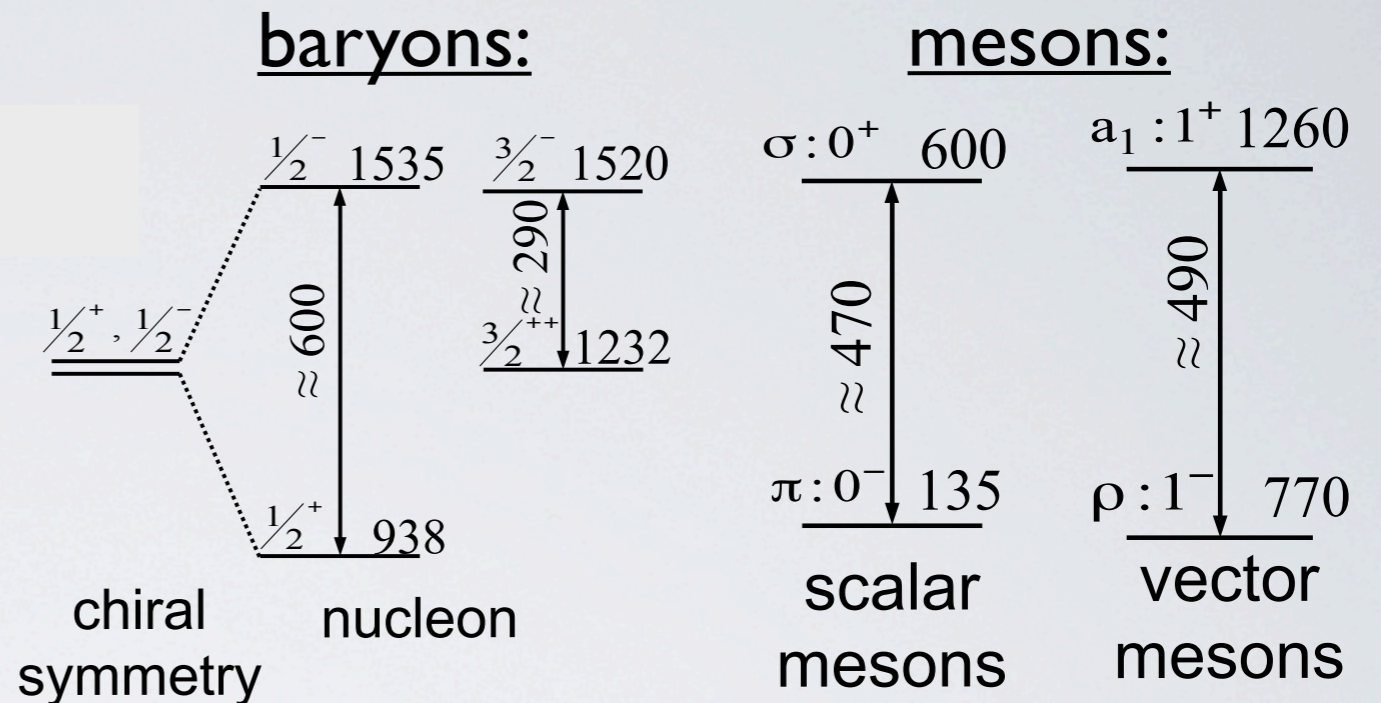
$\chi$ -symmetry restored for  
 $\langle 0|q\bar{q}|0\rangle \rightarrow 0$

# symmetry breaking in the hadronic sector

- for  $\chi$  symmetry chiral partners (hadronic states with same spin but opposite parity) should be degenerate in mass:  $m(J^\pi) = m(J^{-\pi})$

experiment:  $\Delta m \neq 0$

▮▮▮▮▮▮  $\chi$  symmetry

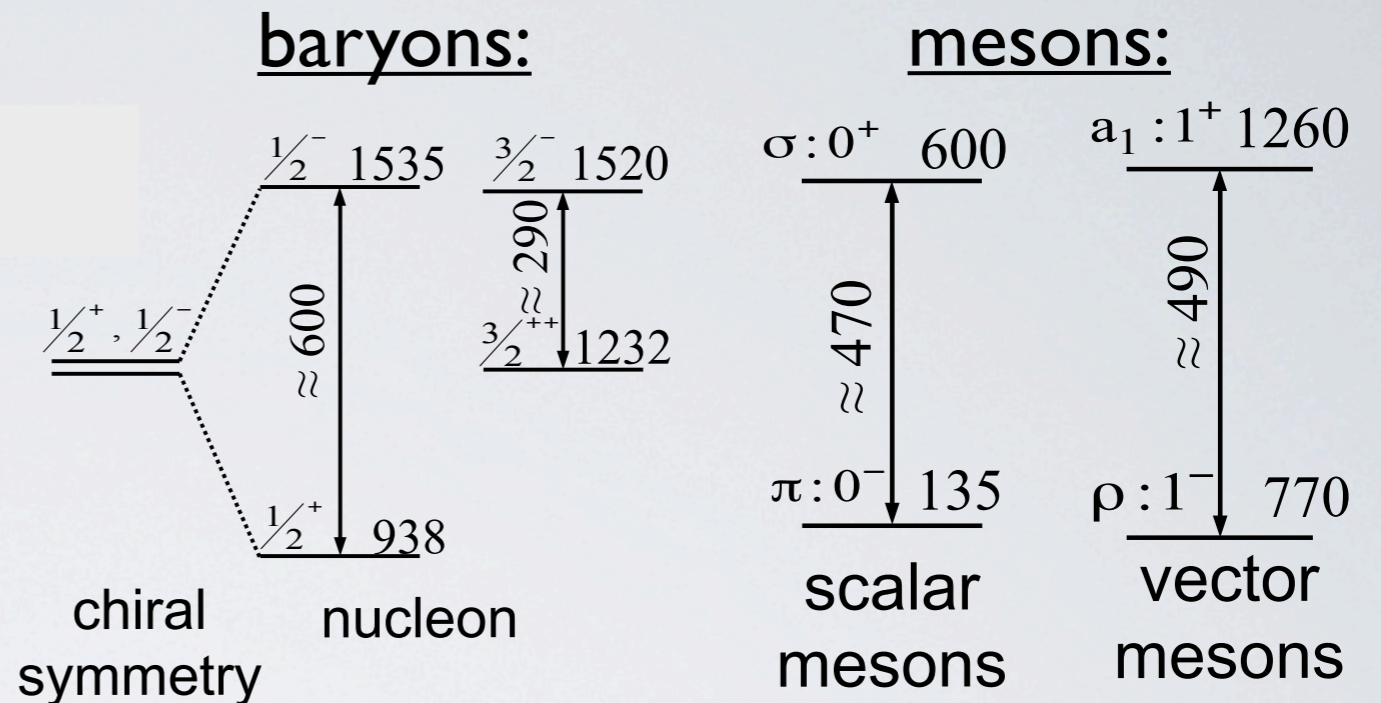


# symmetry breaking in the hadronic sector

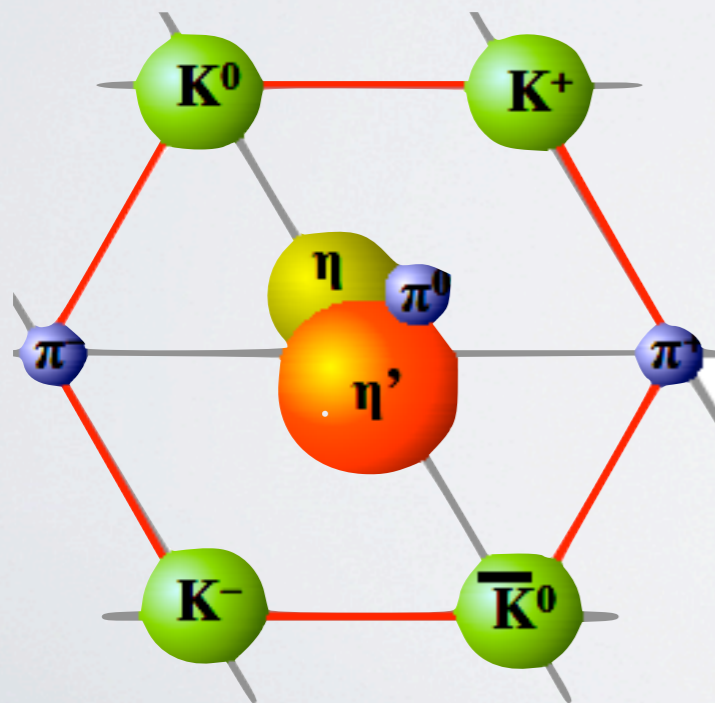
- for  $\chi$  symmetry chiral partners (hadronic states with same spin but opposite parity) should be degenerate in mass:  $m(J^\pi) = m(J^{-\pi})$

experiment:  $\Delta m \neq 0$

➡  $\chi$  symmetry

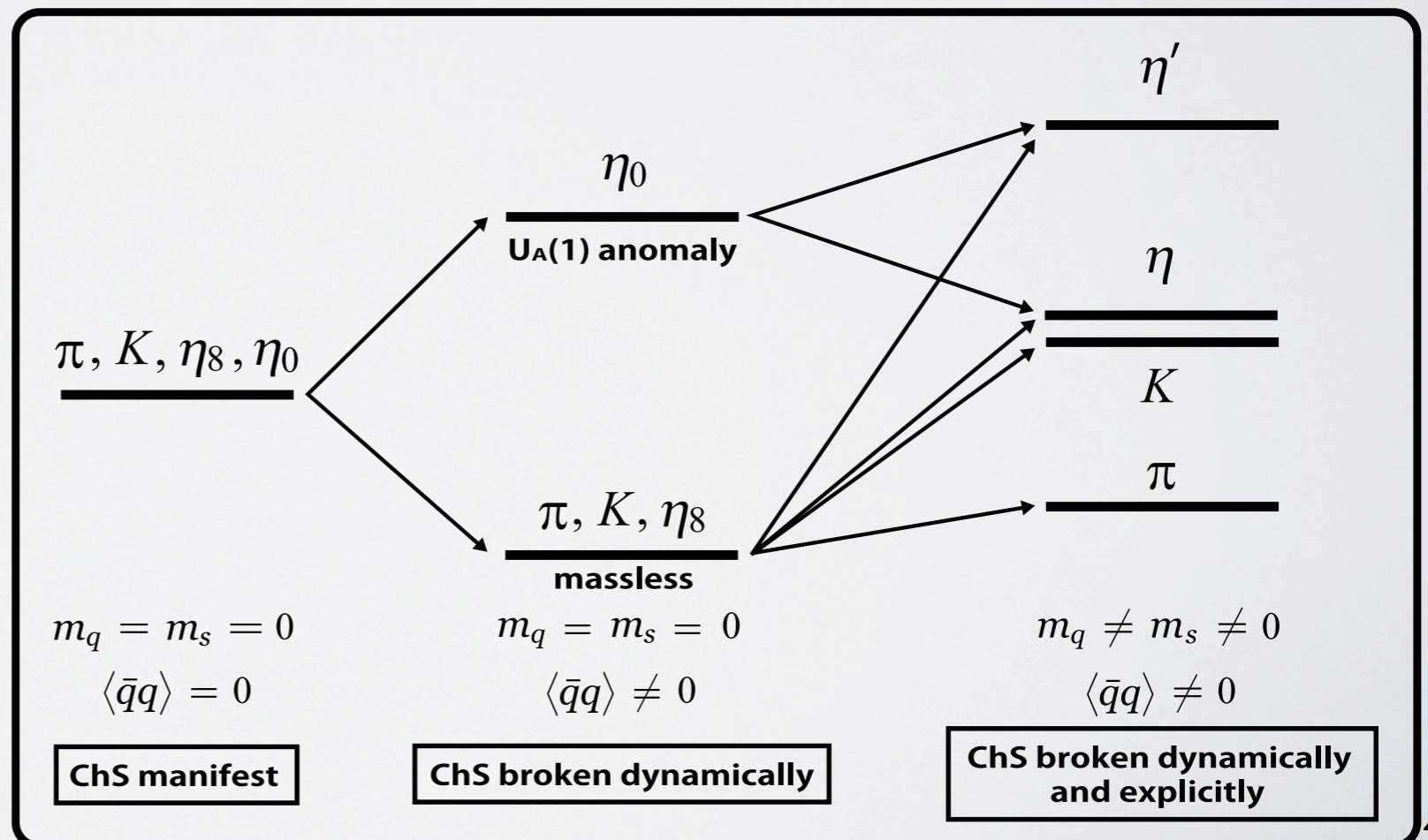


- mass as a result of symmetry breaking



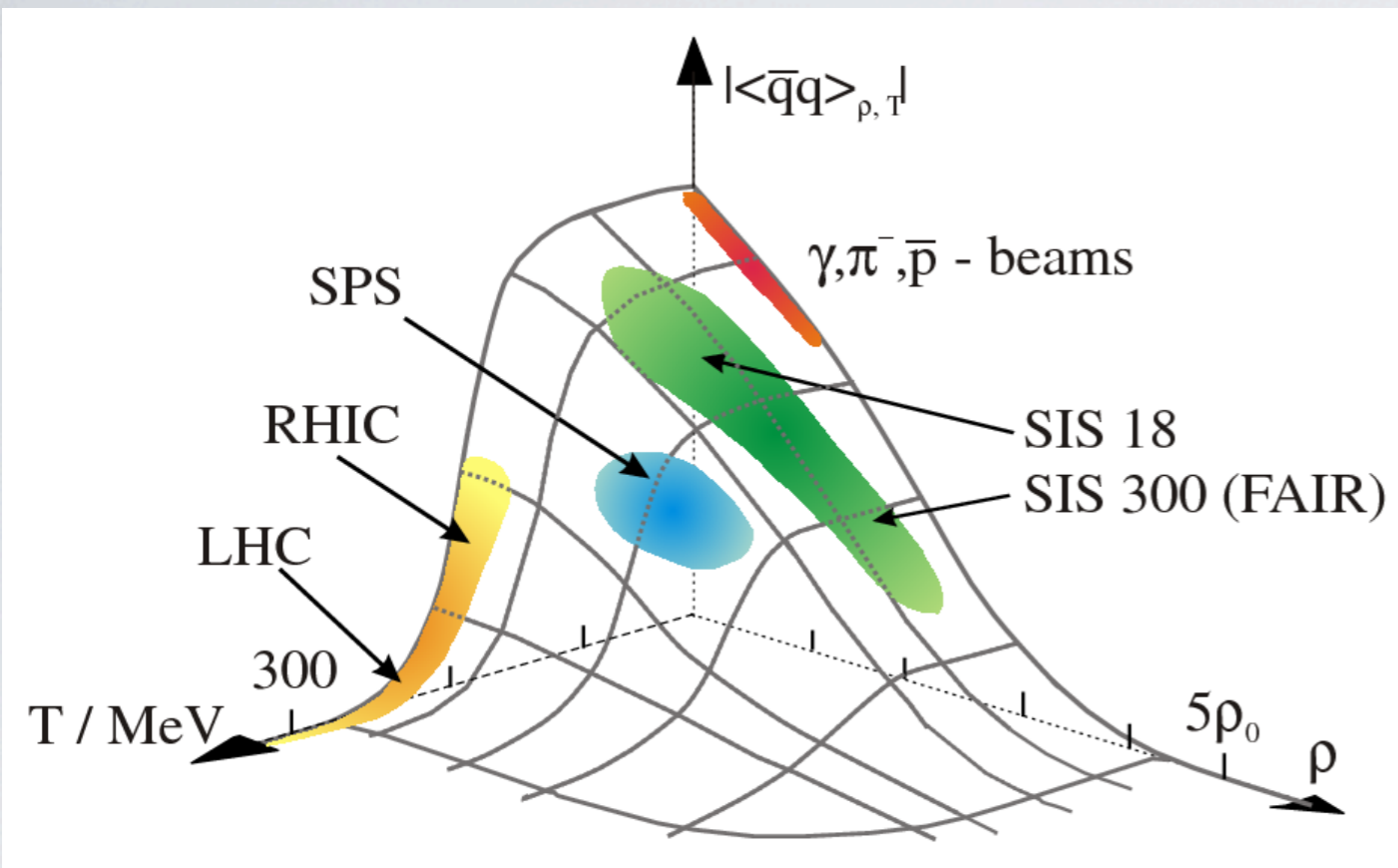
nonet of pseudoscalar mesons

H. Nagahiro et al., PRC 87 (2013) 045201 The NJL Model



# Link between hadronic and QCD- descriptions

chiral condensate as function of baryon density  $\rho_B$  and temperature  $T$



partial restoration of chiral symmetry

$$|\langle \bar{q}q \rangle_{\rho, T}| \rightarrow 0 \text{ for } \rho_B, T \nearrow$$

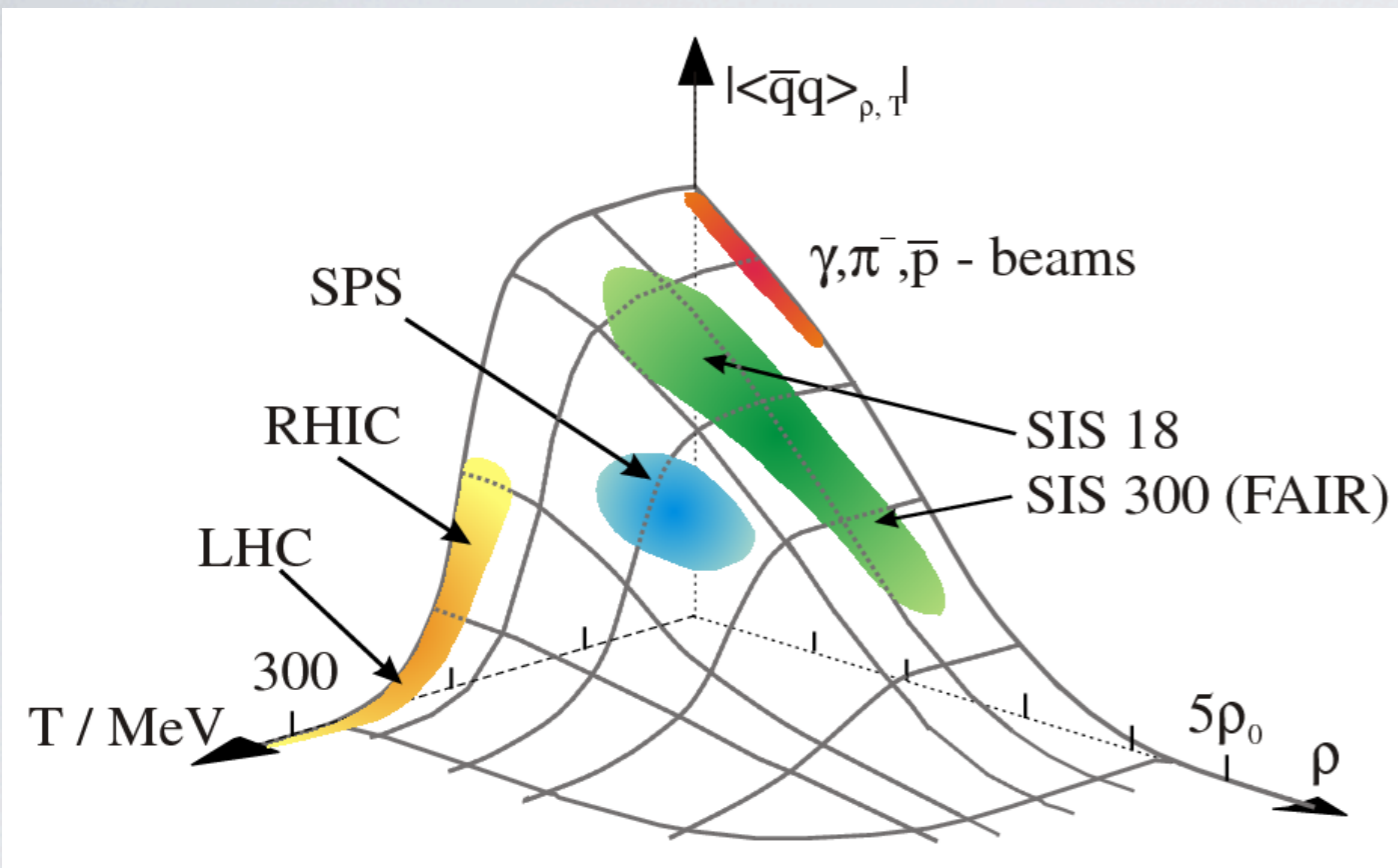
S. Klimt et al., PLB 249 (1990) 386

parameter range  $(\rho_B, T)$  reached in reactions with heavy-ion,  $\gamma, \pi, p$ -beams

**but**, chiral condensate is not an experimental observable

# Link between hadronic and QCD- descriptions

chiral condensate as function of baryon density  $\rho_B$  and temperature  $T$



partial restoration of chiral symmetry

$$|\langle \bar{q}q \rangle_{\rho, T}| \rightarrow 0 \text{ for } \rho_B, T \nearrow$$

S. Klimt et al., PLB 249 (1990) 386

parameter range  $(\rho_B, T)$  reached in reactions with heavy-ion,  $\gamma, \pi, p$ -beams

**but**, chiral condensate is not an experimental observable

## QCD sum rules:

hadronic side

$$\frac{Q^2}{\pi} \int_0^\infty ds \frac{Im\Pi(s)}{s(s+Q^2)} = -\frac{1}{8\pi^2} \left(1 + \frac{\alpha_s}{\pi}\right) \ln \frac{Q^2}{\Lambda^2} + \frac{m_q \langle \bar{q}q \rangle}{Q^4} + \frac{1}{24} \frac{\langle \frac{\alpha_s}{\pi} G^2 \rangle}{Q^4} - \frac{112}{81} \alpha_s \pi \frac{\langle \bar{q}q \rangle^2}{Q^6} + \dots$$

QCD side

no direct relation between in-medium properties of hadrons and QCD condensates

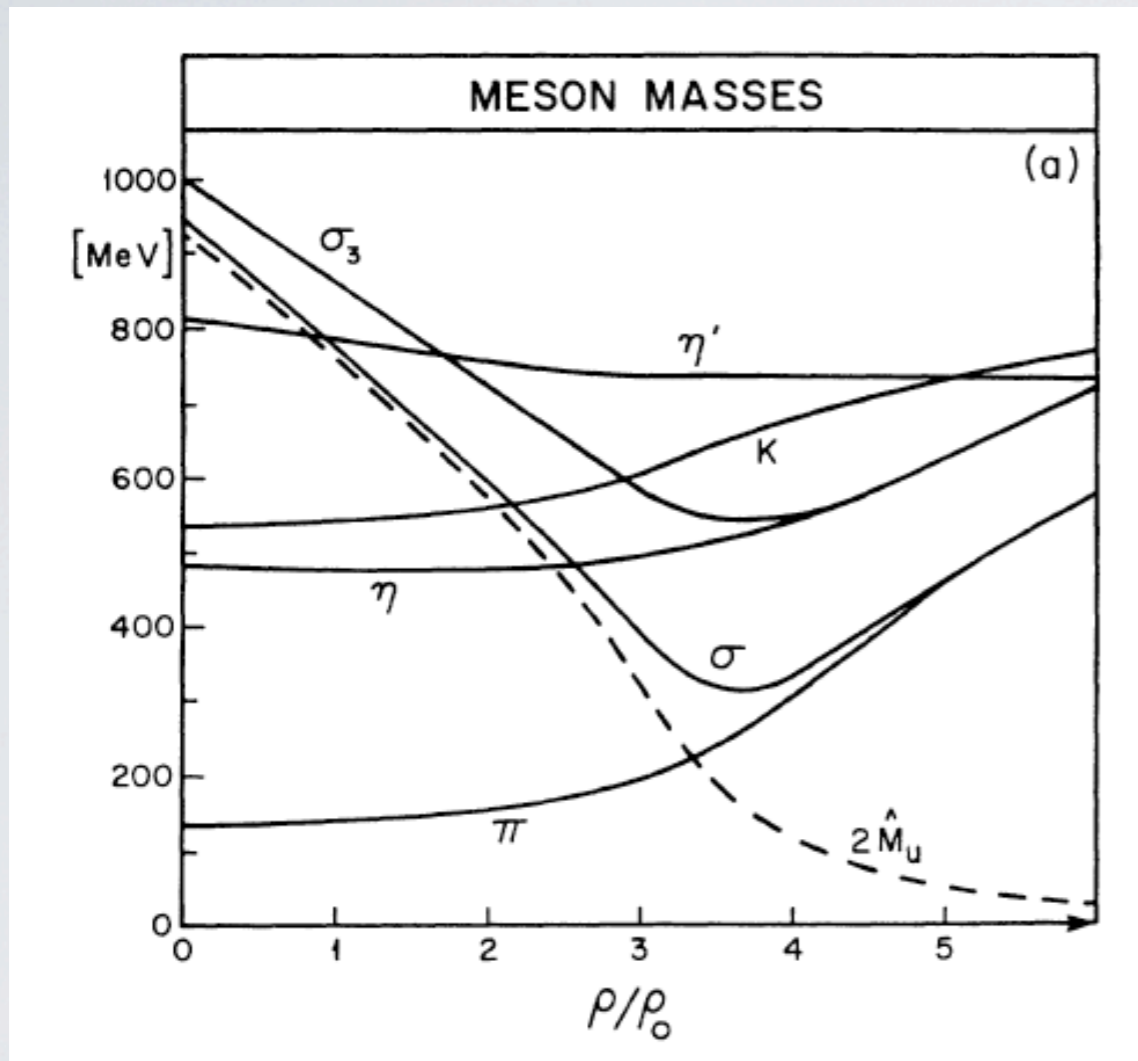
QCD sum rules provide important constraints for hadronic models

**hadronic models needed for quantitative comparison to experiments**

# spectral function of the $\eta'$ meson

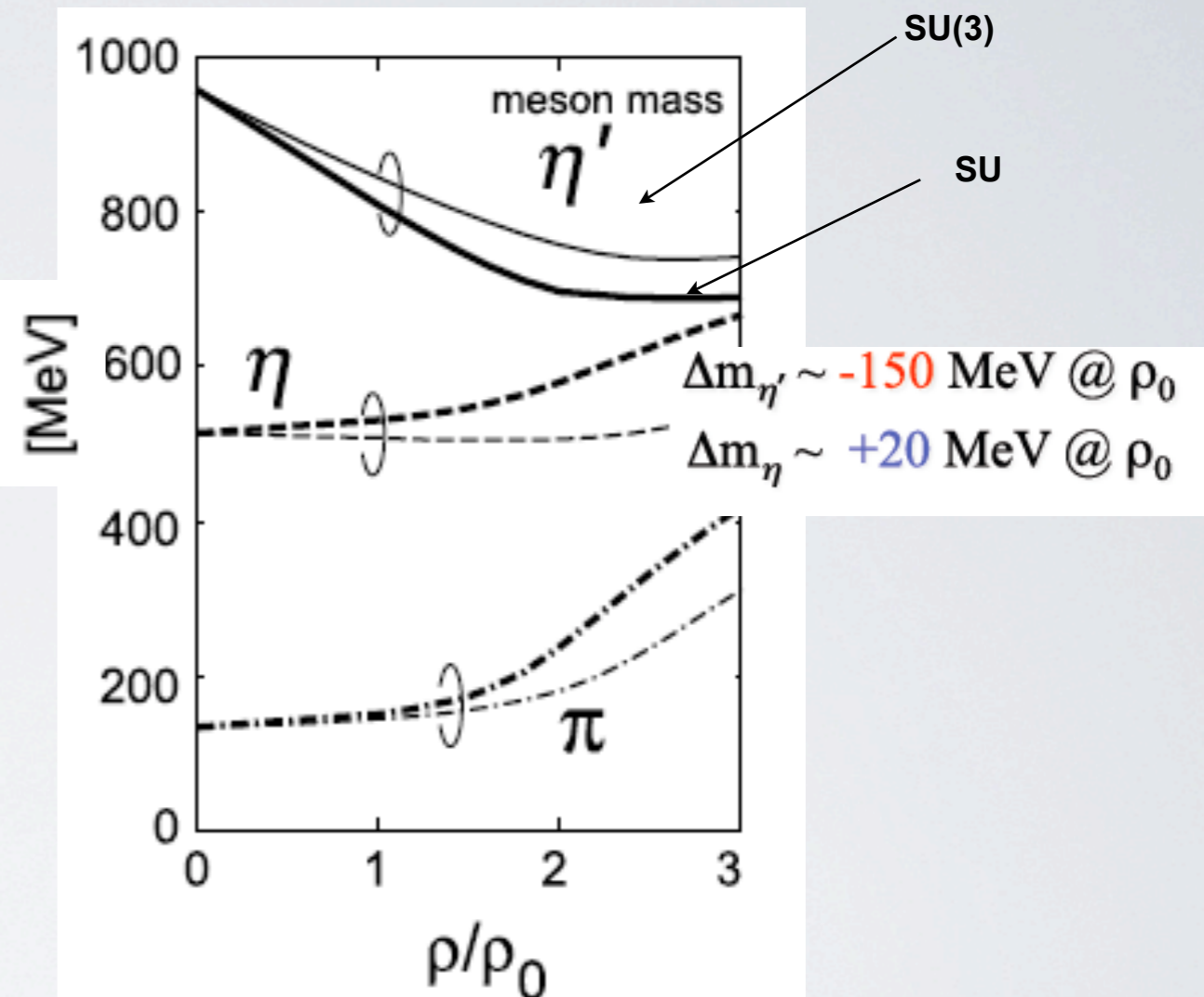
- model predictions - based on NJL

V. Bernard und U.-G. Meißner,  
Phys. Rev. D 38 (1988) 1551



the mass of the  $\eta'$  meson is almost independent of density

H. Nagahiro, M. Takizawa and S. Hirenzaki,  
Phys. Rev. C 74 (2006) 045203



large medium effect could be seen even at normal nuclear density

Y. Kwon, S.H. Lee, K. Morita, and G. Wolf, PRD 86 (2012) 034014

$U_A(1)$  breaking part of  $\eta'$  mass ( $\approx 460$  MeV) lowered by 20%:  $\Delta m_{\eta'}(\rho_0) \approx -90$  MeV

discrepancy between theoretical predictions requires experimental clarification !!



# experimental results on $\eta'$ interactions

- $p p \rightarrow p p \eta'$  @ COSY (P. Moskal et al., PLB 482 (2000) 356)

analysis of final state interactions gives estimate of  $\eta'$ - proton scattering length

$|a_{\eta'p}| \approx 0.1 \text{ fm}$   $\implies$  weak  $\eta'$ - nucleon interaction

- ultra-relativistic heavy-ion collisions @RHIC (Csörgo et al., PRL 105 (2010) 182301)

two-pion Bose-Einstein correlation analysis of PHENIX and STAR data indicates massdrop of  $\eta'$  meson in highly compressed and heated collision zone

$\Delta m_{\eta'} \approx -200 \text{ MeV}$   $\implies$  very strong  $\eta'$ - nucleon interaction

conflicting experimental evidence !!!  
further experiments needed

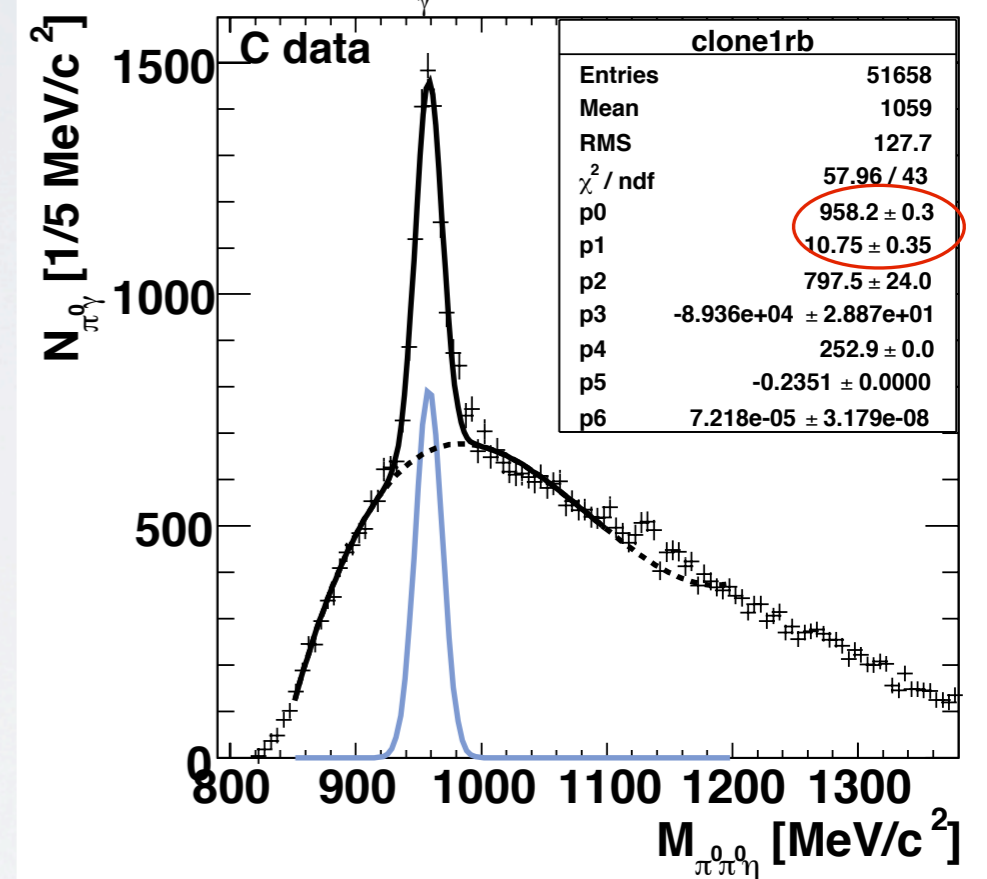
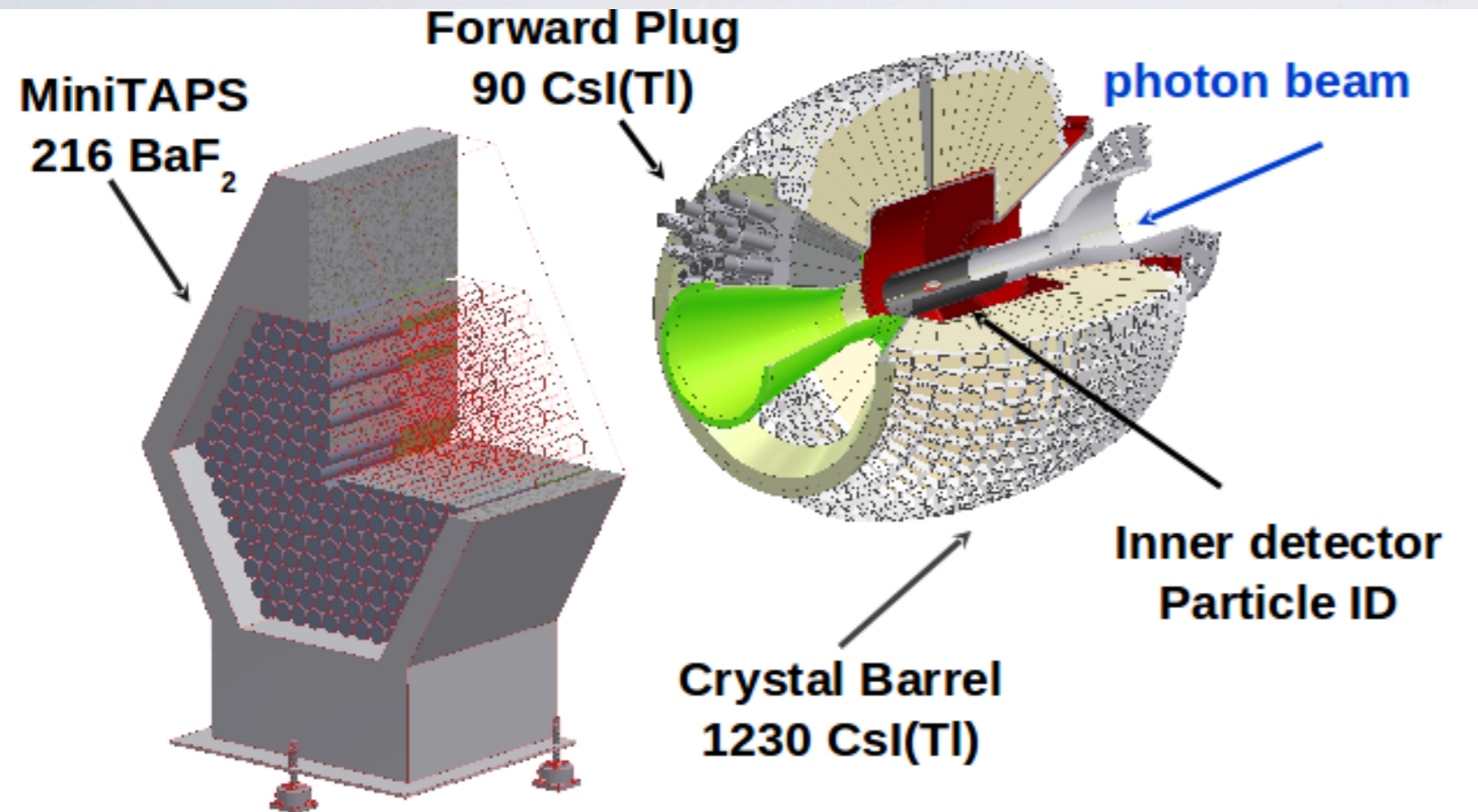
# photoproduction of $\eta'$ mesons off nuclei at ELSA

CBELSA/TAPS-detector system :  $\approx 4\pi$  photon detector system

$$E_\gamma = 1.0\text{-}2.8 \text{ GeV}$$

$$\eta' \rightarrow \pi^0 \pi^0 \eta \rightarrow 6\gamma$$

$E_\gamma = 1250\text{-}2600 \text{ MeV}$



$$m = 958 \text{ MeV}/c^2$$

$$\sigma = 11 \text{ MeV}$$

$$\Delta m/m = 1.1\%$$

# Experimental approaches to determine the meson-nucleus optical potential

meson-nucleus optical potential

$$U(r) = V(r) + iW(r)$$

# Experimental approaches to determine the meson-nucleus optical potential

meson-nucleus optical potential

$$U(r) = V(r) + iW(r)$$

meson mass shift

$$V(r) = \Delta m(\rho_0) \cdot \frac{\rho(r)}{\rho_0}$$

line shape analysis:

direct determination of  $\Delta m$

excitation function:

provides information about the depth of  $V(r)$

meson momentum distribution:

provides information about the depth of  $V(r)$

meson-nucleus-bound states:

direct determination of  $E_{\text{bin}}$  ( $\Delta m$ )

# Experimental approaches to determine the meson-nucleus optical potential

## meson-nucleus optical potential

$$U(r) = V(r) + iW(r)$$

### meson mass shift

$$V(r) = \Delta m(\rho_0) \cdot \frac{\rho(r)}{\rho_0}$$

### meson absorption

$$W(r) = -\Gamma_0/2 \cdot \frac{\rho(r)}{\rho_0} \\ = -\frac{1}{2} \cdot \hbar c \cdot \rho(r) \cdot \sigma_{inel} \cdot \beta$$

#### line shape analysis:

direct determination of  $\Delta m$

#### excitation function:

provides information about the depth of  $V(r)$

#### meson momentum distribution:

provides information about the depth of  $V(r)$

#### meson-nucleus-bound states:

direct determination of  $E_{bin}$  ( $\Delta m$ )

#### Transparency ratio measurement

$$T_A = \frac{\sigma_{\gamma A \rightarrow \eta' X}}{A \cdot \sigma_{\gamma N \rightarrow \eta' X}}$$

# transparency ratio measurement

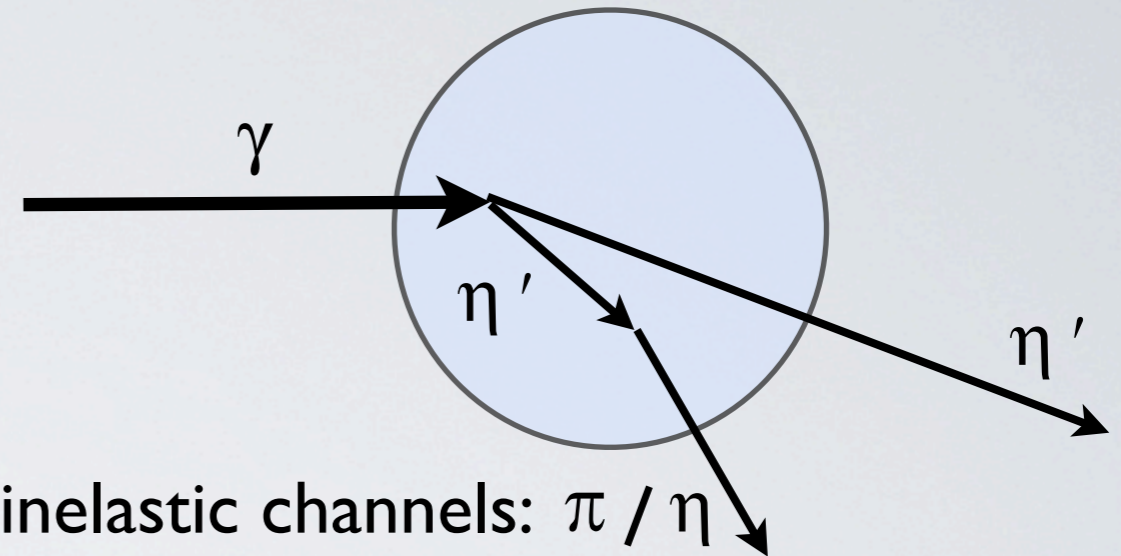
# transparency ratio measurement

attenuation measurement of meson flux:

(D. Cabrera et al., NPA 733 (2004) 130)

$$T_A = \frac{\sigma_{\gamma A \rightarrow \eta' X}}{A \cdot \sigma_{\gamma N \rightarrow \eta' X}}$$

production probability per nucleon  
within the nucleus compared to  
production probability on the free nucleon;



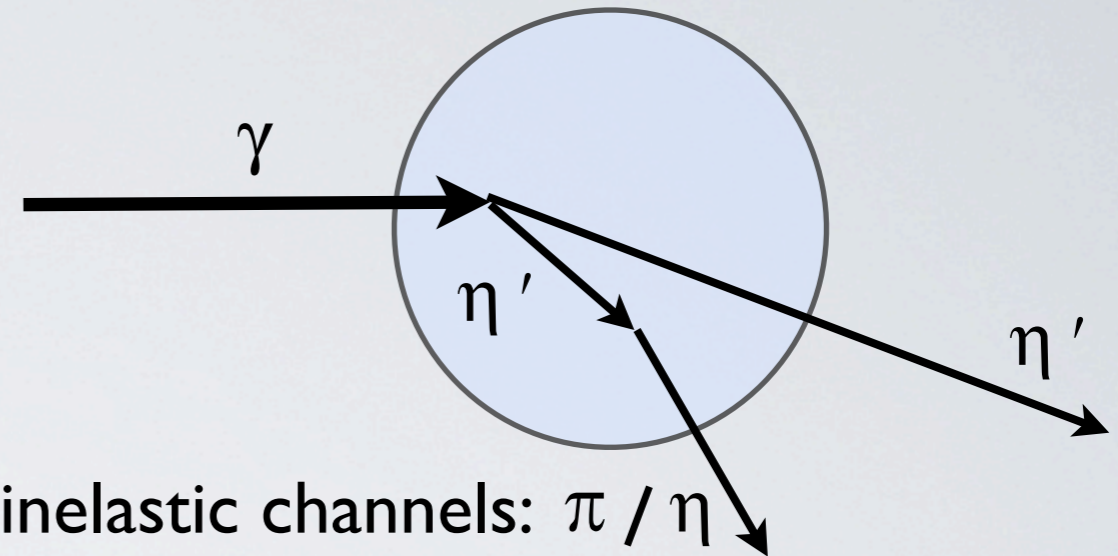
# transparency ratio measurement

attenuation measurement of meson flux:

(D. Cabrera et al., NPA 733 (2004) 130)

$$T_A = \frac{\sigma_{\gamma A \rightarrow \eta' X}}{A \cdot \sigma_{\gamma N \rightarrow \eta' X}}$$

production probability per nucleon within the nucleus compared to production probability on the free nucleon;



inelastic reactions remove  $\omega, \eta'$  mesons, e.g.  $\omega, \eta' N \rightarrow \pi N$

shortening of  $\omega, \eta'$  lifetime in the medium  $\Rightarrow$  increase in width

low density approximation:  $\Gamma(\rho) = -\frac{Im\Pi(\rho)}{E} = \hbar c \cdot \rho \cdot \beta \cdot \sigma_{inel}$ ;  $\Gamma(\rho) = \Gamma(\rho_0) \frac{\rho}{\rho_0}$

information on imaginary part of meson-nucleus potential



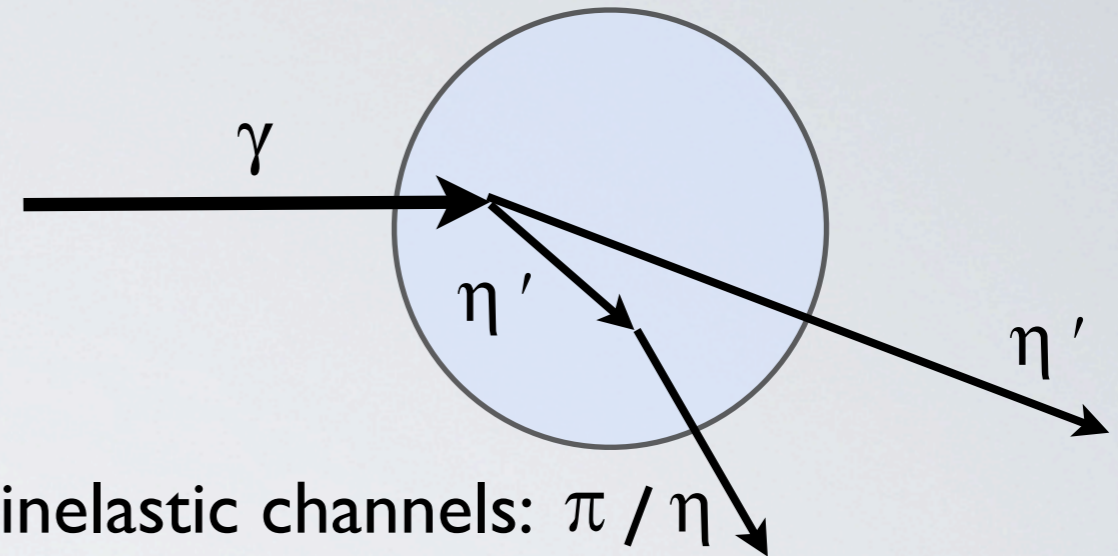
# transparency ratio measurement

attenuation measurement of meson flux:

(D. Cabrera et al., NPA 733 (2004) 130)

$$T_A = \frac{\sigma_{\gamma A \rightarrow \eta' X}}{A \cdot \sigma_{\gamma N \rightarrow \eta' X}}$$

production probability per nucleon within the nucleus compared to production probability on the free nucleon;



inelastic reactions remove  $\omega, \eta'$  mesons, e.g.  $\omega, \eta' N \rightarrow \pi N$

shortening of  $\omega, \eta'$  lifetime in the medium  $\Rightarrow$  increase in width

low density approximation:  $\Gamma(\rho) = -\frac{Im\Pi(\rho)}{E} = \hbar c \cdot \rho \cdot \beta \cdot \sigma_{inel}$ ;  $\Gamma(\rho) = \Gamma(\rho_0) \frac{\rho}{\rho_0}$

information on imaginary part of meson-nucleus potential

applicable to any meson lifetime !!

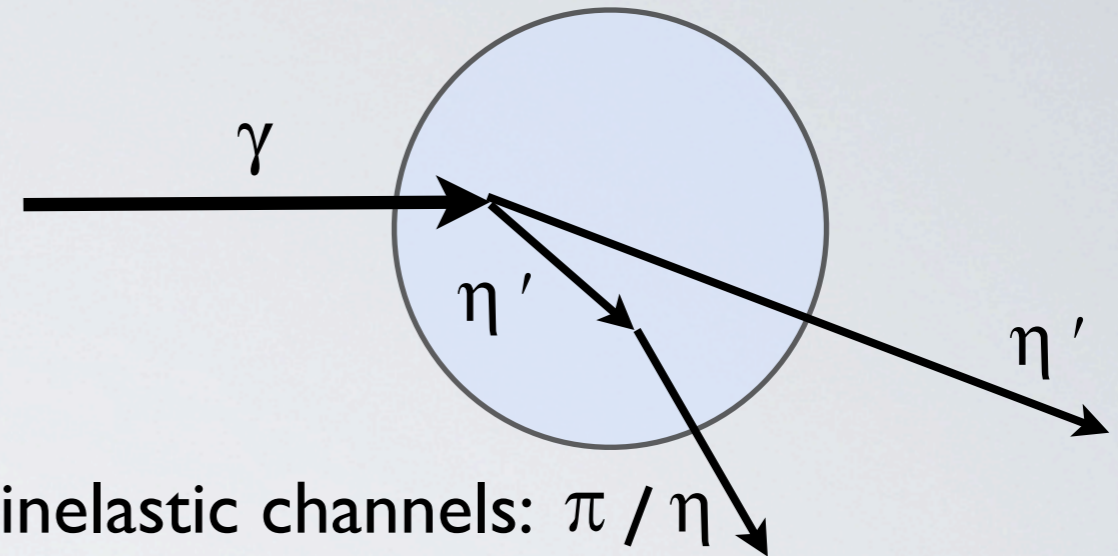
# transparency ratio measurement

attenuation measurement of meson flux:

(D. Cabrera et al., NPA 733 (2004) 130)

$$T_A = \frac{\sigma_{\gamma A \rightarrow \eta' X}}{A \cdot \sigma_{\gamma N \rightarrow \eta' X}}$$

production probability per nucleon within the nucleus compared to production probability on the free nucleon;



inelastic reactions remove  $\omega, \eta'$  mesons, e.g.  $\omega, \eta' N \rightarrow \pi N$

shortening of  $\omega, \eta'$  lifetime in the medium  $\Rightarrow$  increase in width

low density approximation:  $\Gamma(\rho) = -\frac{Im\Pi(\rho)}{E} = \hbar c \cdot \rho \cdot \beta \cdot \sigma_{inel}$ ;  $\Gamma(\rho) = \Gamma(\rho_0) \frac{\rho}{\rho_0}$

information on imaginary part of meson-nucleus potential

applicable to any meson lifetime !!

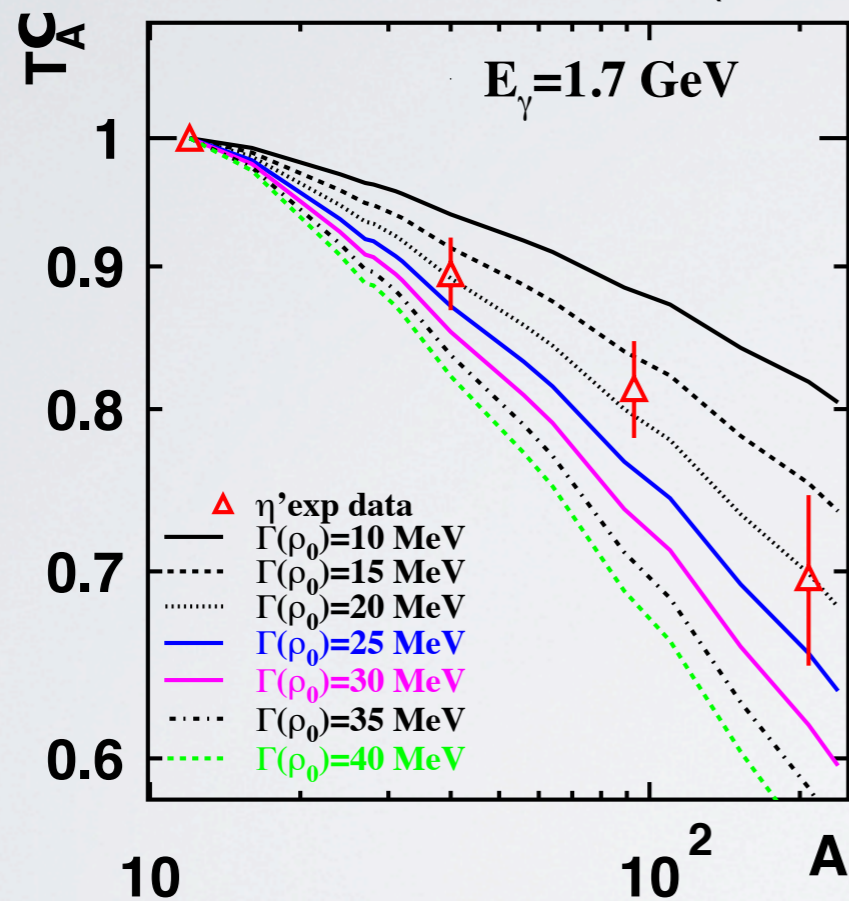
information on in-medium properties of mesons from measurement of their decay outside of the nucleus

# The imaginary part of the $\eta'$ -nucleus potential

$E_\gamma = 1500 - 2200$  MeV; photoproduction of  $\eta'$  meson off  $^{12}\text{C}$ ,  $^{40}\text{Ca}$ ,  $^{93}\text{Nb}$  and  $^{208}\text{Pb}$

$$T_A^C = \frac{12 \cdot \sigma_{\gamma A \rightarrow \eta' X}}{A \cdot \sigma_{\gamma C \rightarrow \eta' X}} \quad \text{normalized to carbon}$$

M. Nanova et al., PLB 710 (2012) 600



at low density approximation:

$$\Gamma(\rho) = -\frac{\text{Im}\Pi(\rho)}{E} \sim \rho v \sigma_{inel} \quad ; \quad \Gamma(\rho) = \Gamma(\rho_0) \frac{\rho}{\rho_0}$$

$$\Rightarrow \Gamma_{\eta'}(\langle p_{\eta'} \rangle \approx 1.05 \text{ GeV}/c) \approx 15-25 \text{ MeV};$$

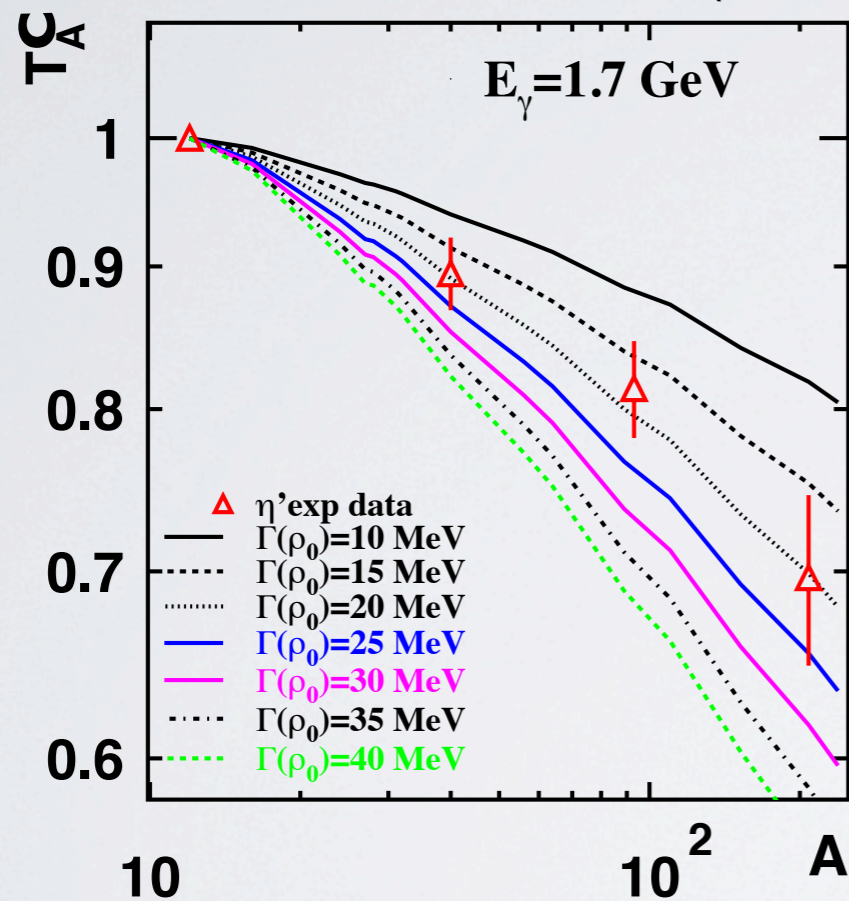
$$\rho_0 = 0.17 \text{ fm}^{-3}; \quad \sigma_{\eta'}^{inel} \approx 3 - 10 \text{ mb}$$

# The imaginary part of the $\eta'$ -nucleus potential

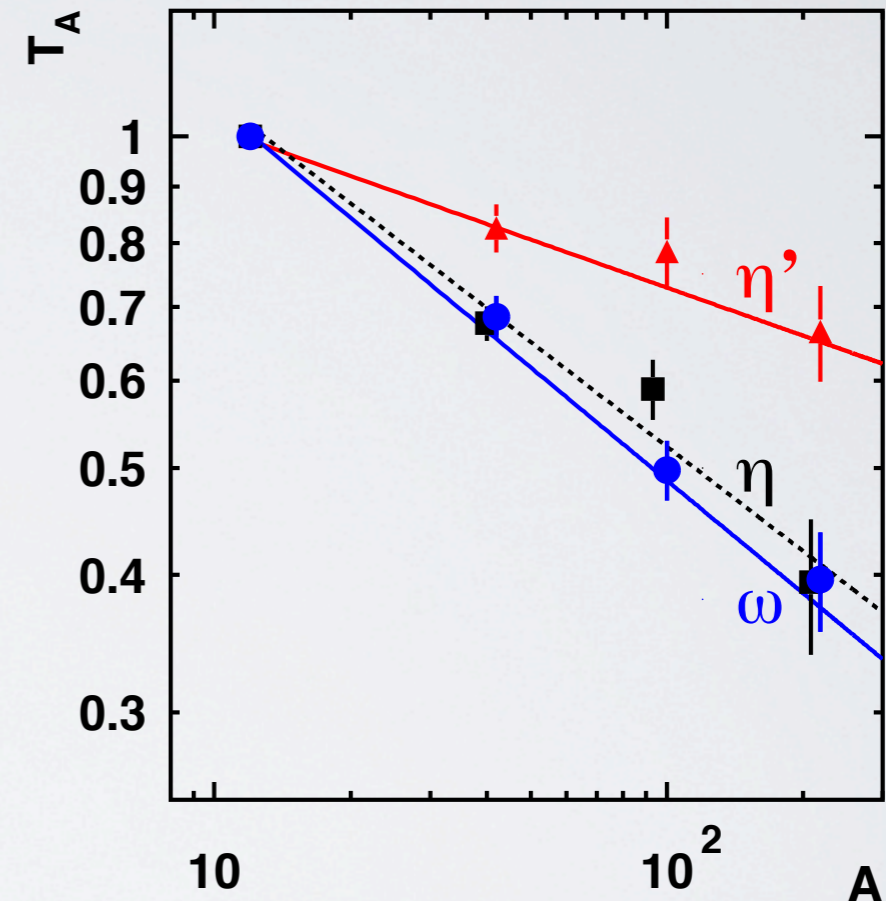
$E_\gamma = 1500 - 2200$  MeV; photoproduction of  $\eta'$  meson off  $^{12}\text{C}$ ,  $^{40}\text{Ca}$ ,  $^{93}\text{Nb}$  and  $^{208}\text{Pb}$

$$T_A^C = \frac{12 \cdot \sigma_{\gamma A \rightarrow \eta' X}}{A \cdot \sigma_{\gamma C \rightarrow \eta' X}} \quad \text{normalized to carbon}$$

M. Nanova et al., PLB 710 (2012) 600



comparison with other mesons



$\eta'$  interaction with nuclear matter  
much weaker than for  $\eta$ ,  $\omega$   
mesons

at low density approximation:

$$\Gamma(\rho) = -\frac{\text{Im}\Pi(\rho)}{E} \sim \rho v \sigma_{inel} \quad ; \quad \Gamma(\rho) = \Gamma(\rho_0) \frac{\rho}{\rho_0}$$

$$\Rightarrow \Gamma_{\eta'}(\langle p_{\eta'} \rangle \approx 1.05 \text{ GeV}/c) \approx 15-25 \text{ MeV};$$

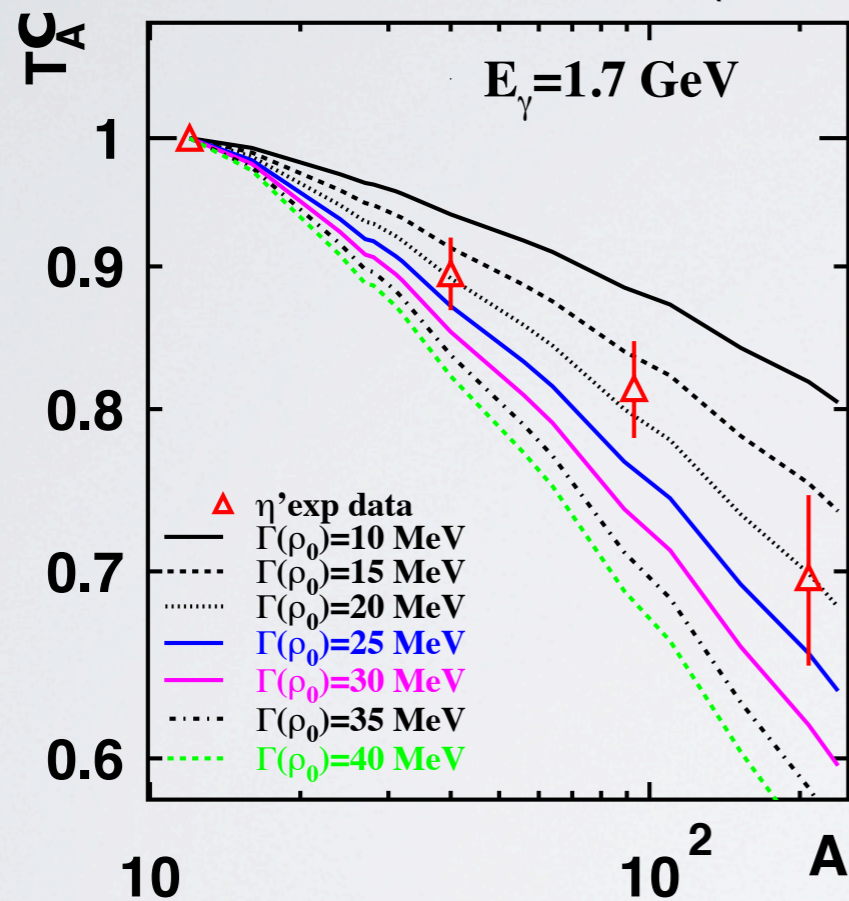
$$\rho_0 = 0.17 \text{ fm}^{-3}; \quad \sigma_{inel}^{\eta'} \approx 3-10 \text{ mb}$$

# The imaginary part of the $\eta'$ -nucleus potential

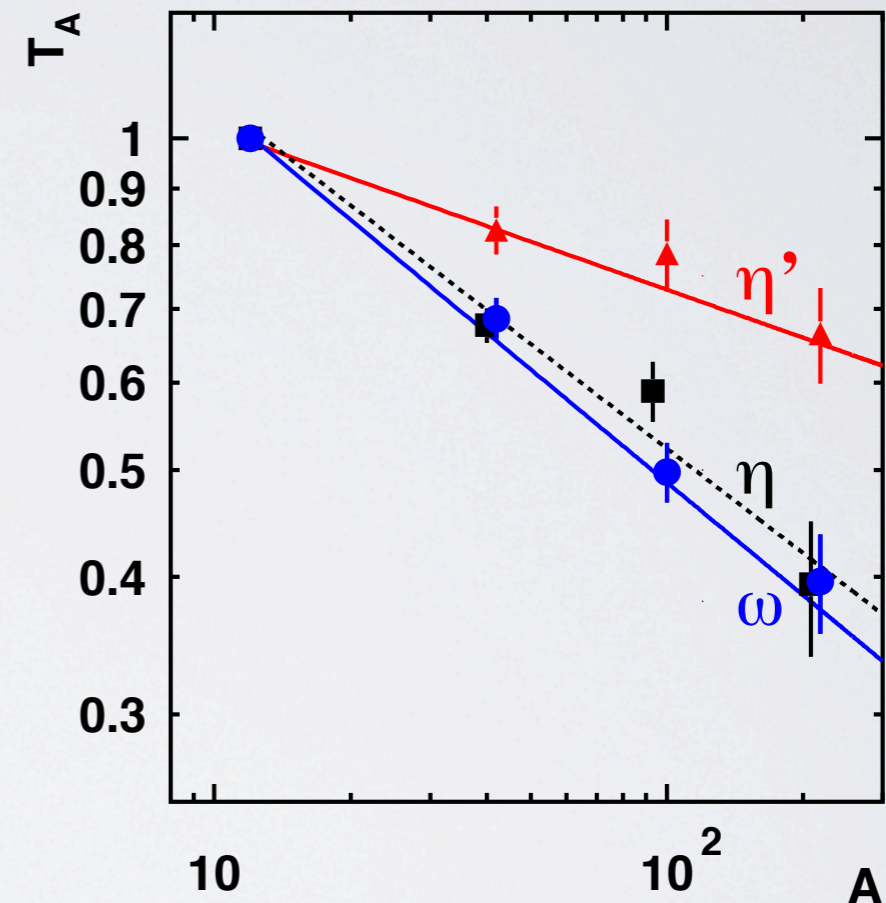
$E_\gamma = 1500 - 2200$  MeV; photoproduction of  $\eta'$  meson off  $^{12}\text{C}$ ,  $^{40}\text{Ca}$ ,  $^{93}\text{Nb}$  and  $^{208}\text{Pb}$

$$T_A^C = \frac{12 \cdot \sigma_{\gamma A \rightarrow \eta' X}}{A \cdot \sigma_{\gamma C \rightarrow \eta' X}} \quad \text{normalized to carbon}$$

M. Nanova et al., PLB 710 (2012) 600



comparison with other mesons



$\eta'$  interaction with nuclear matter  
much weaker than for  $\eta$ ,  $\omega$   
mesons

at low density approximation:

$$\Gamma(\rho) = -\frac{\text{Im}\Pi(\rho)}{E} \sim \rho v \sigma_{inel} \quad ; \quad \Gamma(\rho) = \Gamma(\rho_0) \frac{\rho}{\rho_0}$$

$$\Rightarrow \Gamma_{\eta'}(\langle p_{\eta'} \rangle \approx 1.05 \text{ GeV}/c) \approx 15-25 \text{ MeV};$$

$$\rho_0 = 0.17 \text{ fm}^{-3}; \quad \sigma_{\eta'}^{inel} \approx 3-10 \text{ mb}$$

$$W_{\eta'}(\rho = \rho_0) = -\Gamma_0/2 = -(7.5-12.5) \text{ MeV}$$

# Determination of the real part of the $\eta'$ -nucleus potential

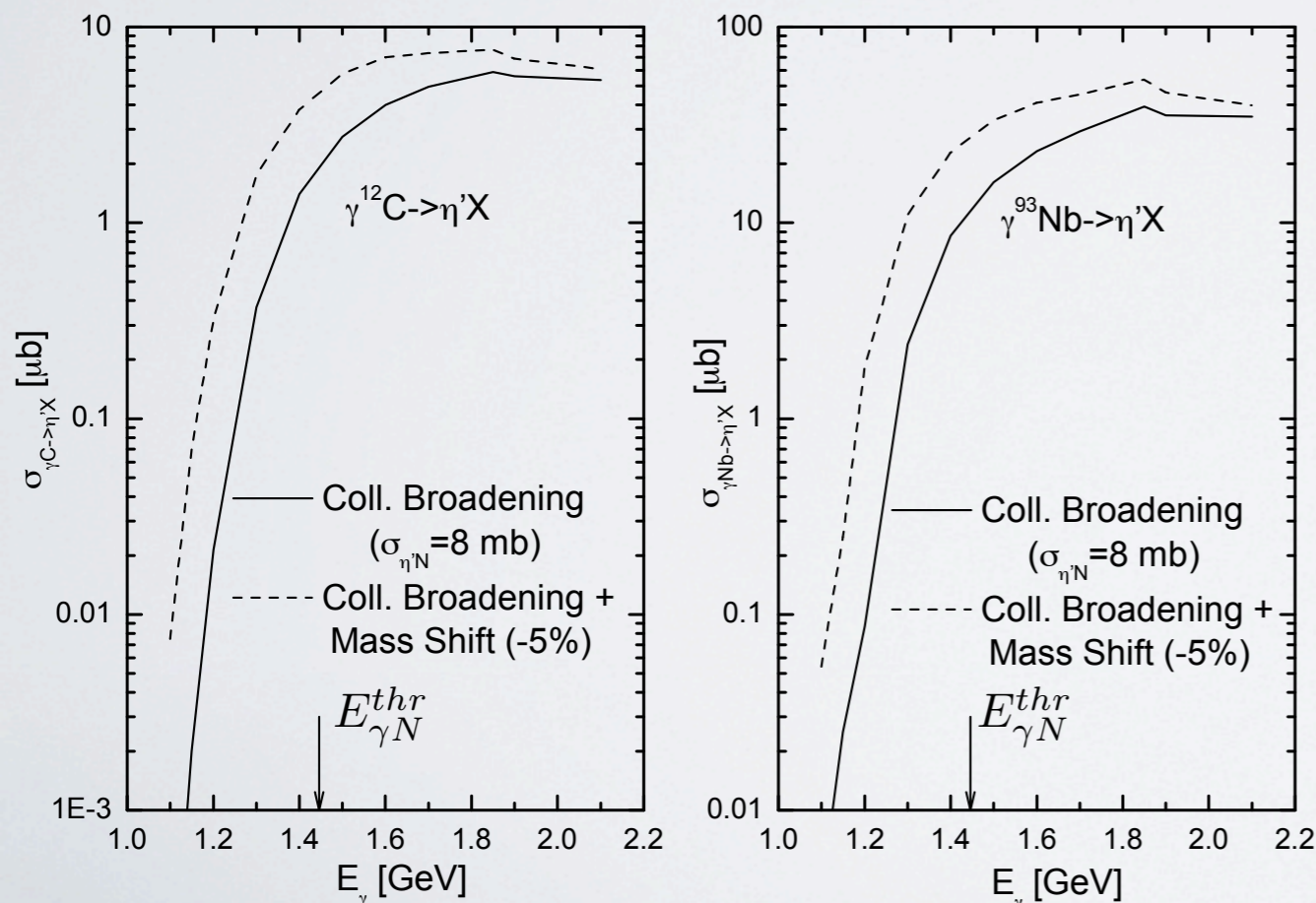
J.Weil, U. Mosel and V. Metag, PLB 723 (2013) 120

E. Paryev, J. Phys. G: Nucl. Part. Phys. 40 (2013) 025201

- measurement of the excitation function:

in case of dropping mass - higher meson yield for given  $\sqrt{s}$  because of increased phase space due to lowering of the production threshold

## $\eta'$ excitation function



# Determination of the real part of the $\eta'$ -nucleus potential

J.Weil, U.Mosel and V.Metag, PLB 723 (2013) 120

E.Paryev, J. Phys. G: Nucl. Part. Phys. 40 (2013) 025201

- measurement of the excitation function:

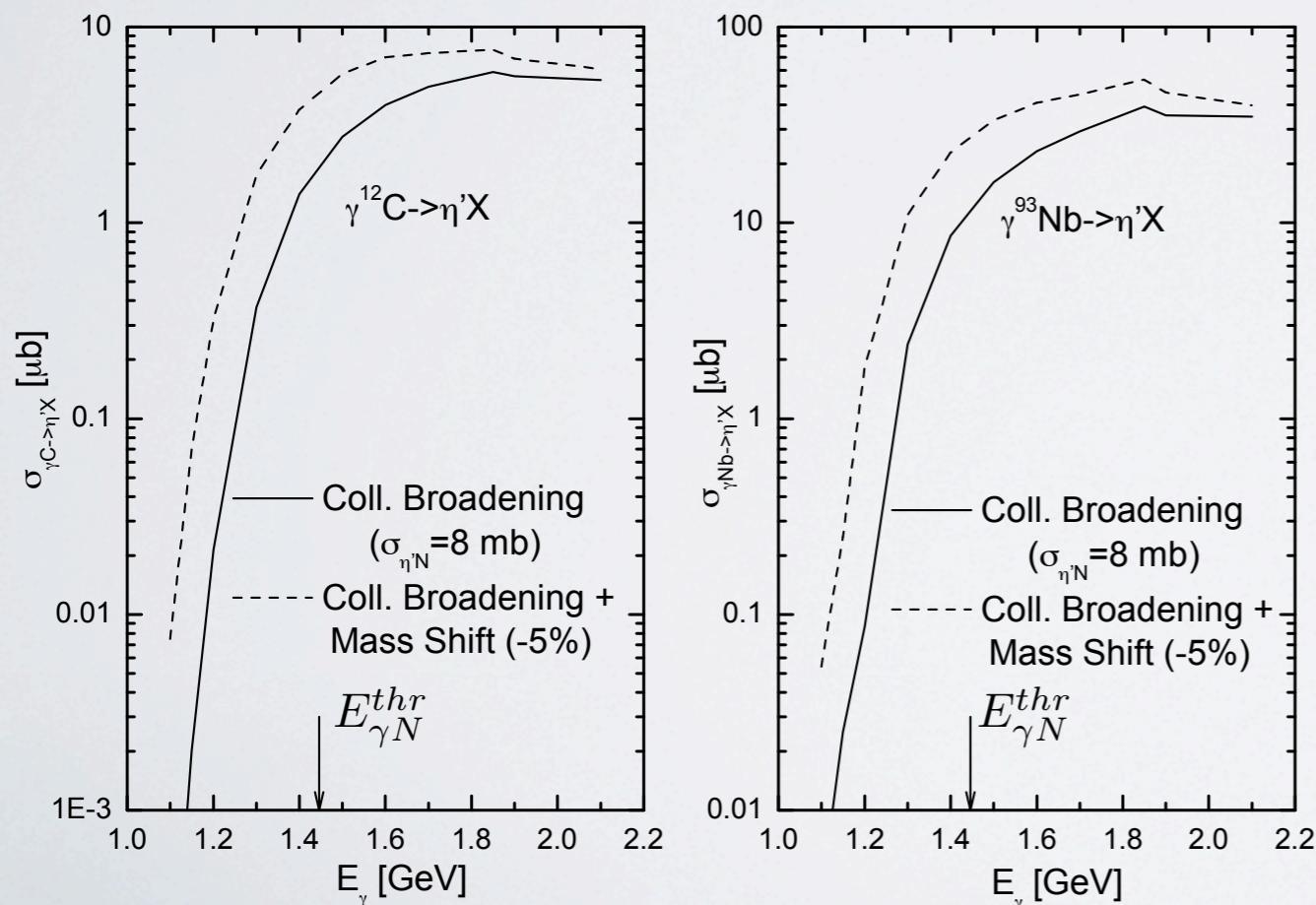
in case of dropping mass - higher meson yield for given  $\sqrt{s}$  because of increased phase space due to lowering of the production threshold

- measurement of the momentum distribution:

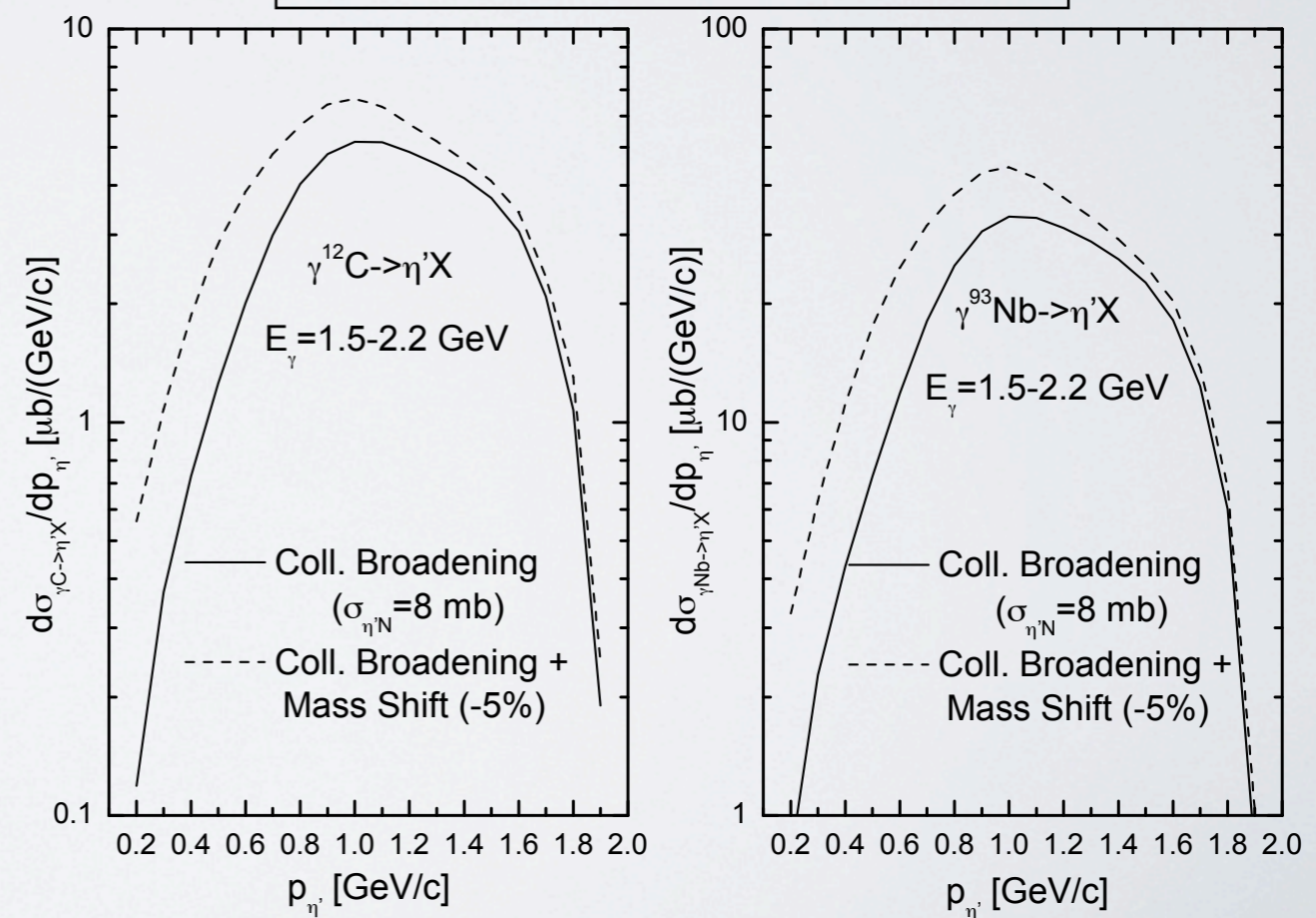
in case of dropping mass - when leaving the nucleus hadron has to become on-shell; mass generated at the expense of kinetic energy

⇒ downward shift of momentum distribution

$\eta'$  excitation function

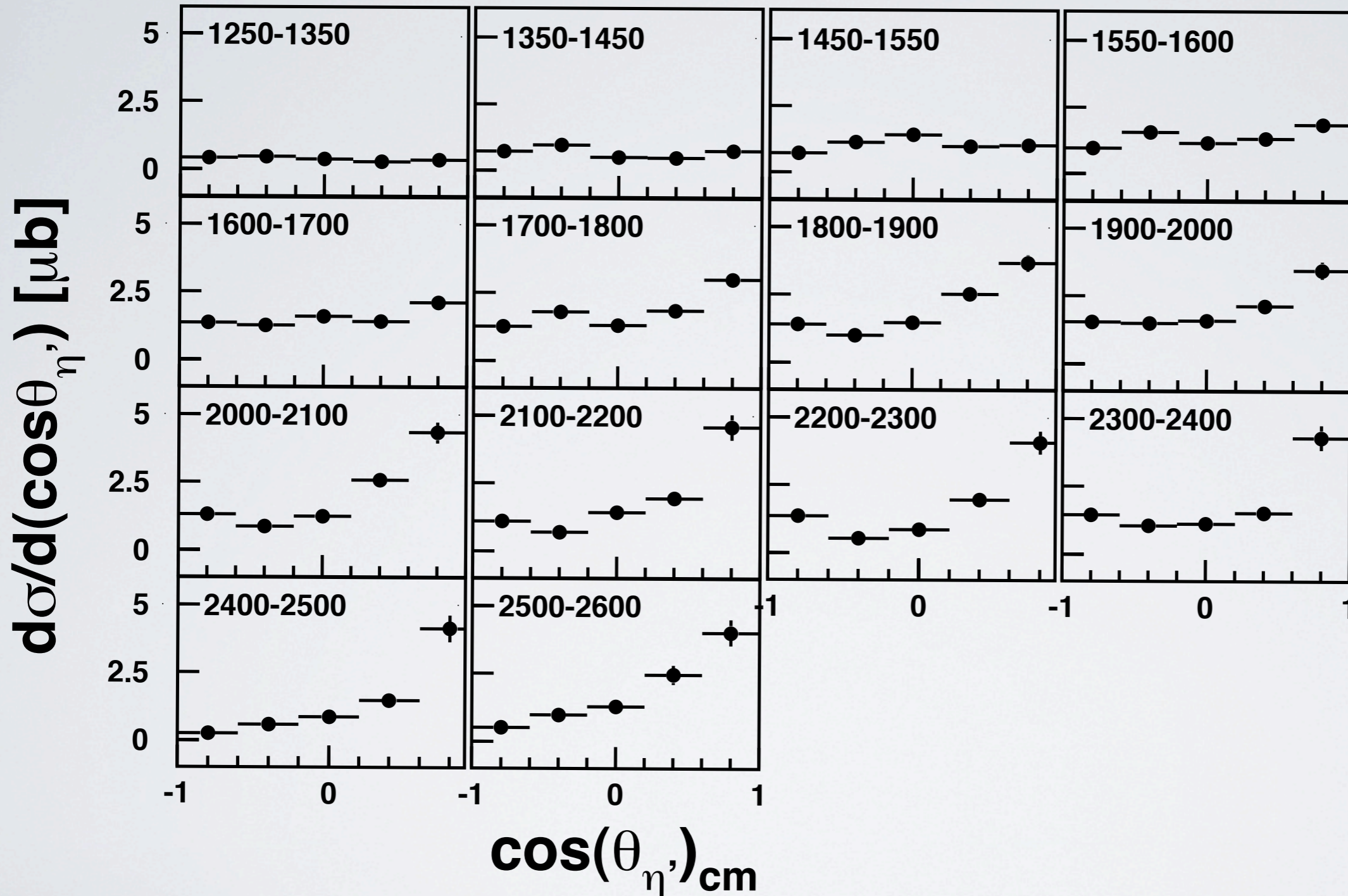


$\eta'$  momentum distribution



# differential cross sections for $\eta'$ photo production off carbon

M. Nanova et al., arXiv:1311.0122; accepted for publication in PLB



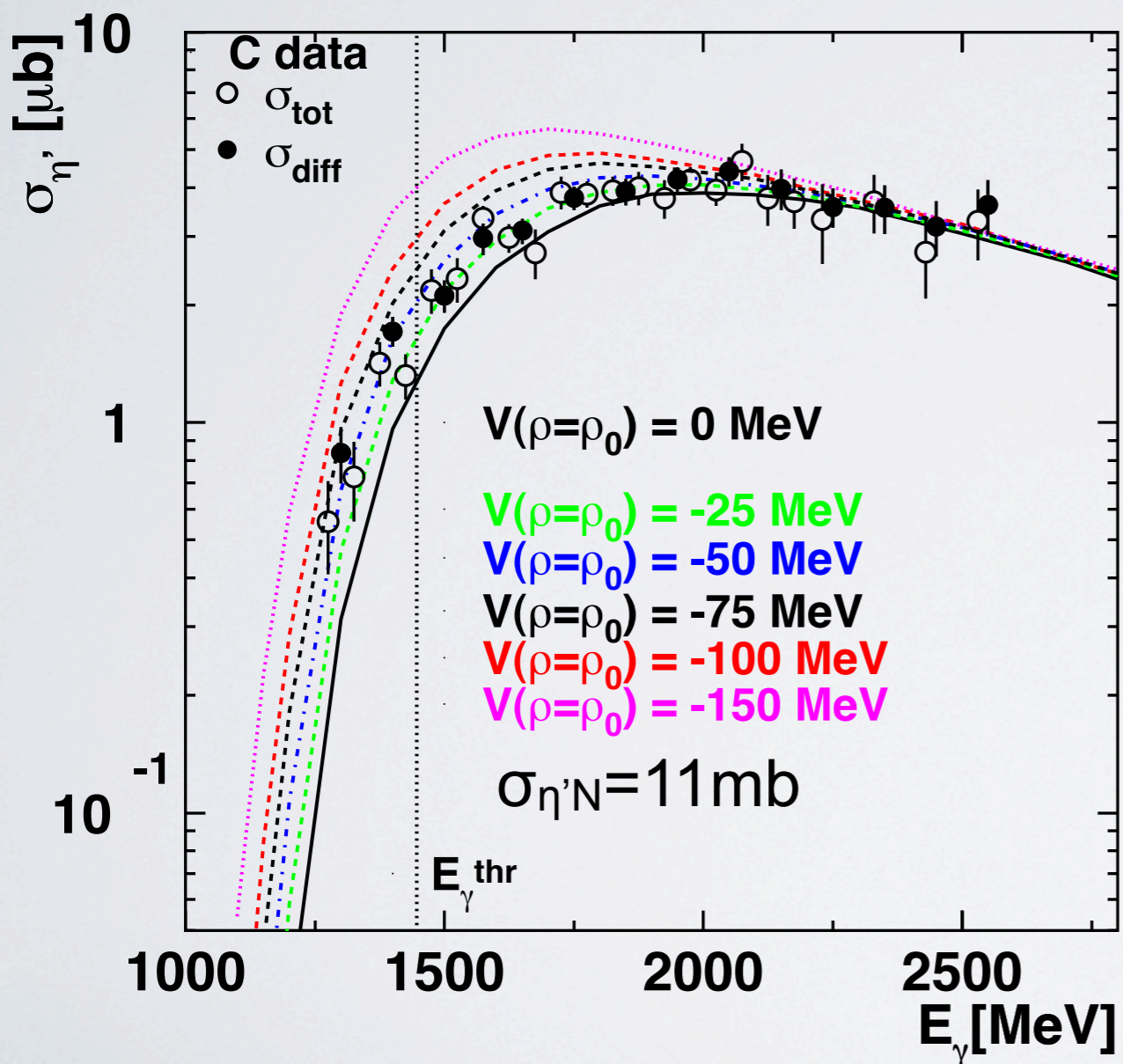
forward rise of cross section with increasing incident photon energy:  
t-channel production mechanism



# excitation function for $\eta'$ photoproduction off C

comparison of CBELSA/TAPS data with  
calculations by E. Paryev, J. Phys. G: Nucl. Part. Phys. 40 (2013) 025201  
and priv. communication

decay mode:  $\eta' \rightarrow \pi^0\pi^0\eta$   
excitation function



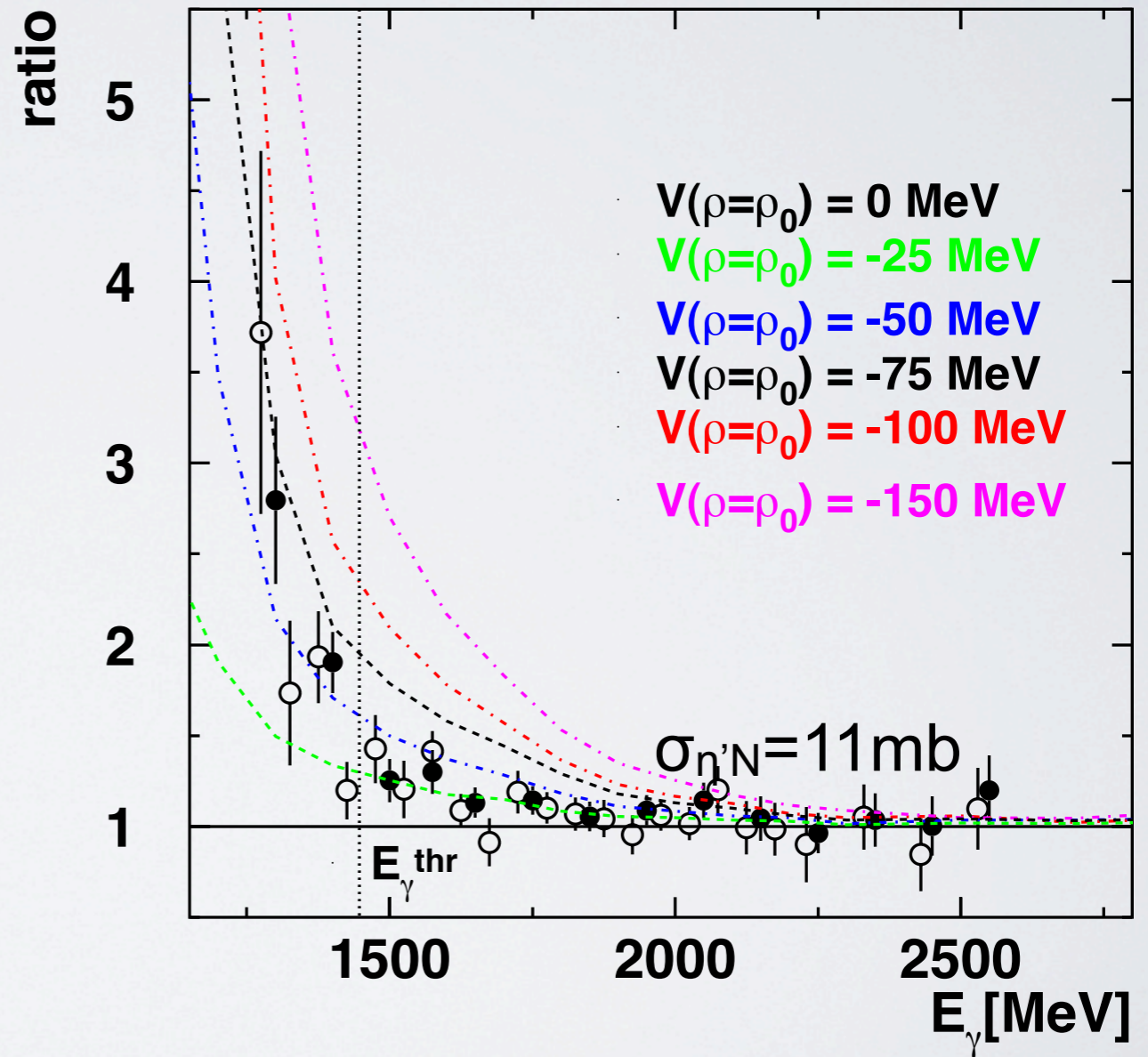
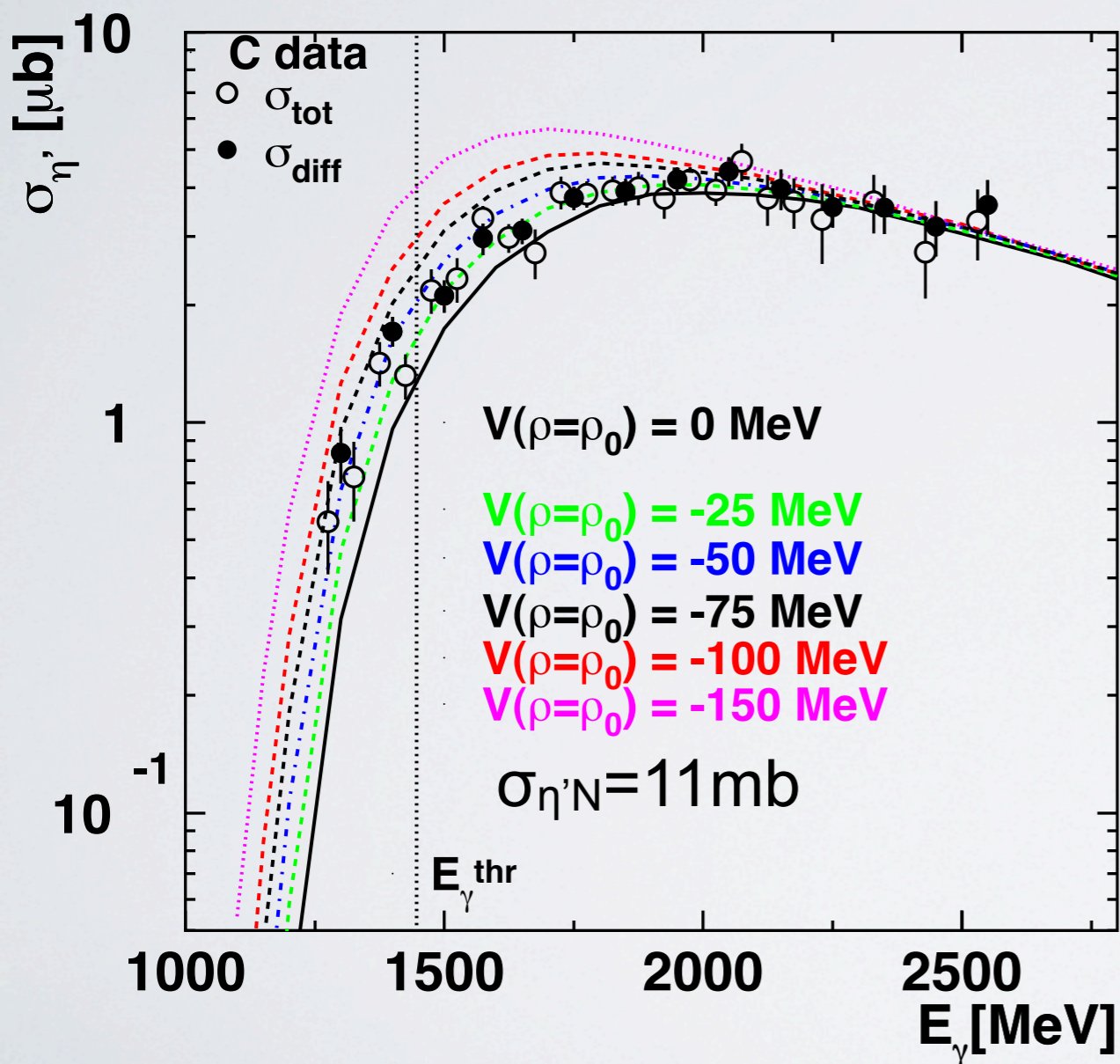
calculations normalized to data for  
 $E_{\gamma} = 2000\text{-}2500 \text{ MeV}$ ; downscaled by 1.2

# excitation function for $\eta'$ photoproduction off C

comparison of CBELSA/TAPS data with  
 calculations by E. Paryev, J. Phys. G: Nucl. Part. Phys. 40 (2013) 025201  
 and priv. communication

decay mode:  $\eta' \rightarrow \pi^0\pi^0\eta$   
 excitation function

exp. data and the 5 scenarios divided by the  
 calculation for scenario  $V(\rho=\rho_0)=0$  MeV



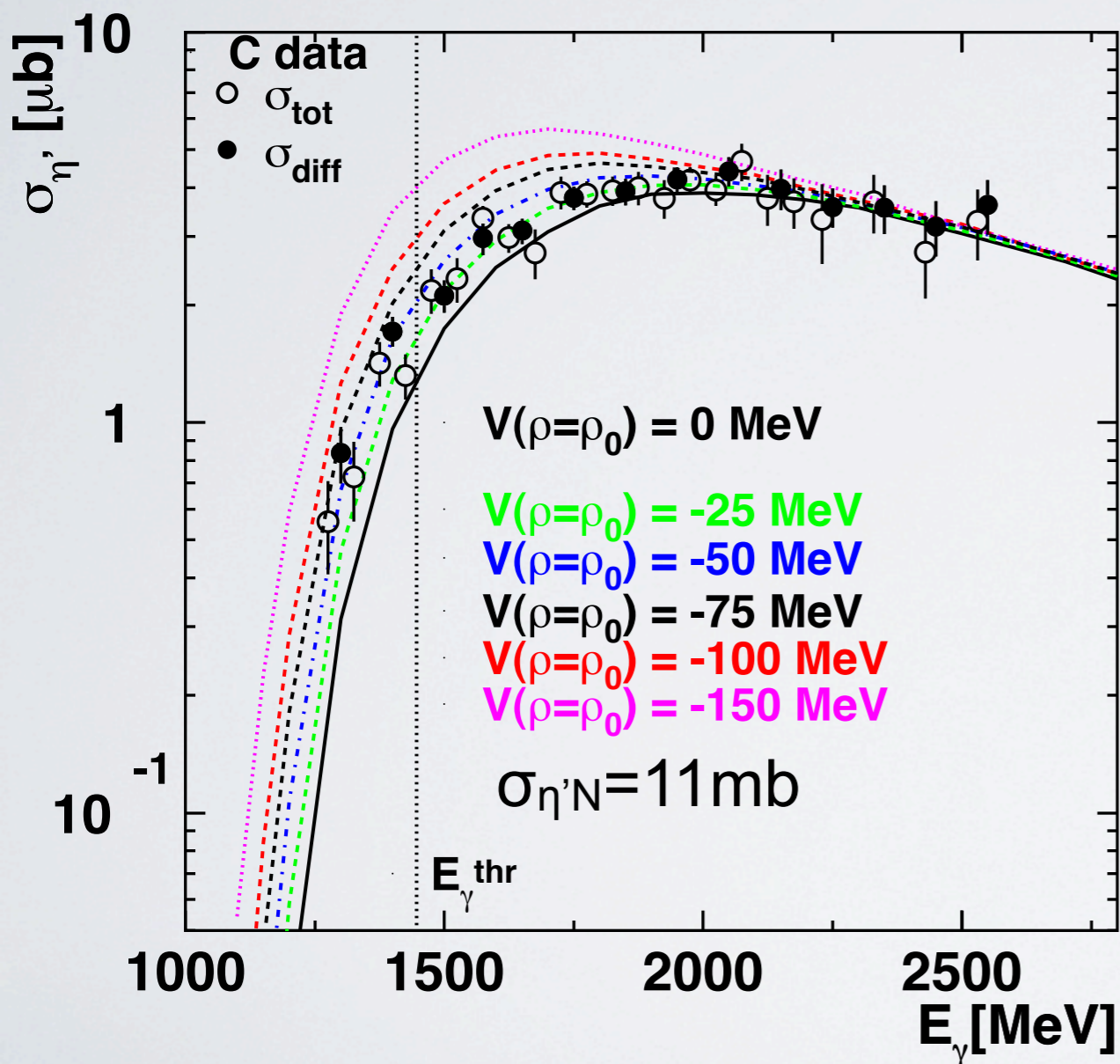
calculations normalized to data for  
 $E_\gamma = 2000\text{-}2500$  MeV; downscaled by 1.2

# excitation function for $\eta'$ photoproduction off C

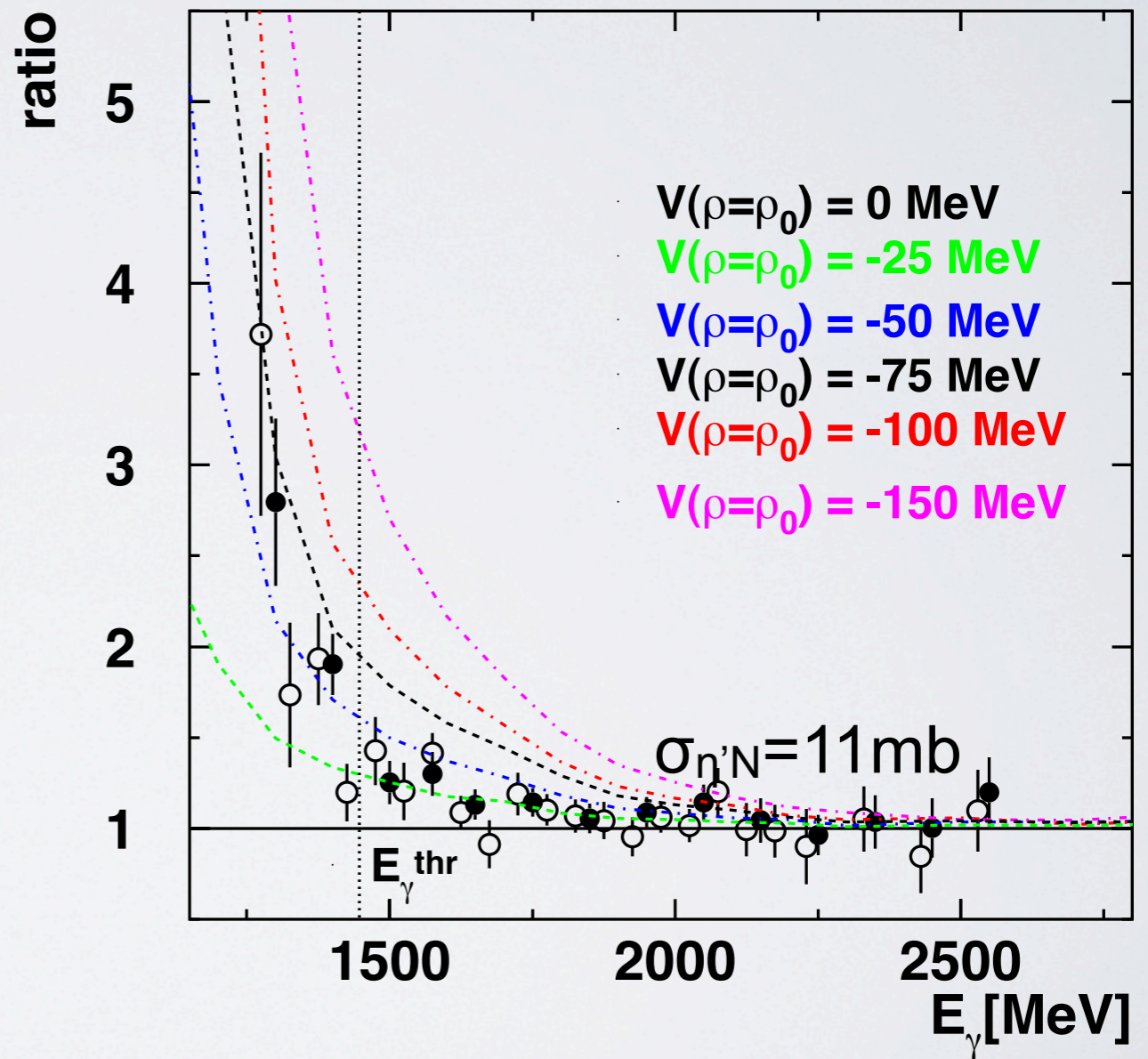
comparison of CBELSA/TAPS data with  
 calculations by E. Paryev, J. Phys. G: Nucl. Part. Phys. 40 (2013) 025201  
 and priv. communication

decay mode:  $\eta' \rightarrow \pi^0\pi^0\eta$   
 excitation function

exp. data and the 5 scenarios divided by the  
 calculation for scenario  $V(\rho=\rho_0)=0$  MeV



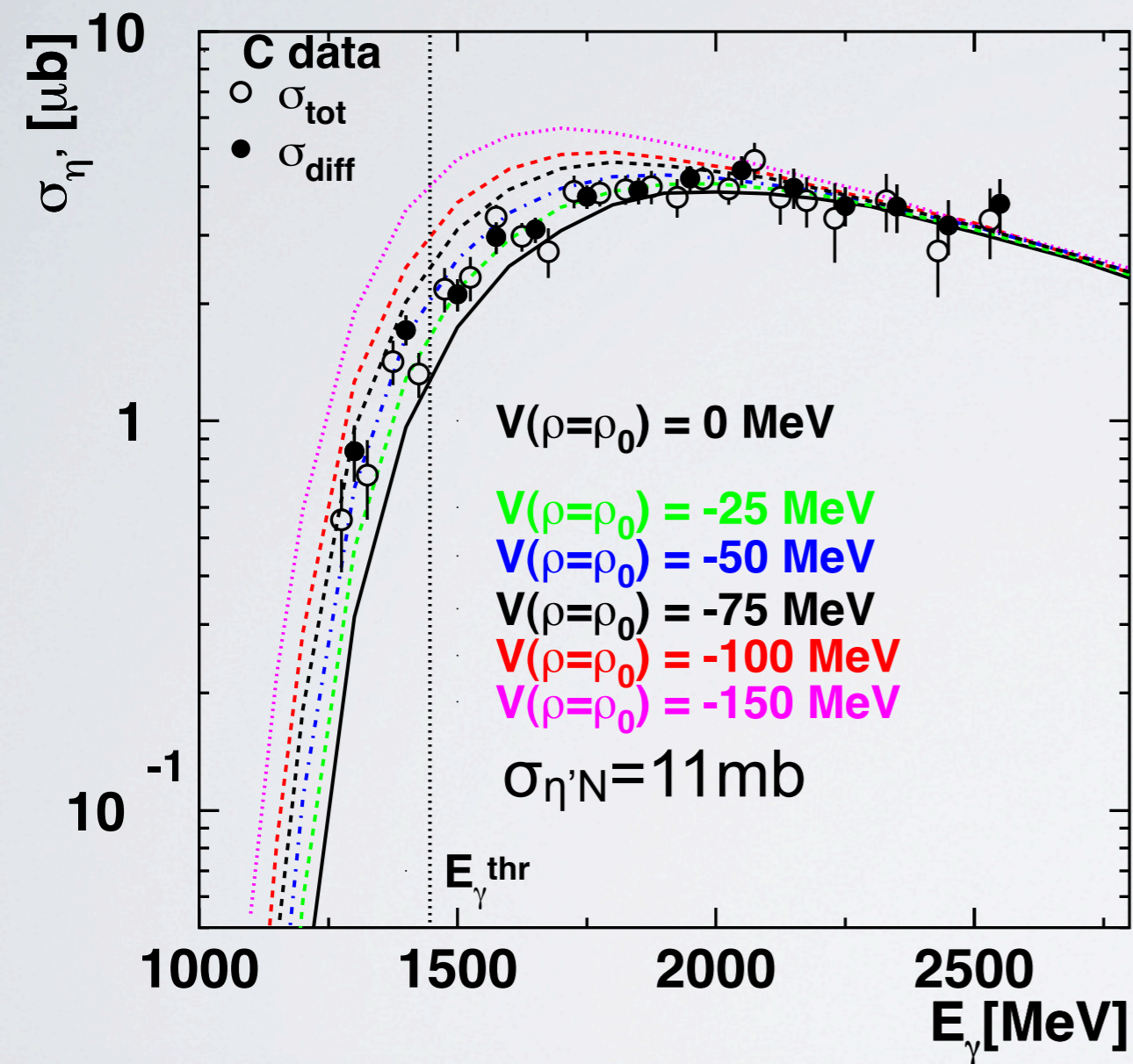
calculations normalized to data for  
 $E_\gamma = 2000\text{-}2500$  MeV; downscaled by 1.2



strong mass shift not supported by data

# estimation of the real part of the $\eta'$ -nucleus potential from the $\eta'$ excitation function

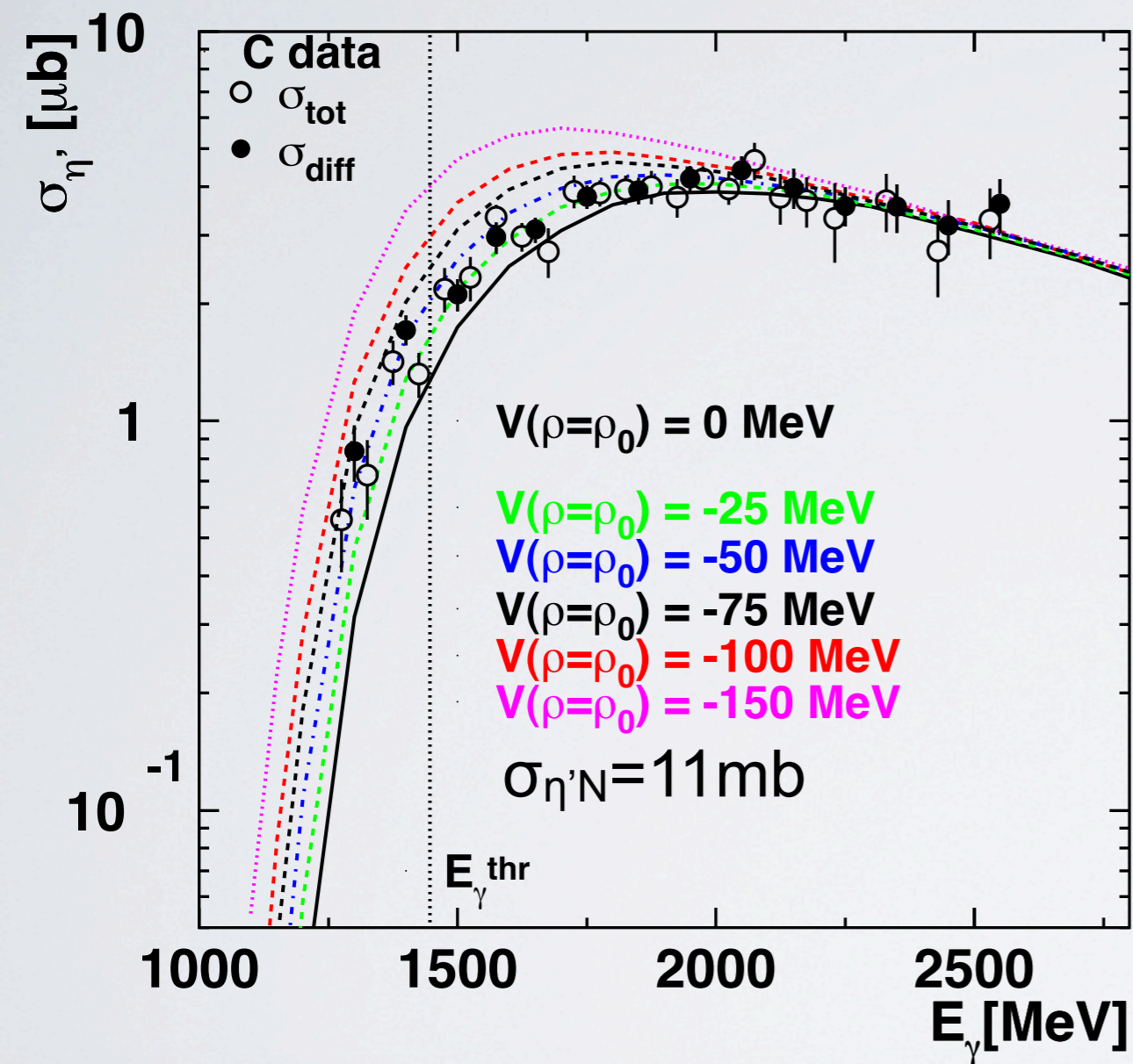
excitation function



# estimation of the real part of the $\eta'$ -nucleus potential from the $\eta'$ excitation function

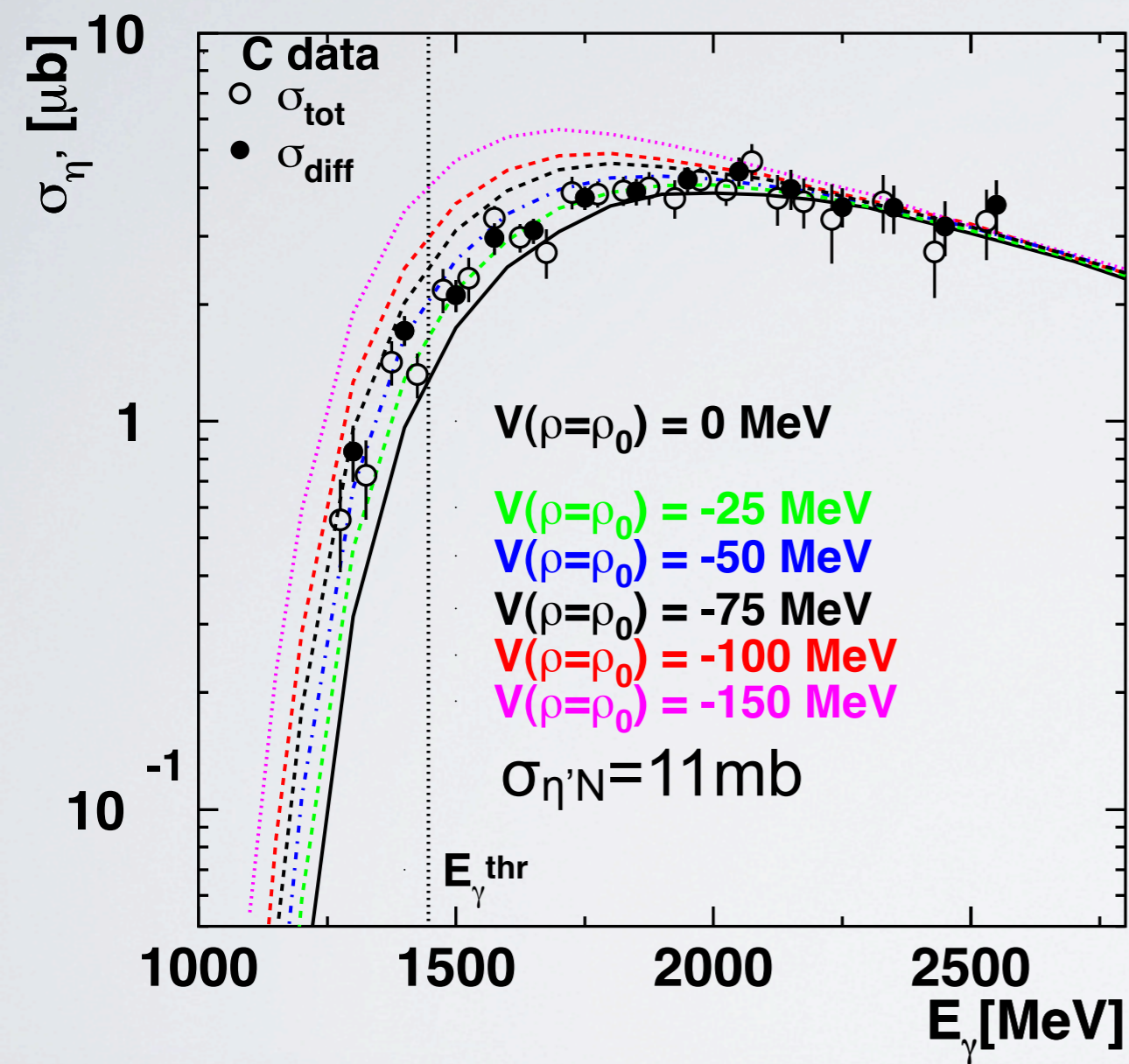
excitation function

significance test

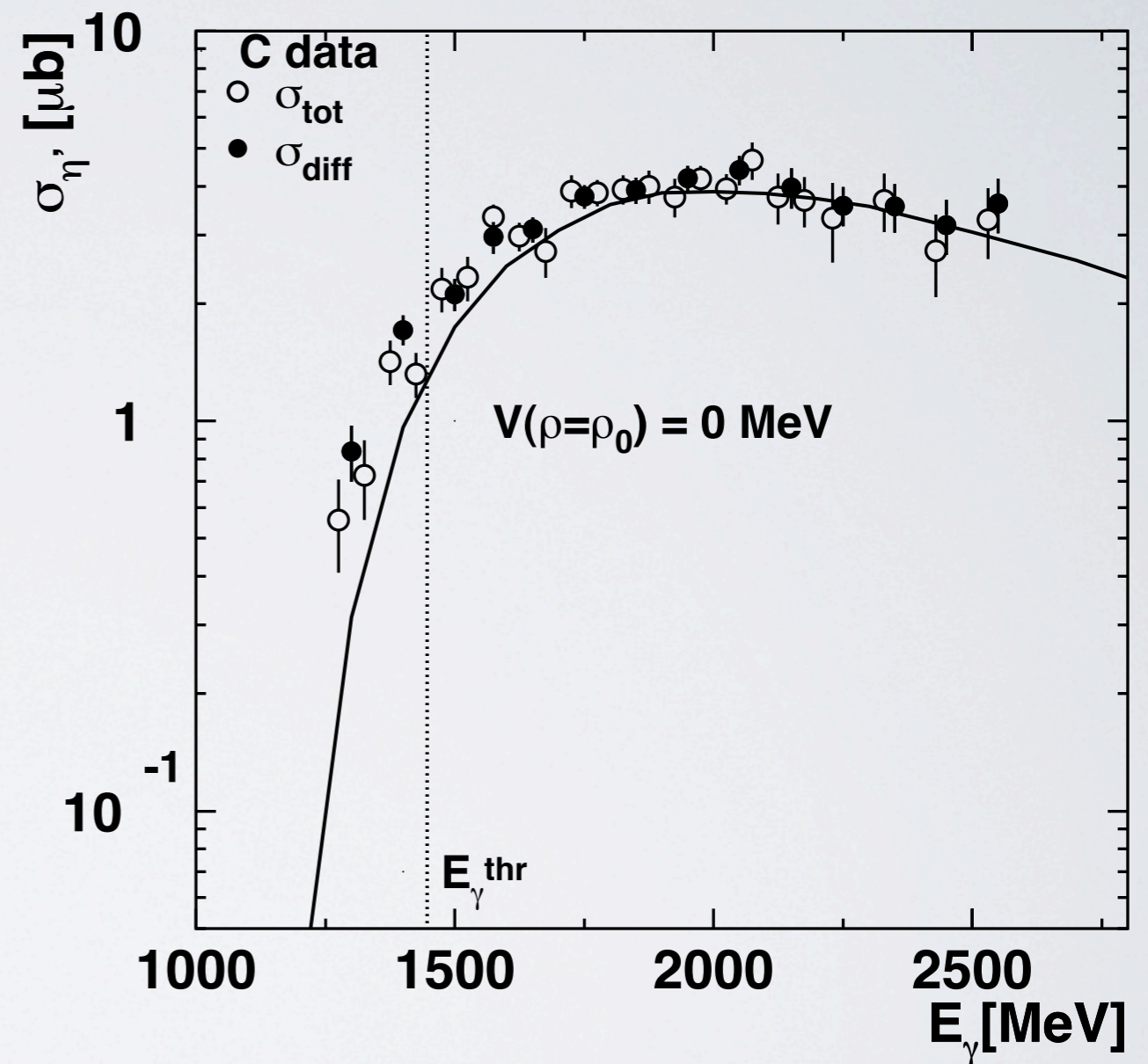


# estimation of the real part of the $\eta'$ -nucleus potential from the $\eta'$ excitation function

excitation function



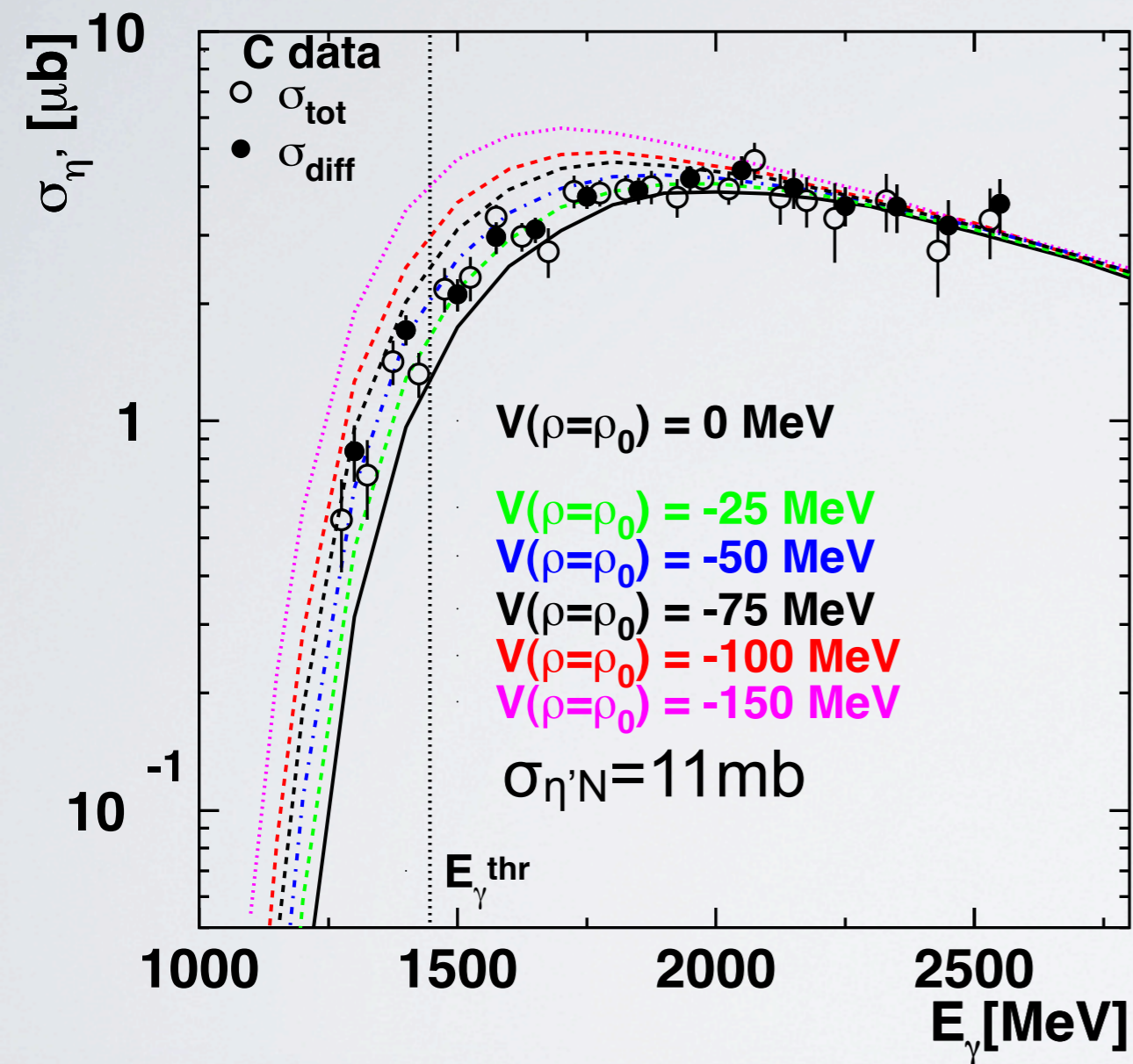
significance test



# estimation of the real part of the $\eta'$ -nucleus potential from the $\eta'$ excitation function

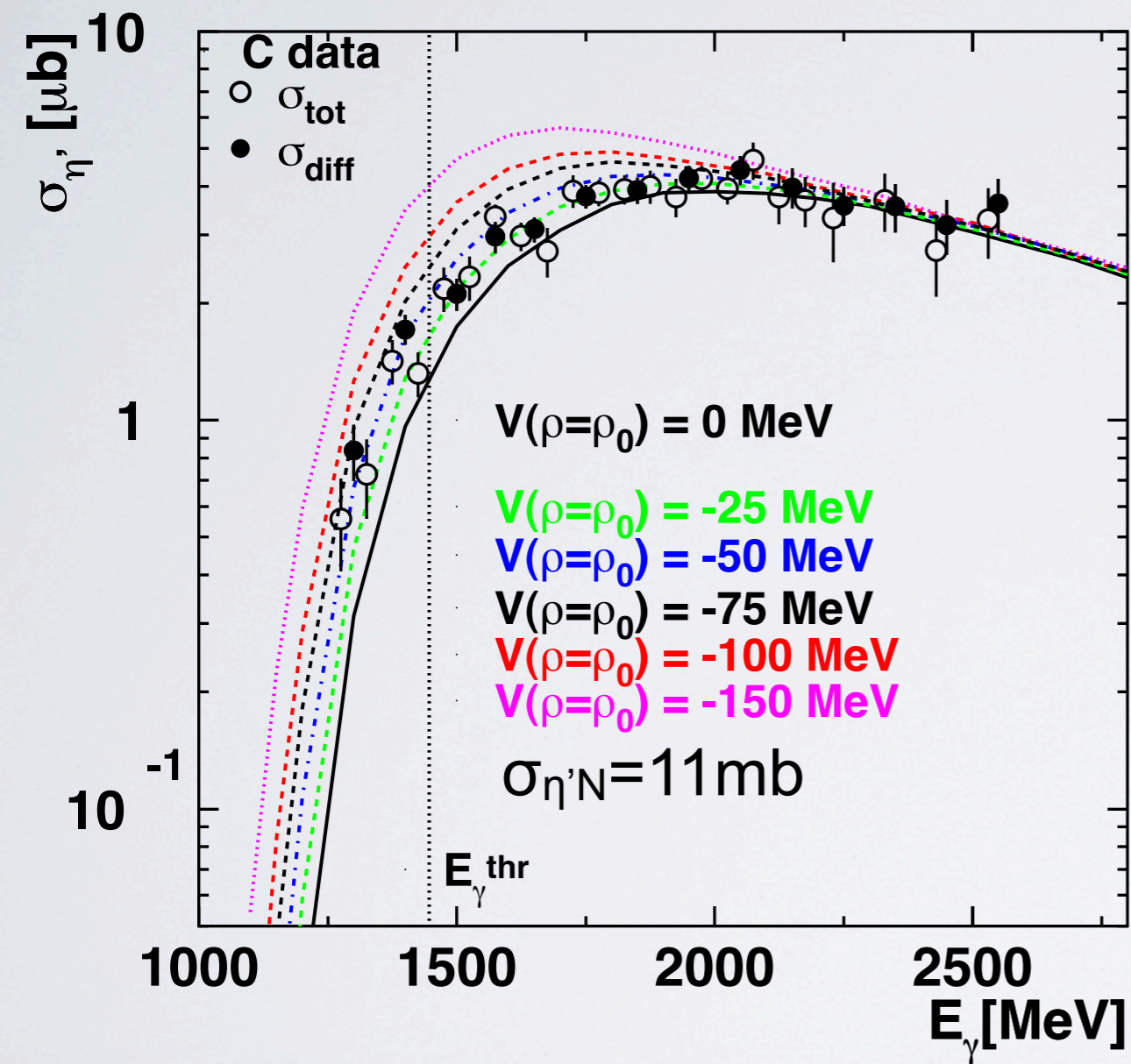
excitation function

significance test

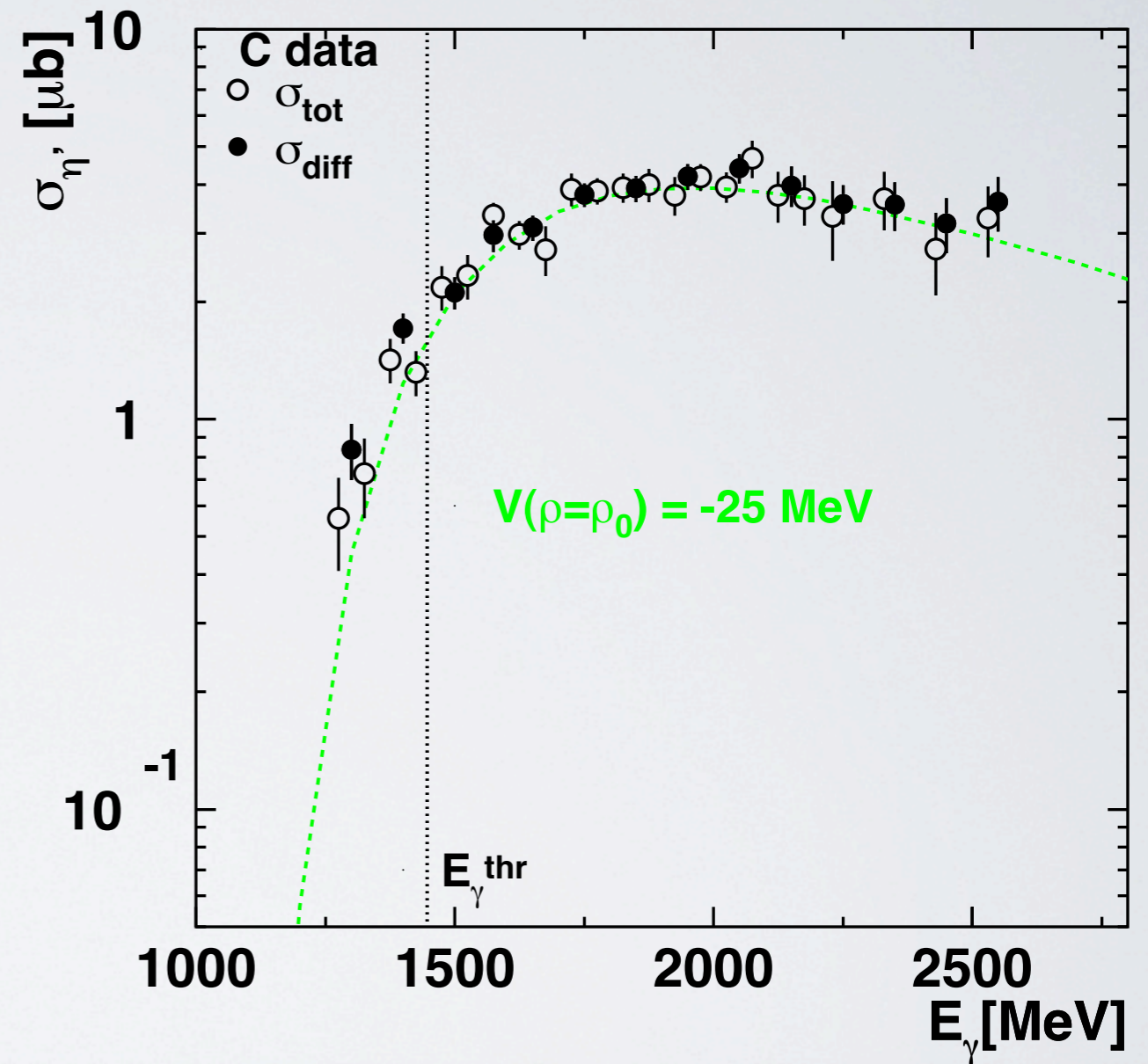


# estimation of the real part of the $\eta'$ -nucleus potential from the $\eta'$ excitation function

excitation function



significance test

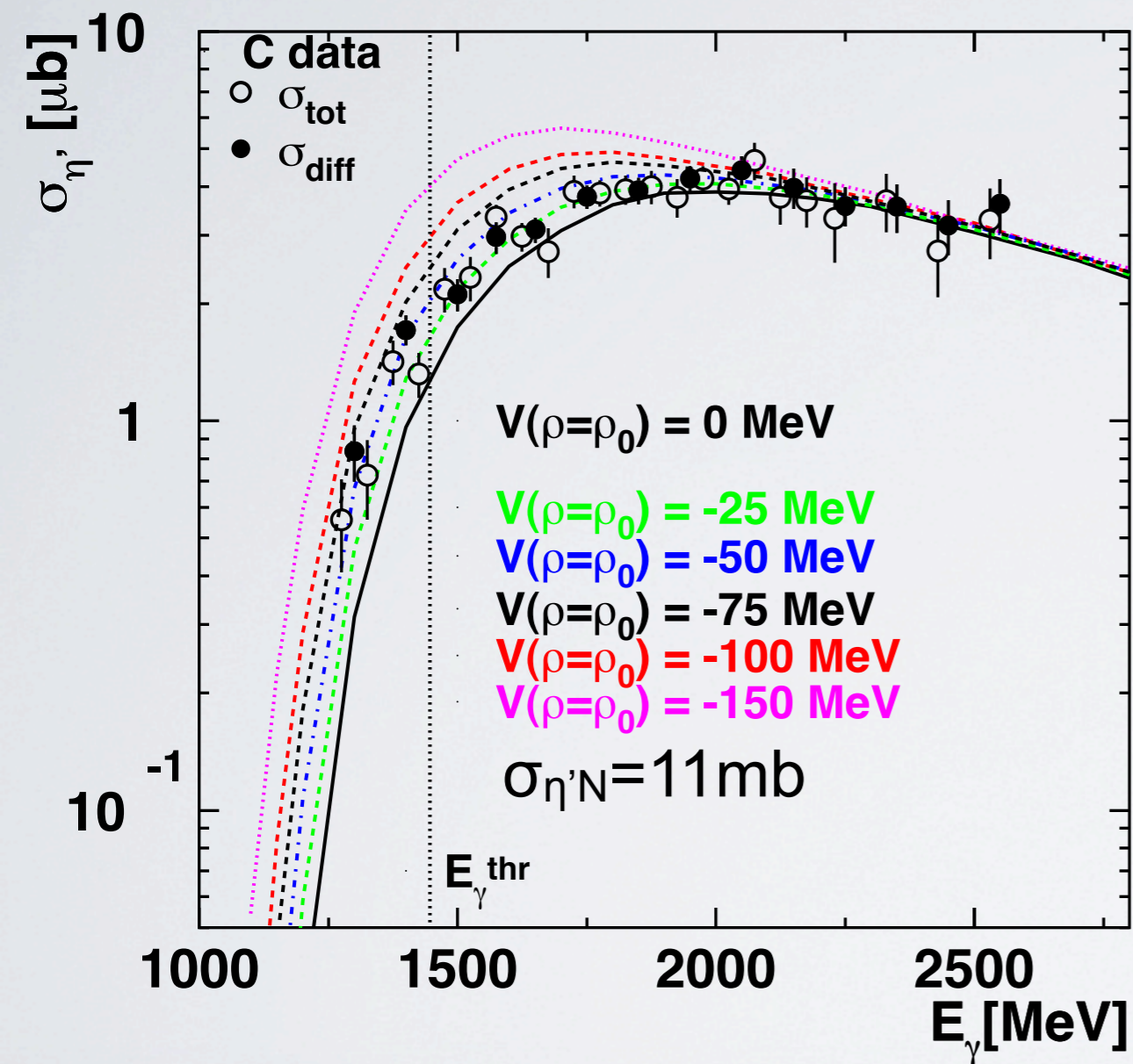




# estimation of the real part of the $\eta'$ -nucleus potential from the $\eta'$ excitation function

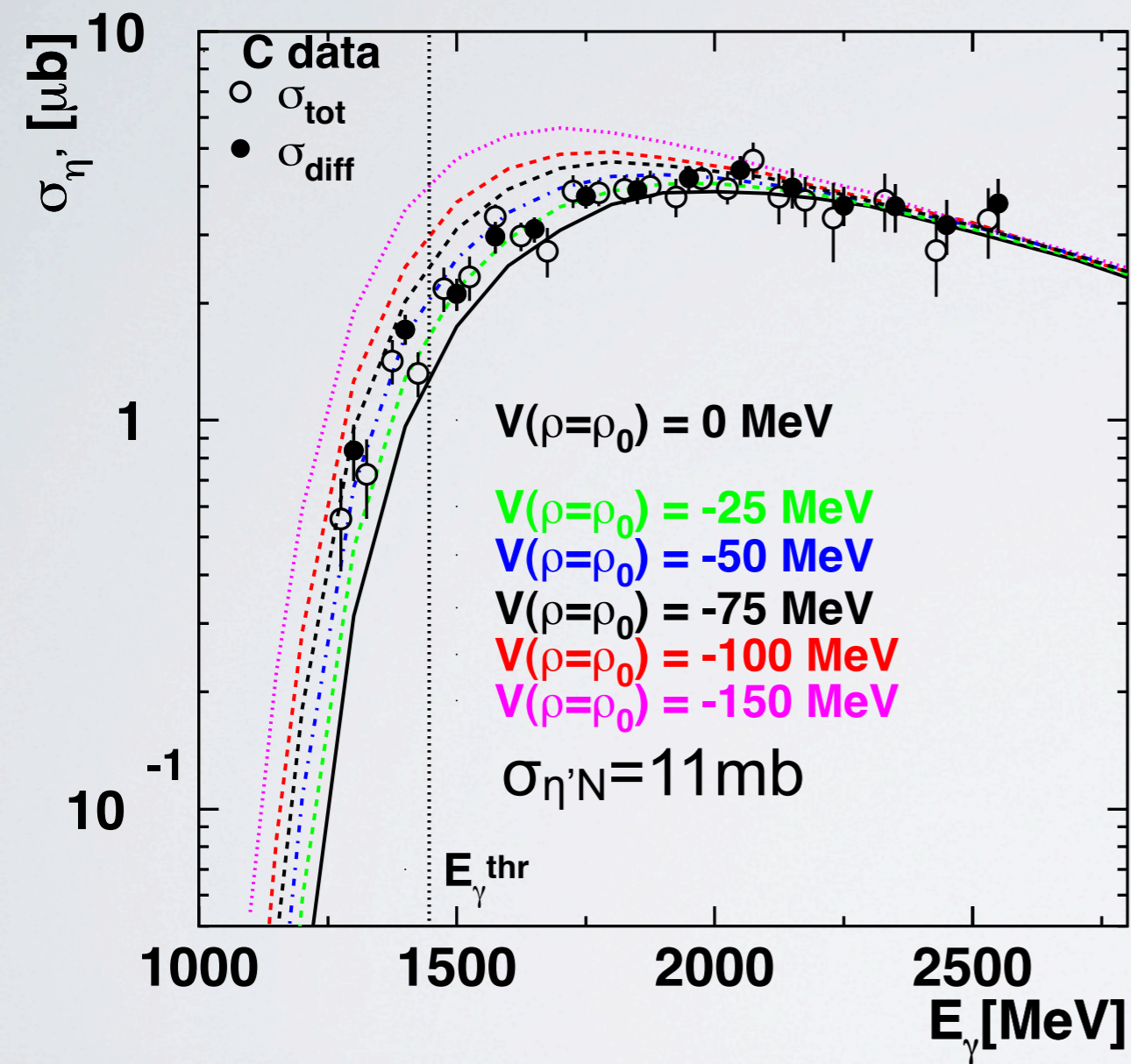
excitation function

significance test

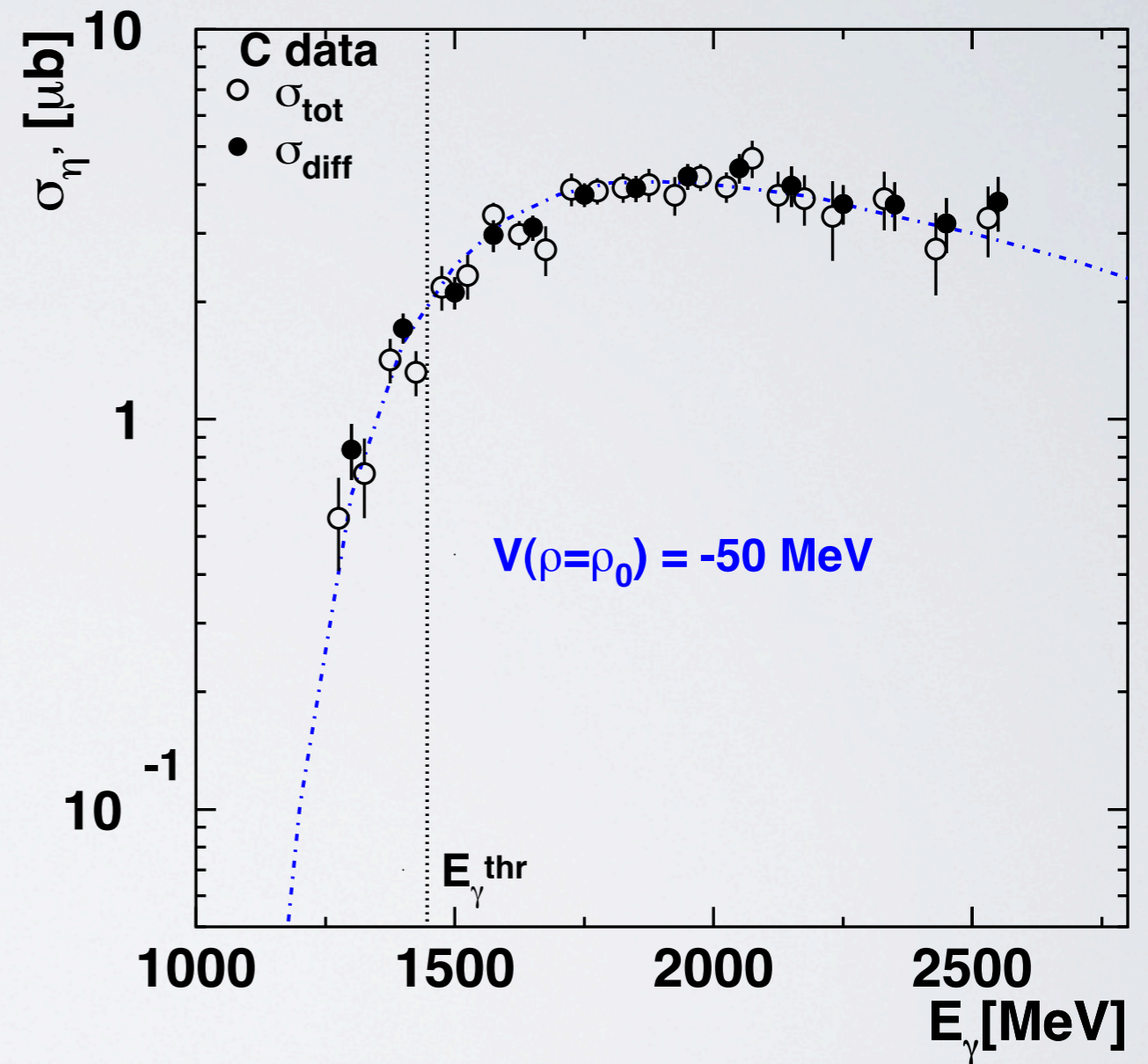


# estimation of the real part of the $\eta'$ -nucleus potential from the $\eta'$ excitation function

excitation function



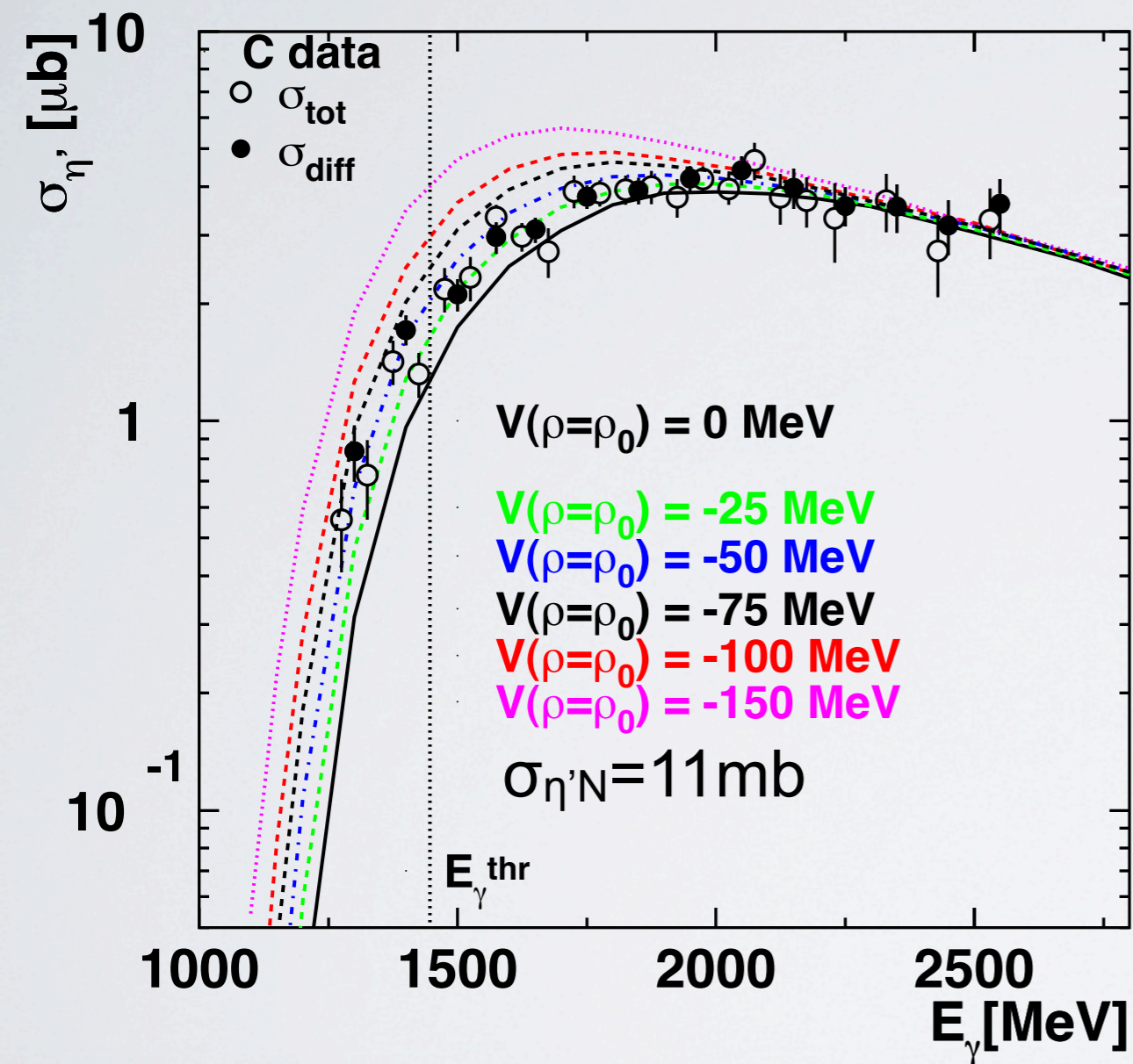
significance test



# estimation of the real part of the $\eta'$ -nucleus potential from the $\eta'$ excitation function

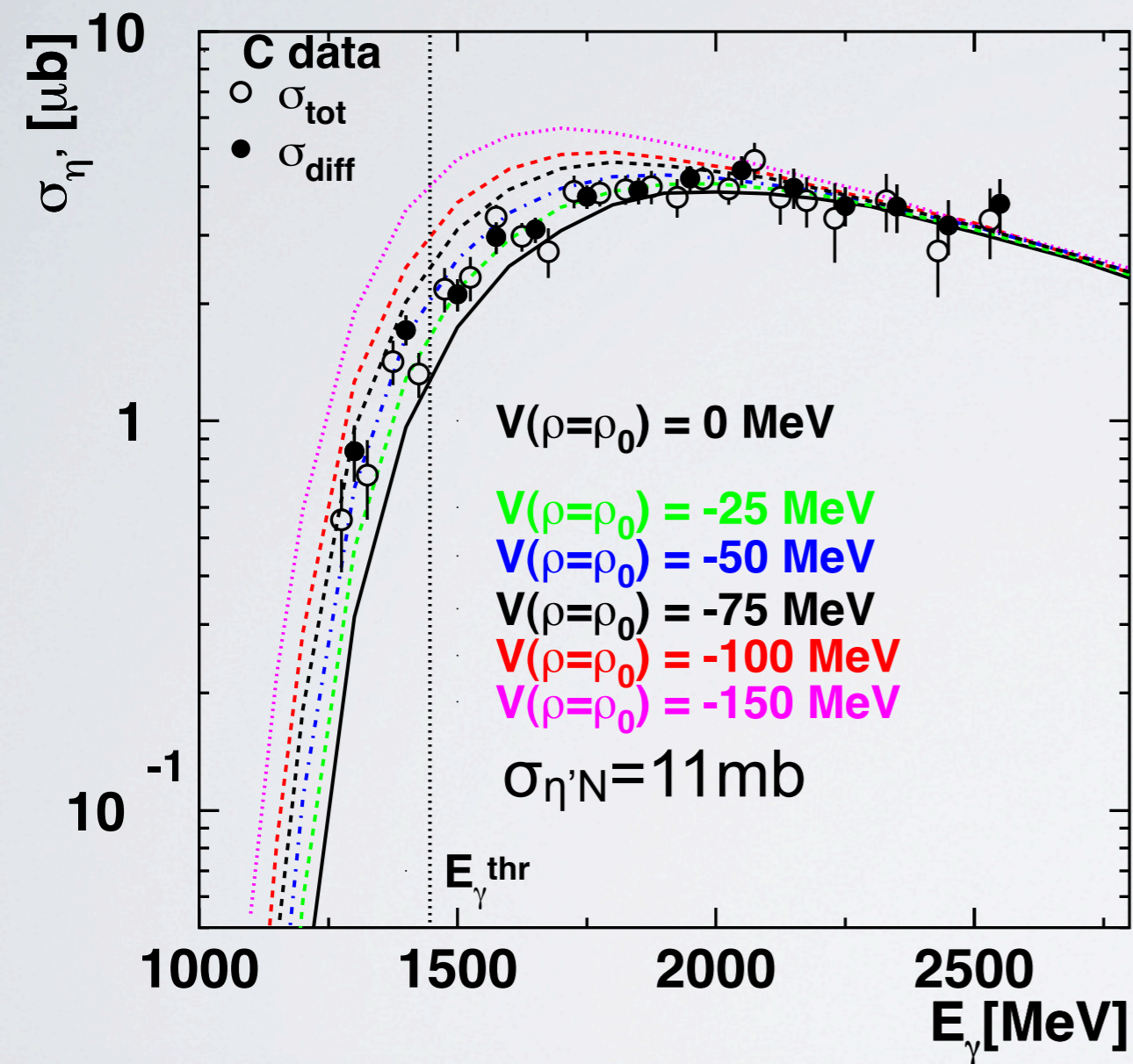
excitation function

significance test

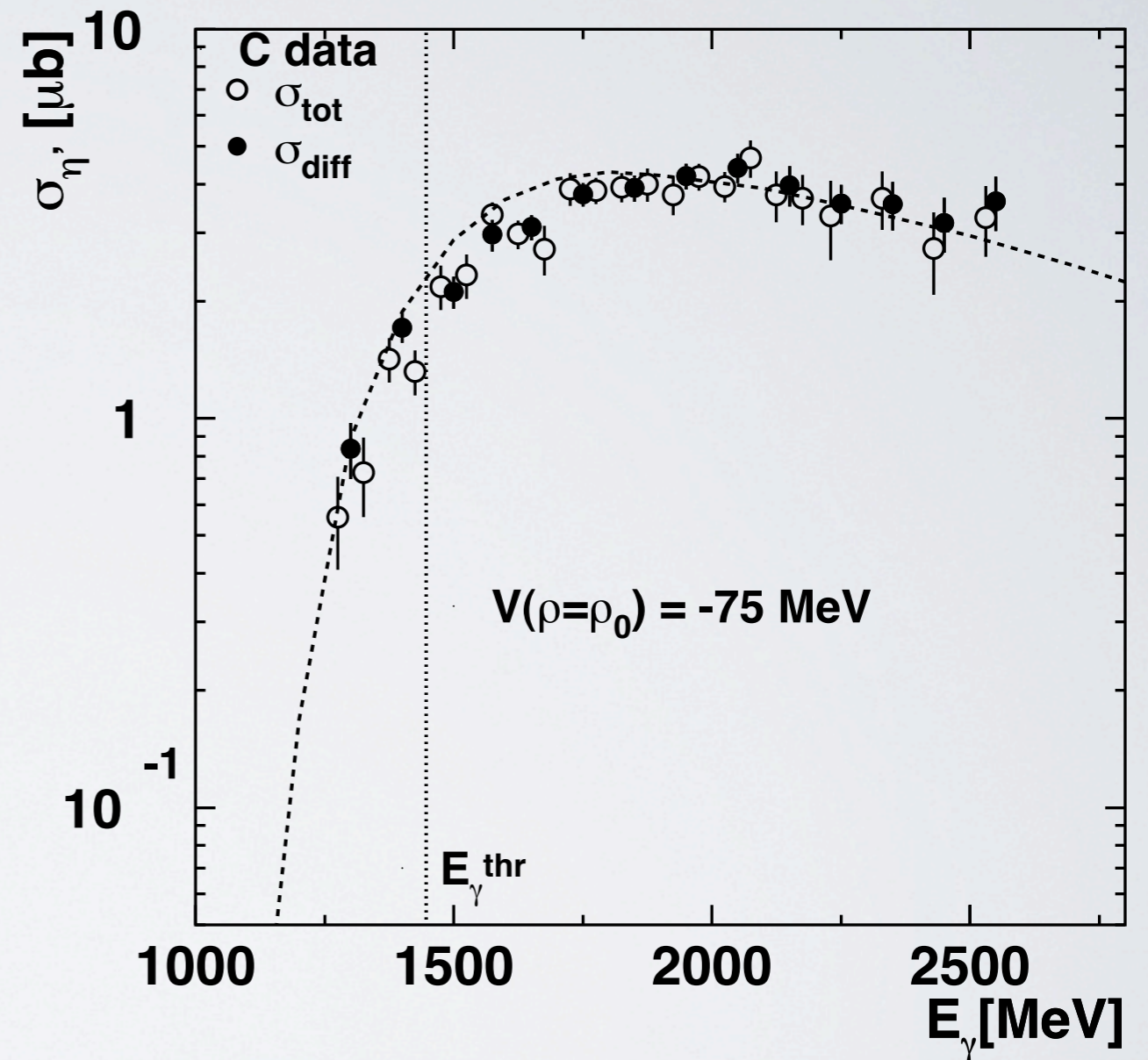


# estimation of the real part of the $\eta'$ -nucleus potential from the $\eta'$ excitation function

excitation function



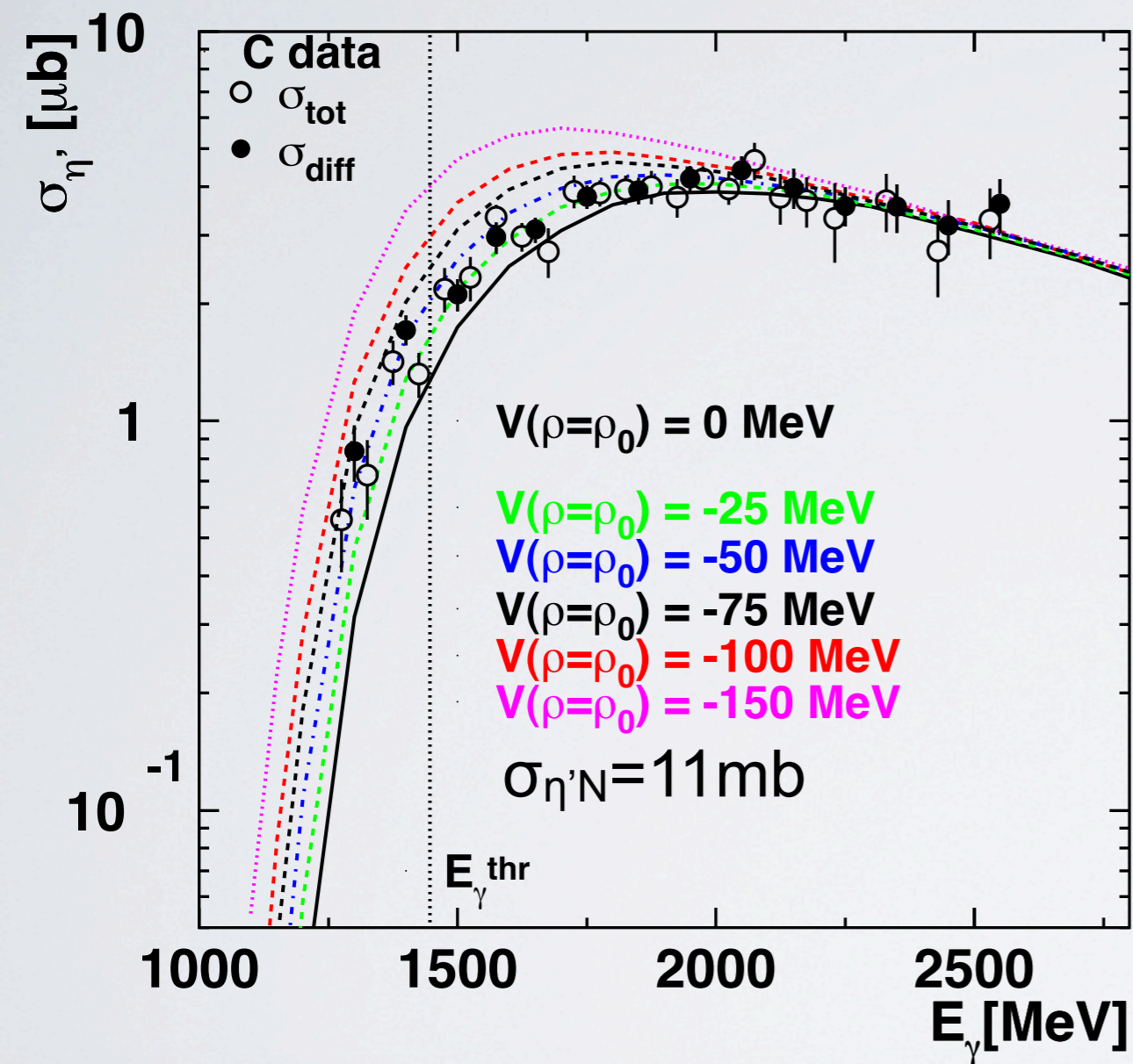
significance test



# estimation of the real part of the $\eta'$ -nucleus potential from the $\eta'$ excitation function

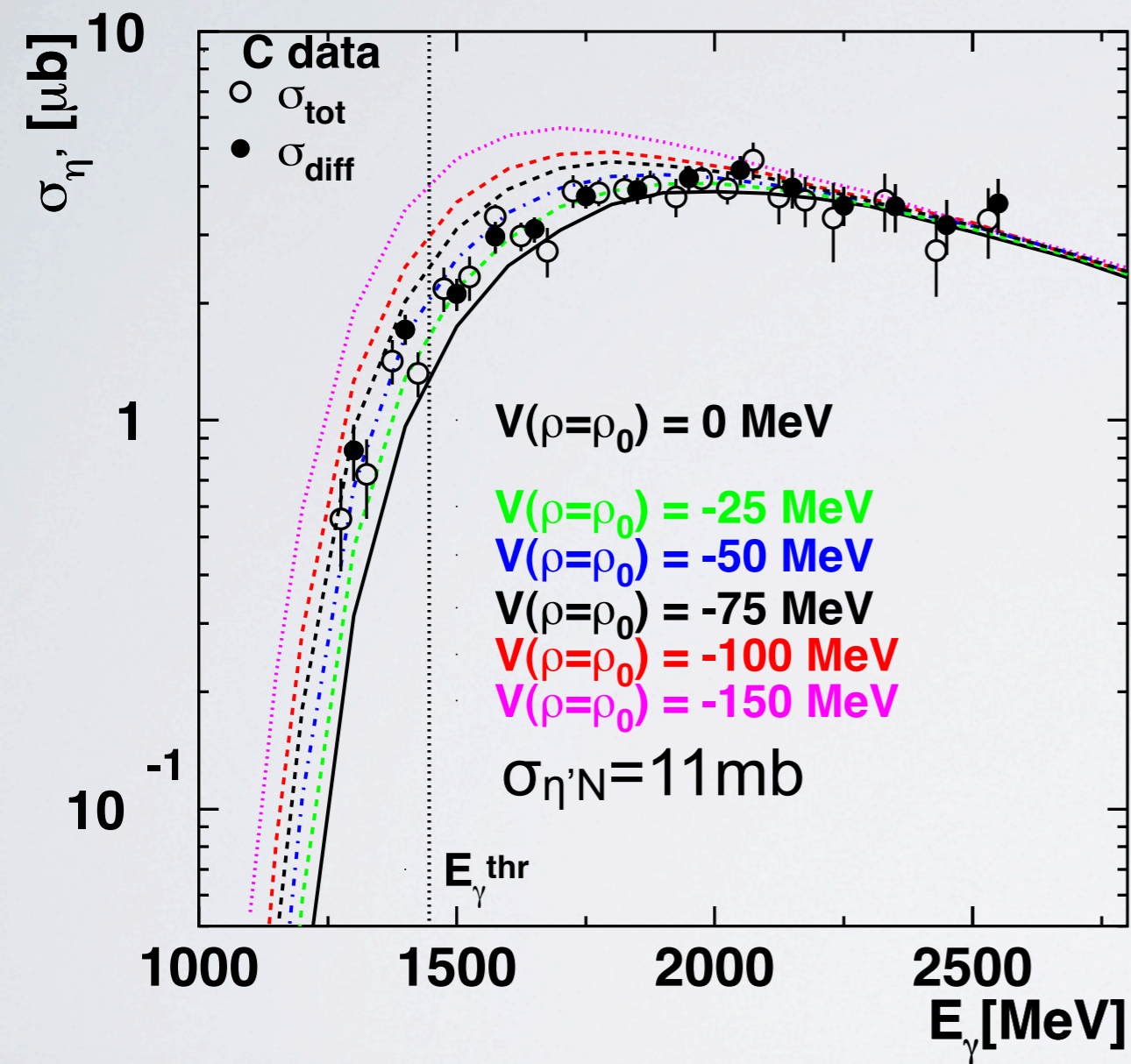
excitation function

significance test

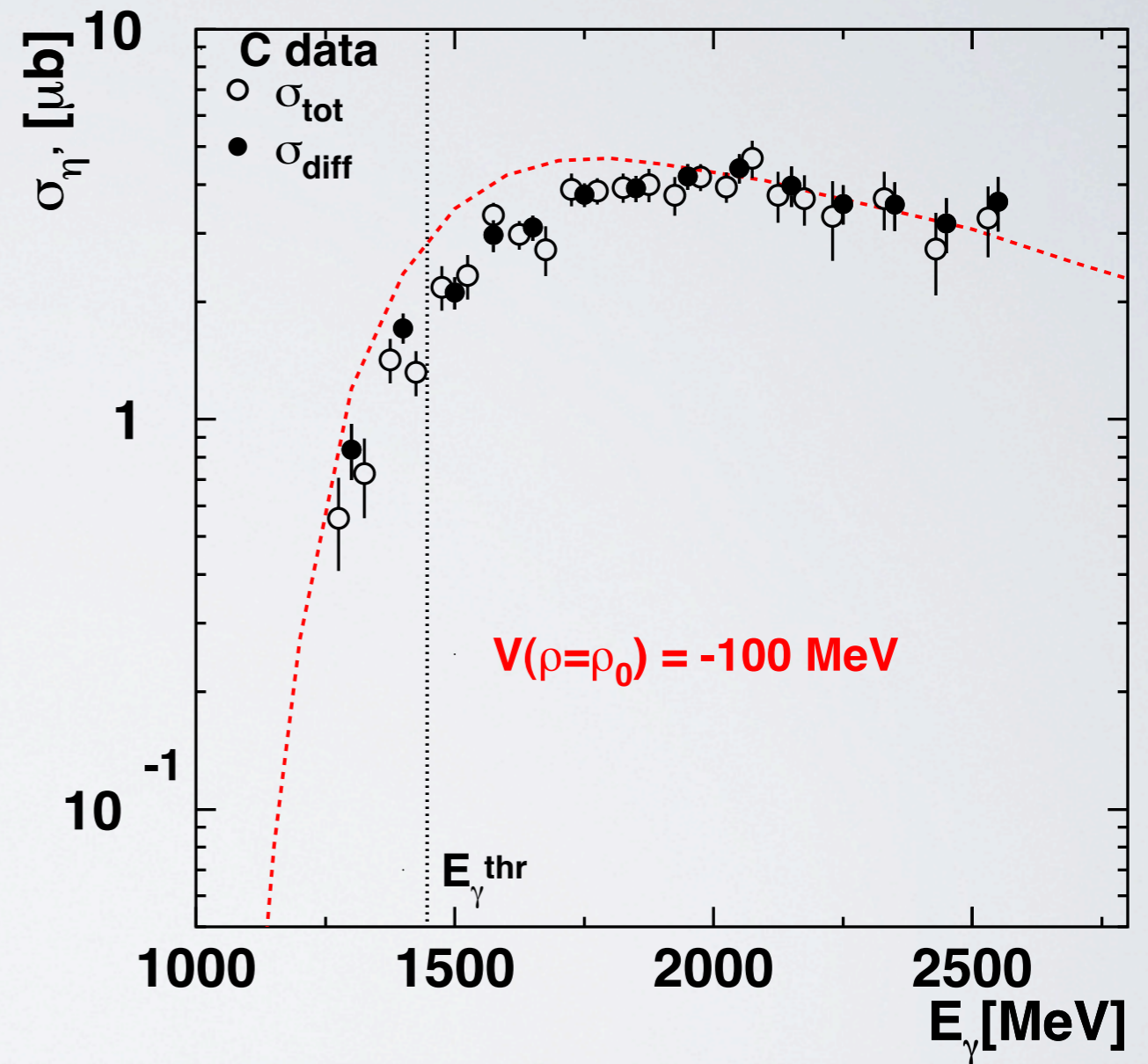


# estimation of the real part of the $\eta'$ -nucleus potential from the $\eta'$ excitation function

excitation function



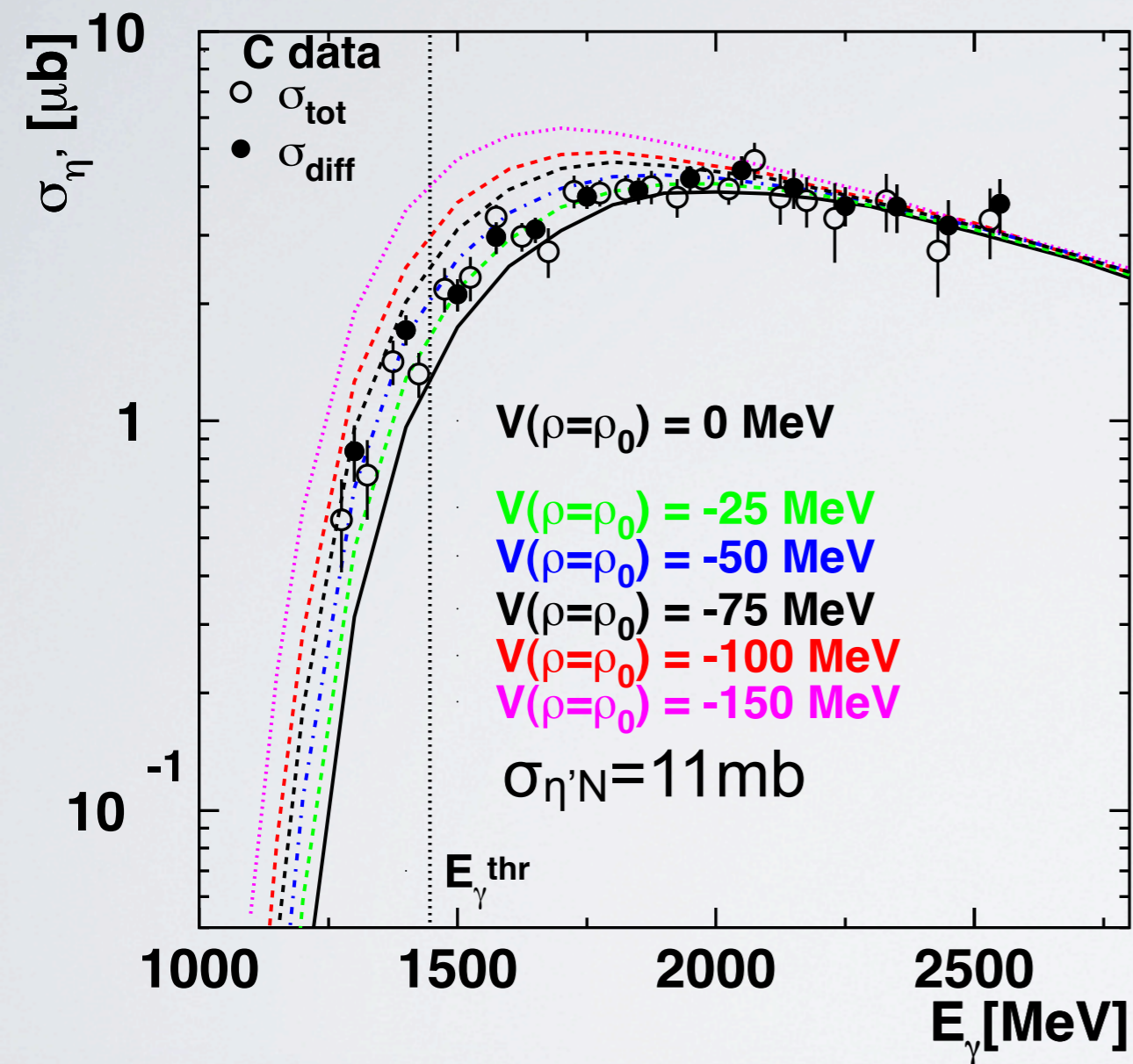
significance test



# estimation of the real part of the $\eta'$ -nucleus potential from the $\eta'$ excitation function

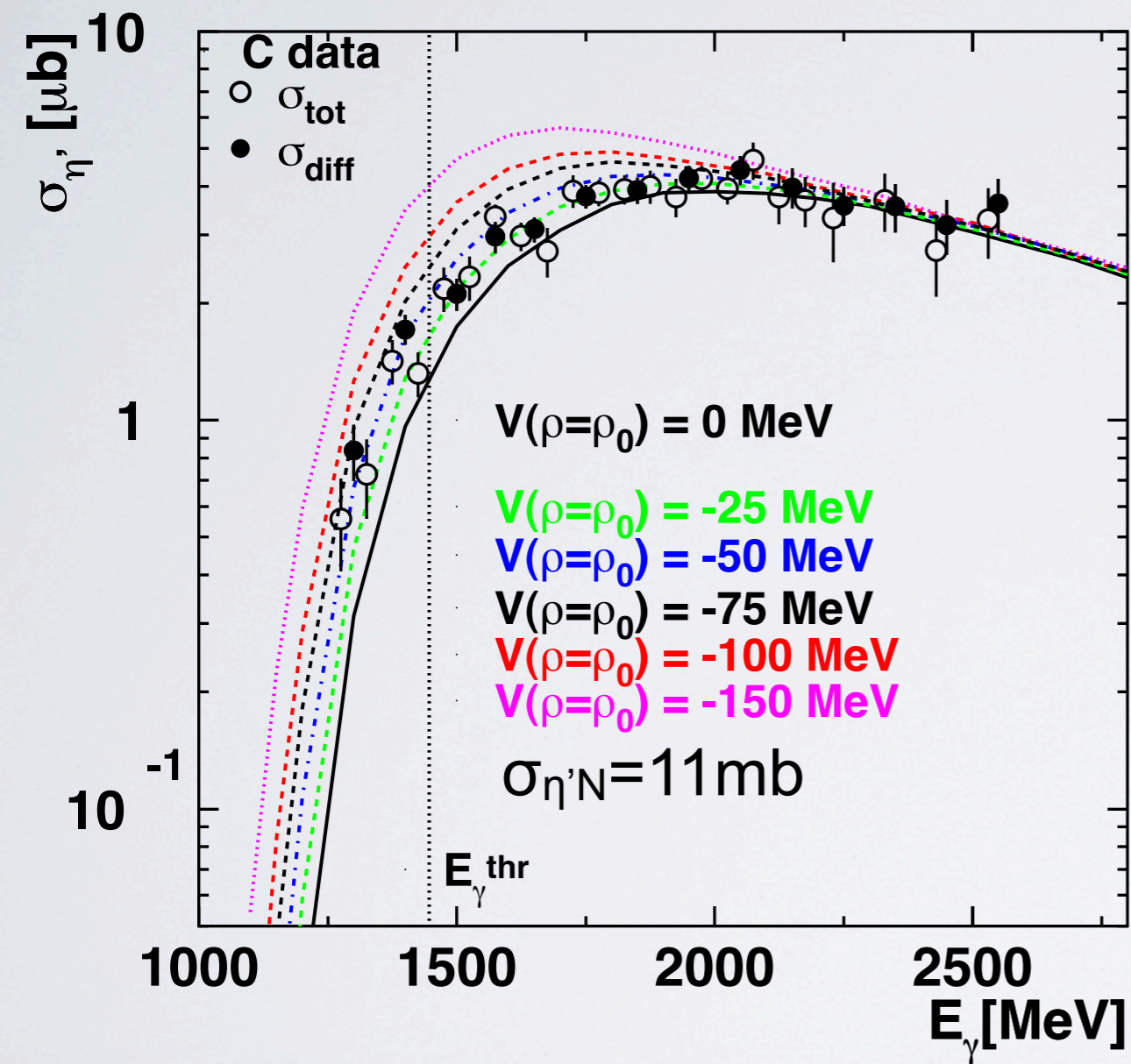
excitation function

significance test

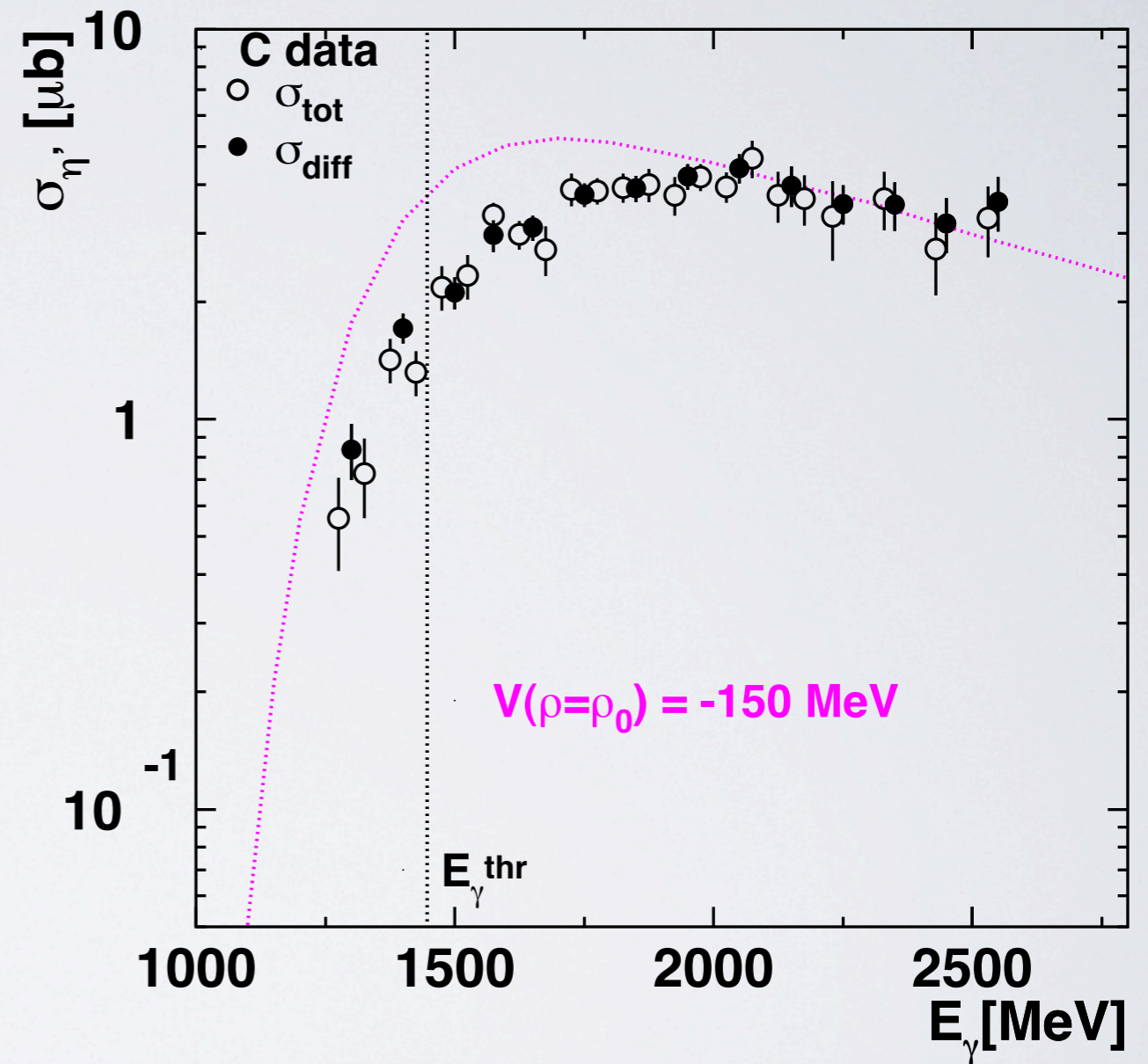


# estimation of the real part of the $\eta'$ -nucleus potential from the $\eta'$ excitation function

excitation function



significance test

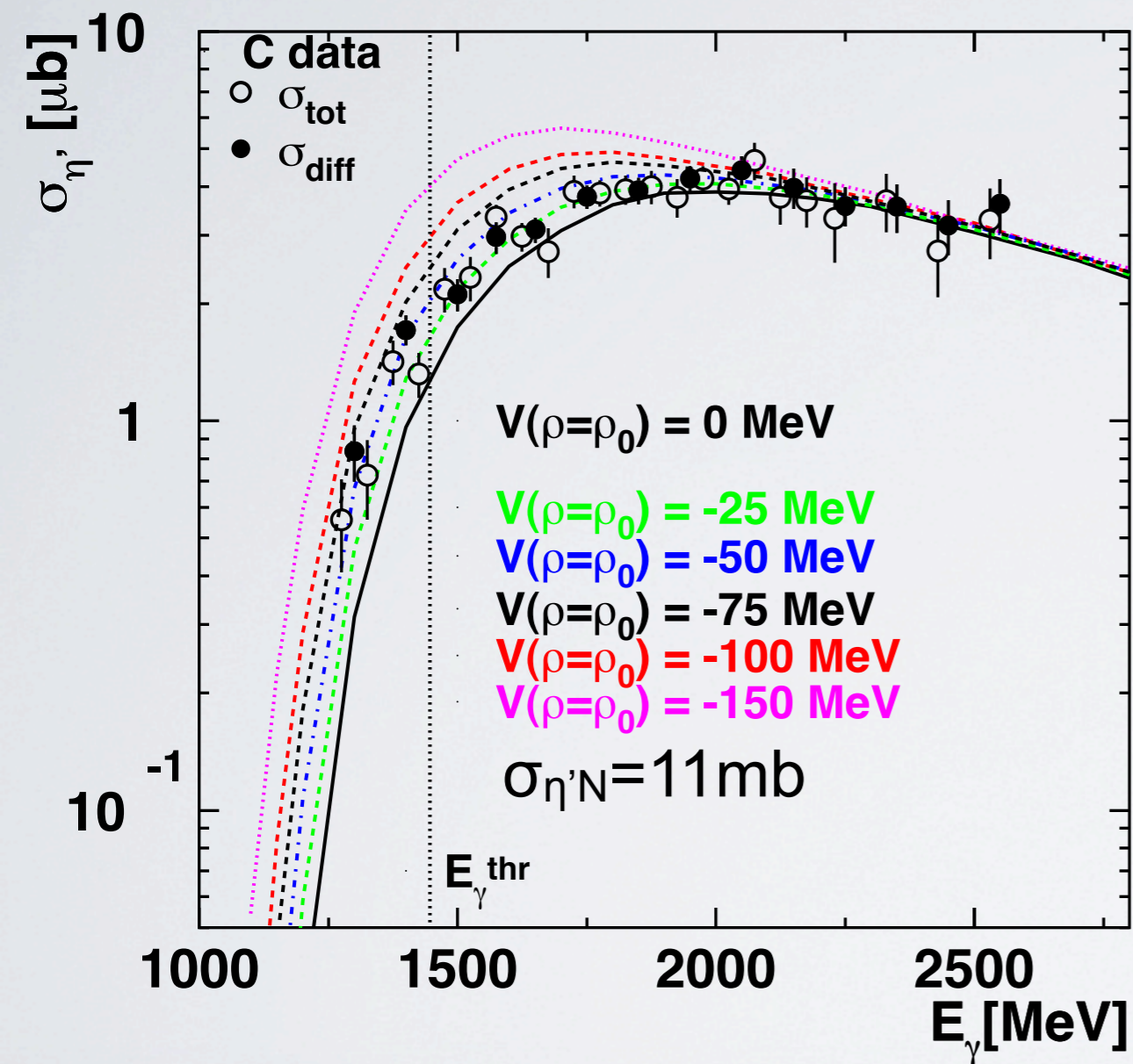




# estimation of the real part of the $\eta'$ -nucleus potential from the $\eta'$ excitation function

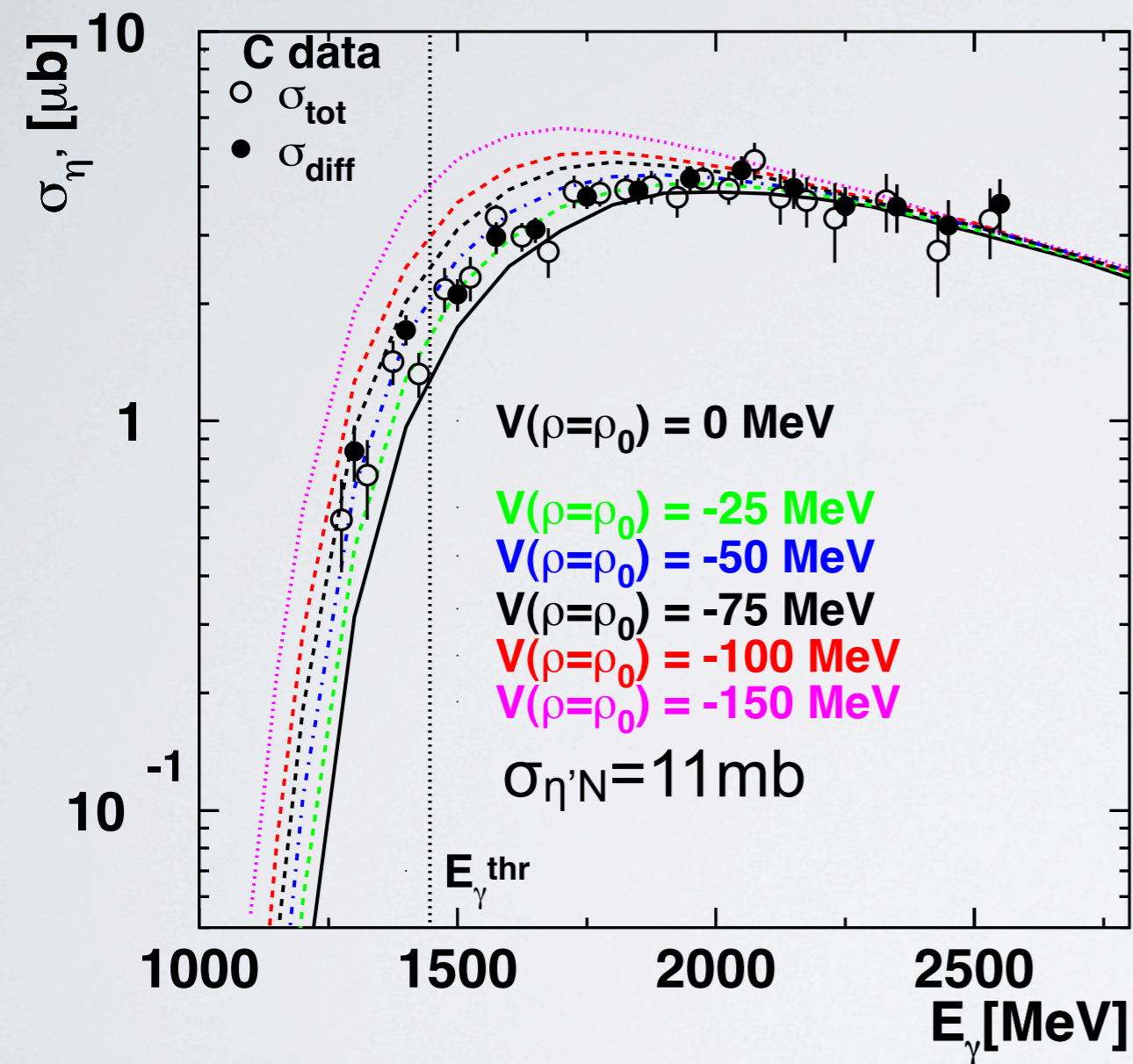
excitation function

significance test

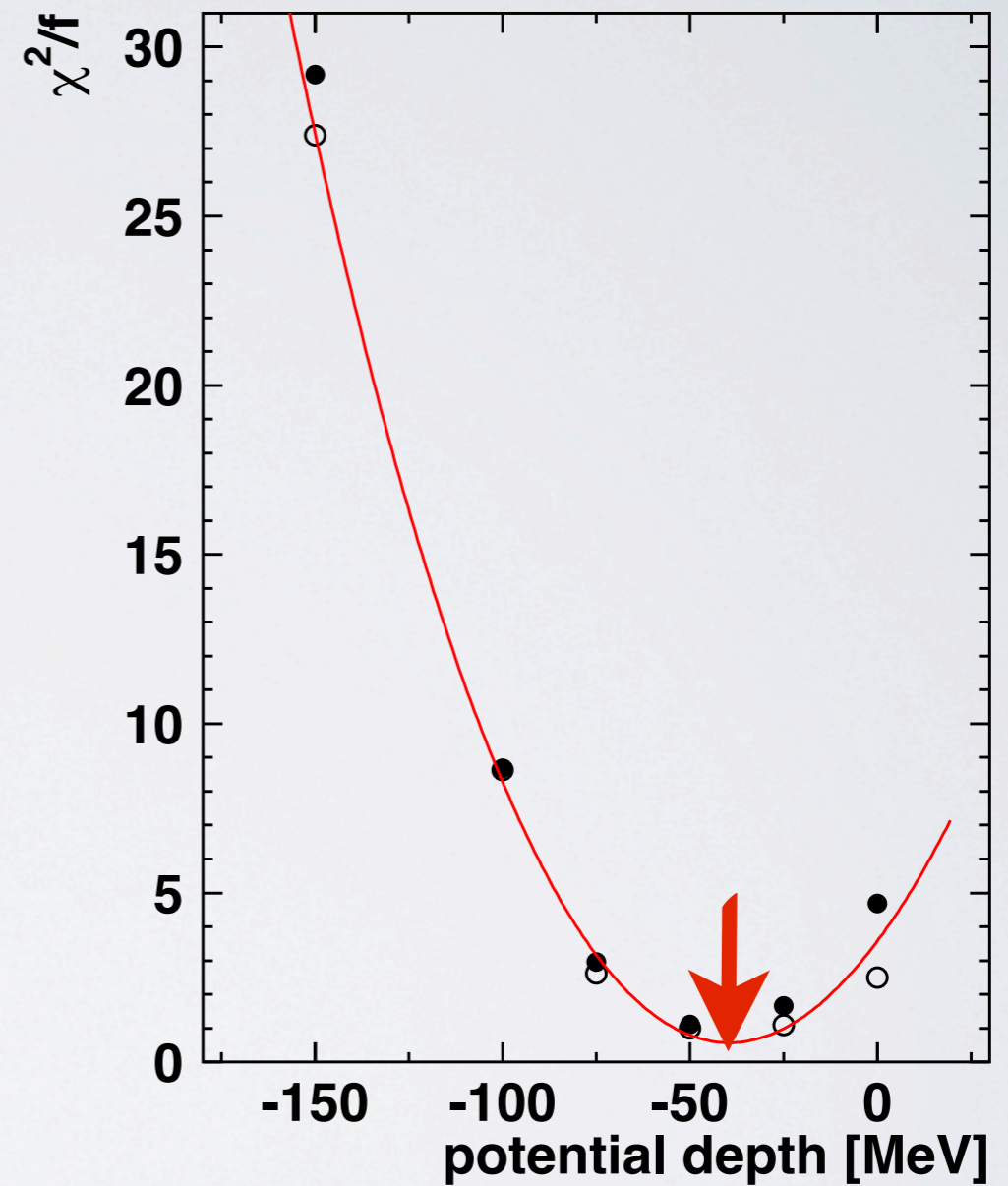


# estimation of the real part of the $\eta'$ -nucleus potential from the $\eta'$ excitation function

excitation function



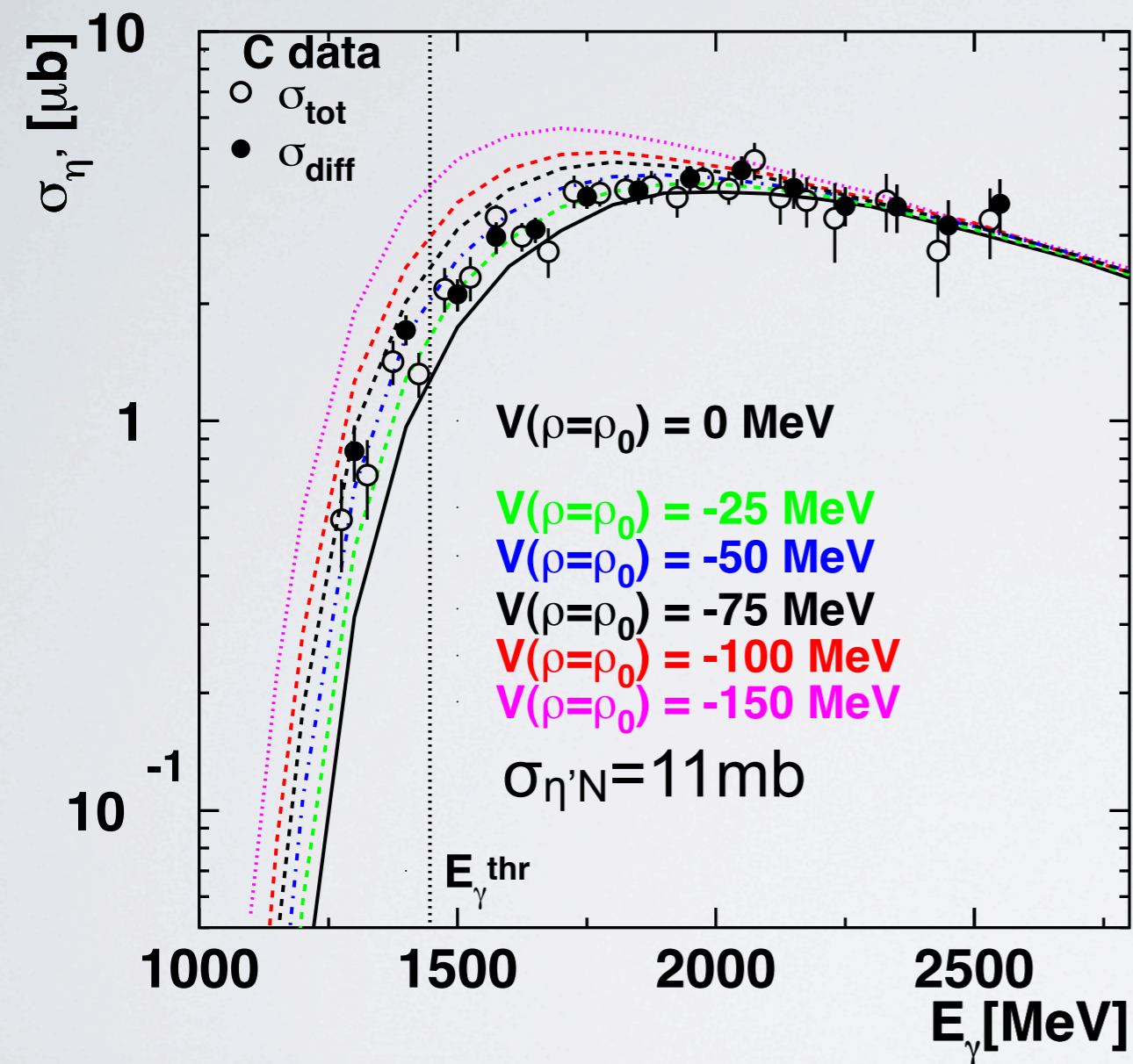
significance test



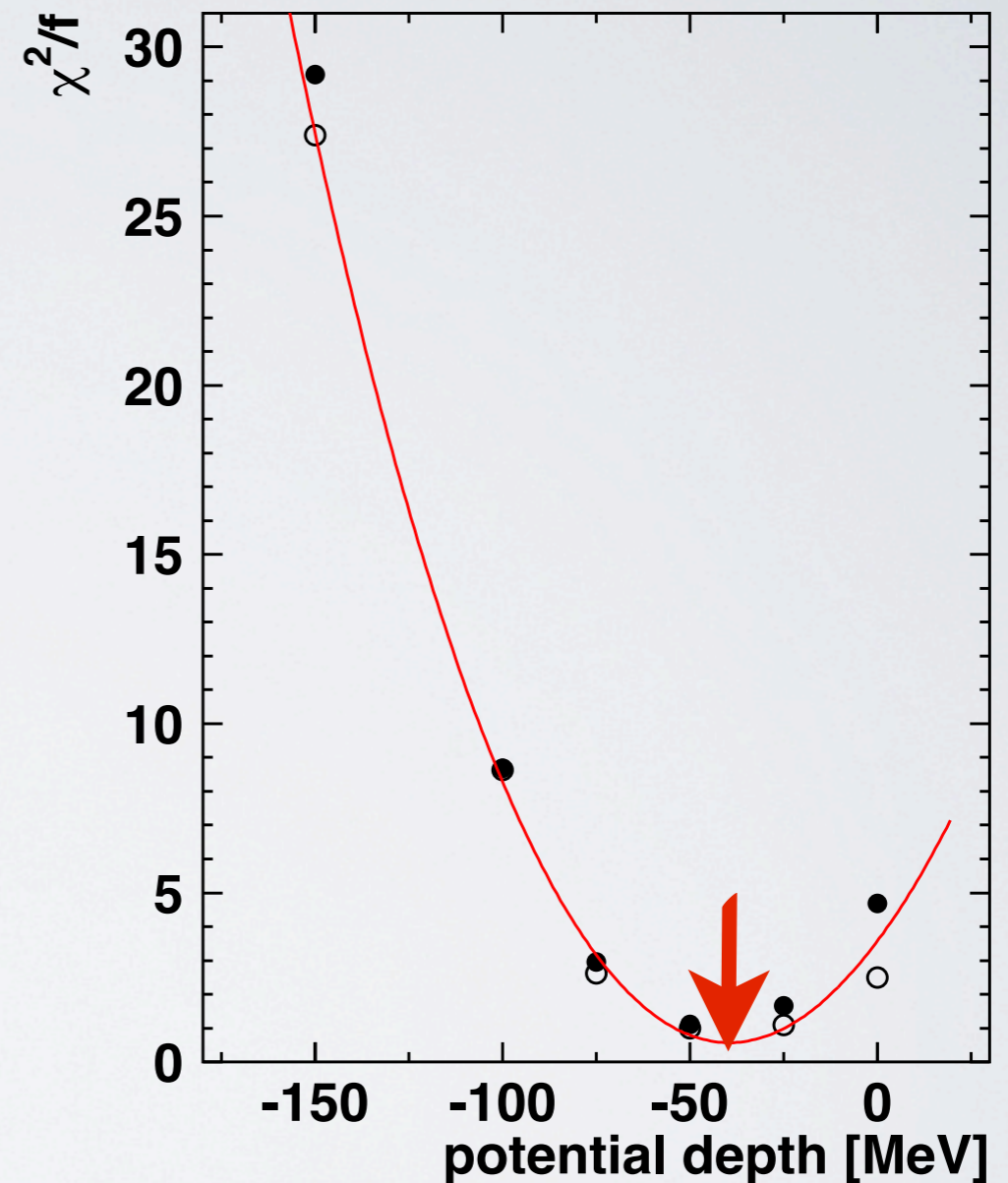
$\chi^2$ -fit of the data with the calculated excitation functions for the 6 scenarios

# estimation of the real part of the $\eta'$ -nucleus potential from the $\eta'$ excitation function

excitation function



significance test



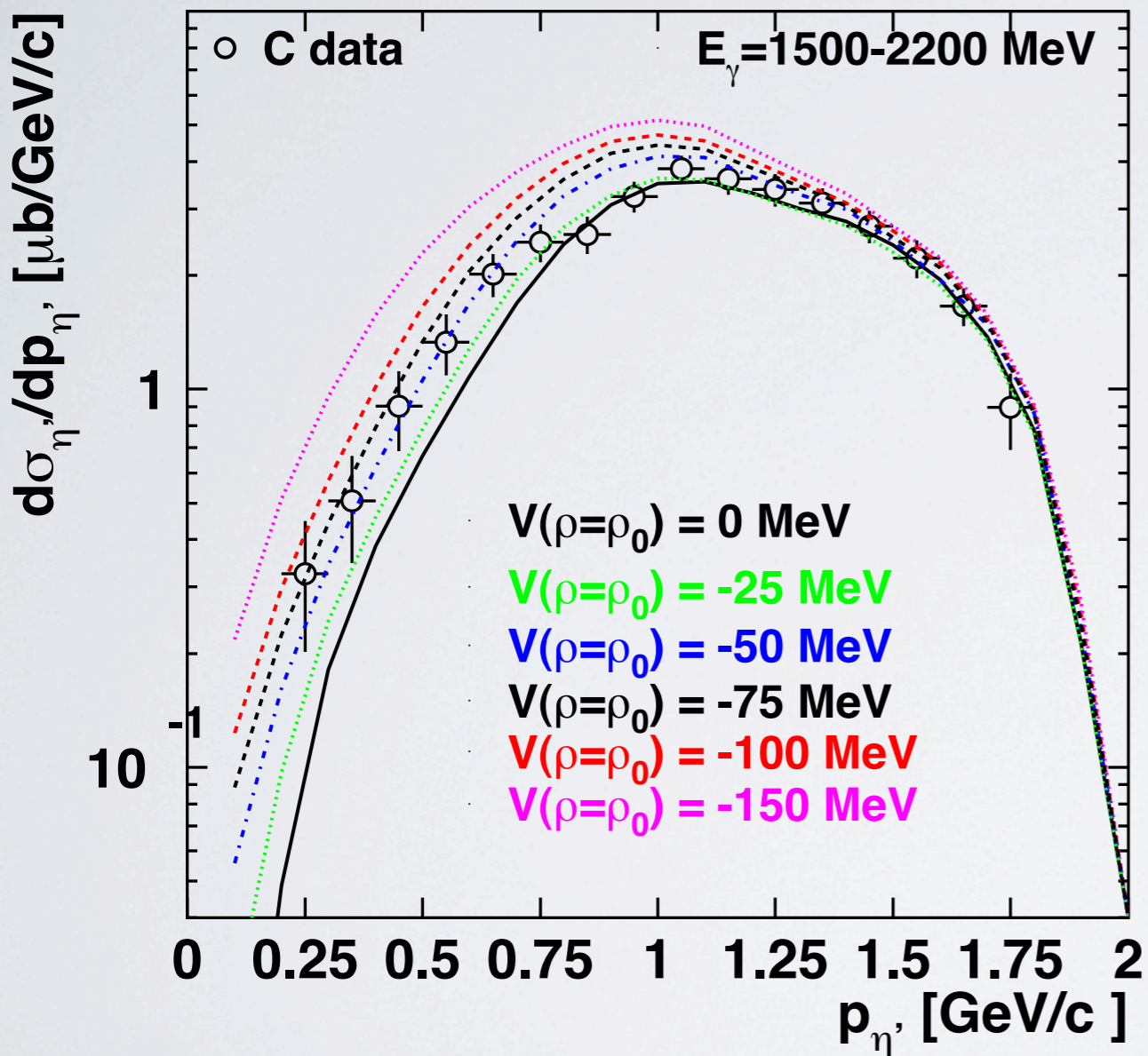
$\chi^2$ -fit of the data with the calculated excitation functions for the 6 scenarios

$$V(\rho=\rho_0) = -40 \pm 6 \text{ MeV}$$

# $\eta'$ momentum distribution off C

comparison of CBELSA/TAPS data with calculations by  
E. Paryev, J. Phys. G: Nucl. Part. Phys. 40 (2013) 025201 and priv. communication

momentum distribution

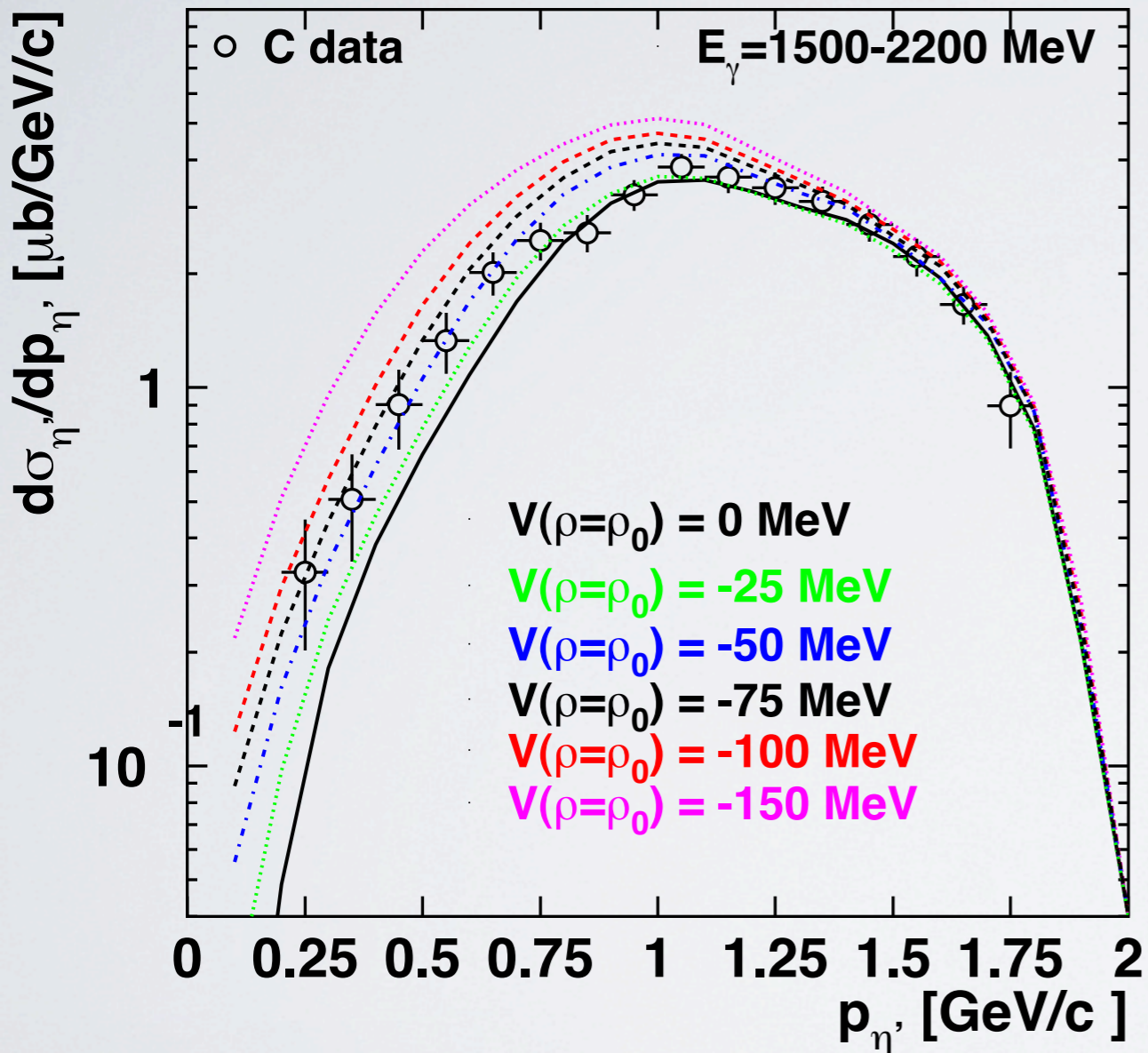


calculation normalized to data in  $p = 1.5-1.8$  GeV/c,  
downscaled by 1.2

# $\eta'$ momentum distribution off C

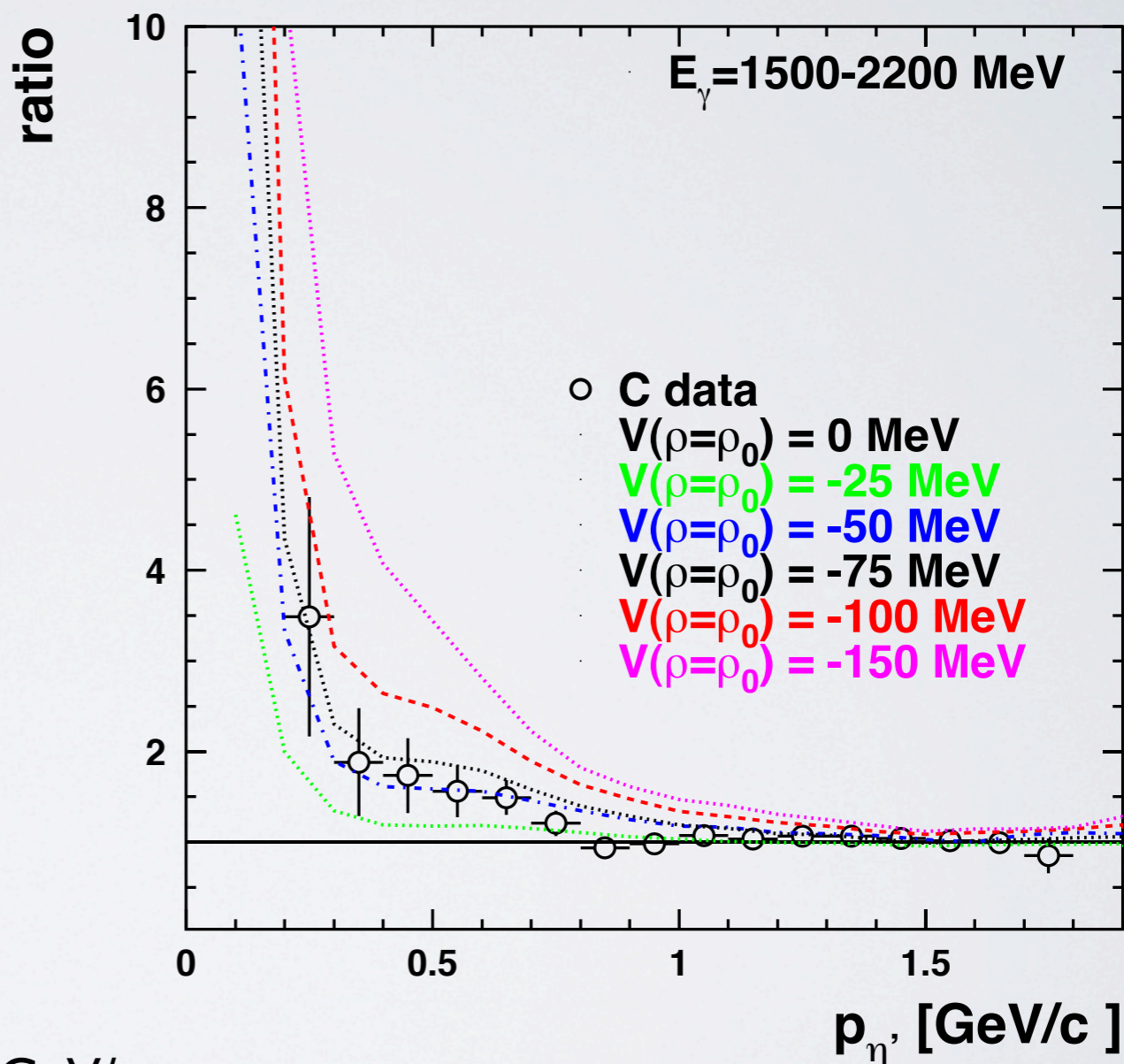
comparison of CBELSA/TAPS data with calculations by  
E. Paryev, J. Phys. G: Nucl. Part. Phys. 40 (2013) 025201 and priv. communication

momentum distribution

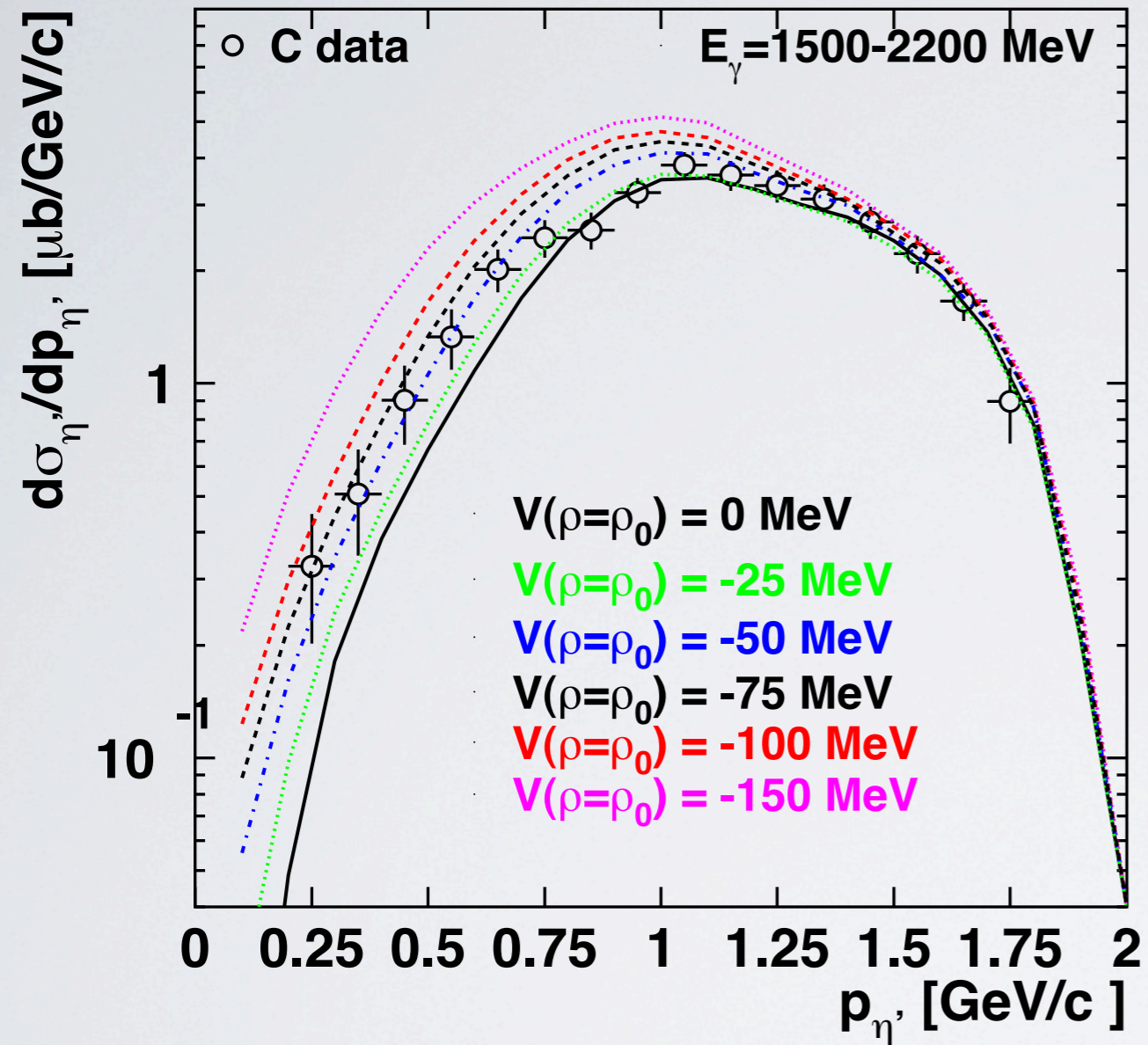


calculation normalized to data in  $p = 1.5-1.8$  GeV/c,  
downscaled by 1.2

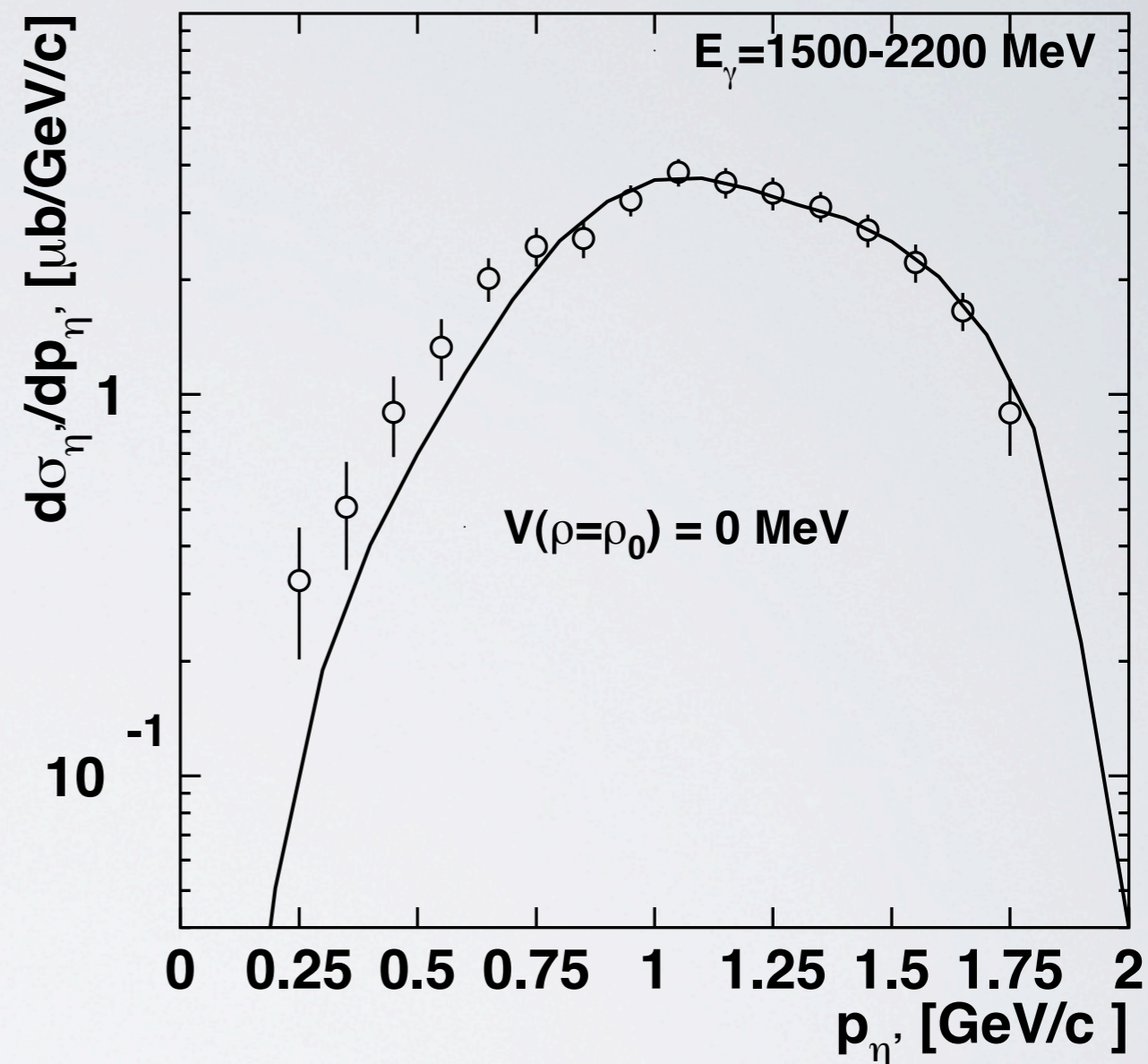
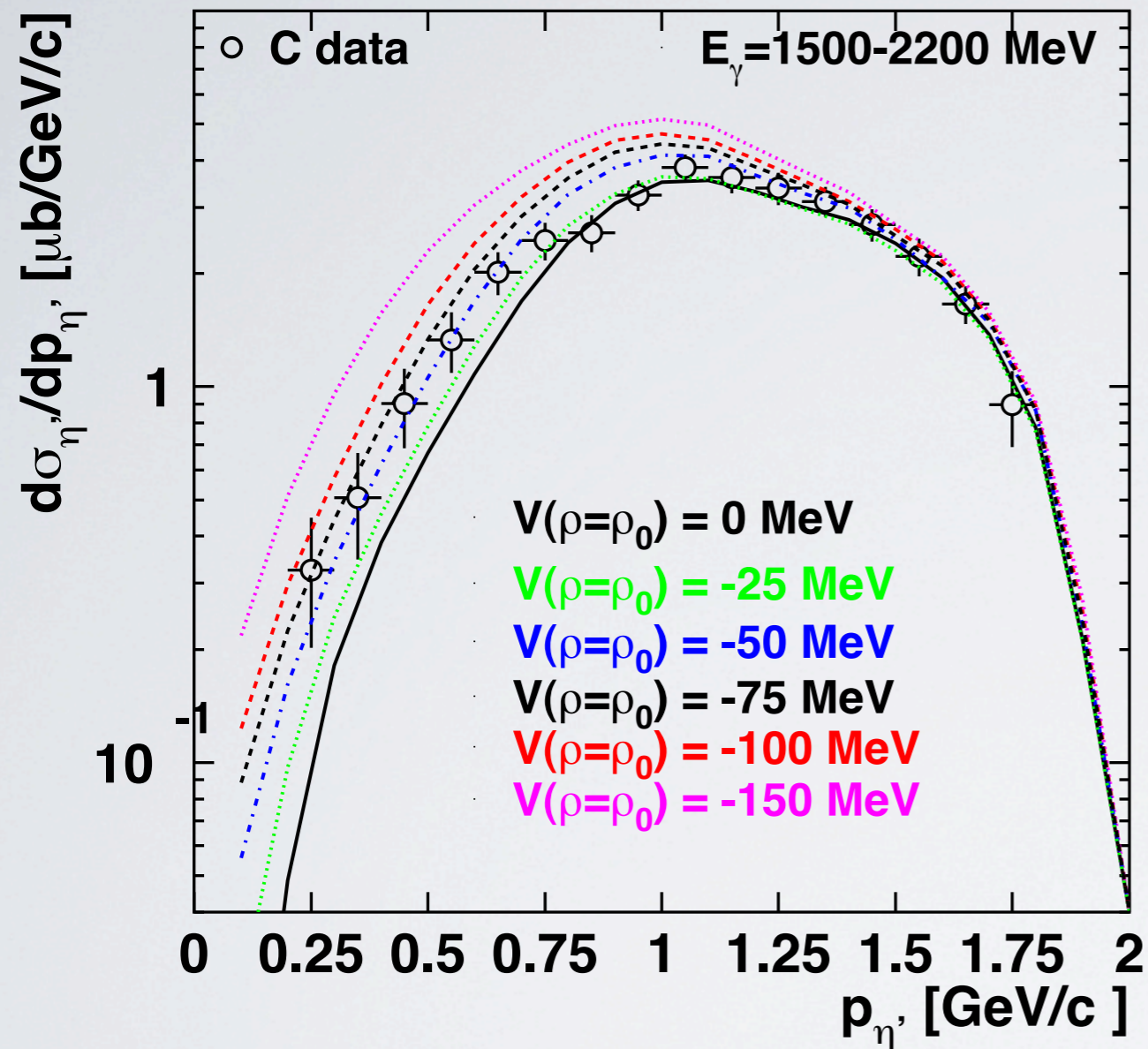
exp. data and the 5 scenarios divided by the  
calculation for scenario  $V(\rho=\rho_0)=0$  MeV



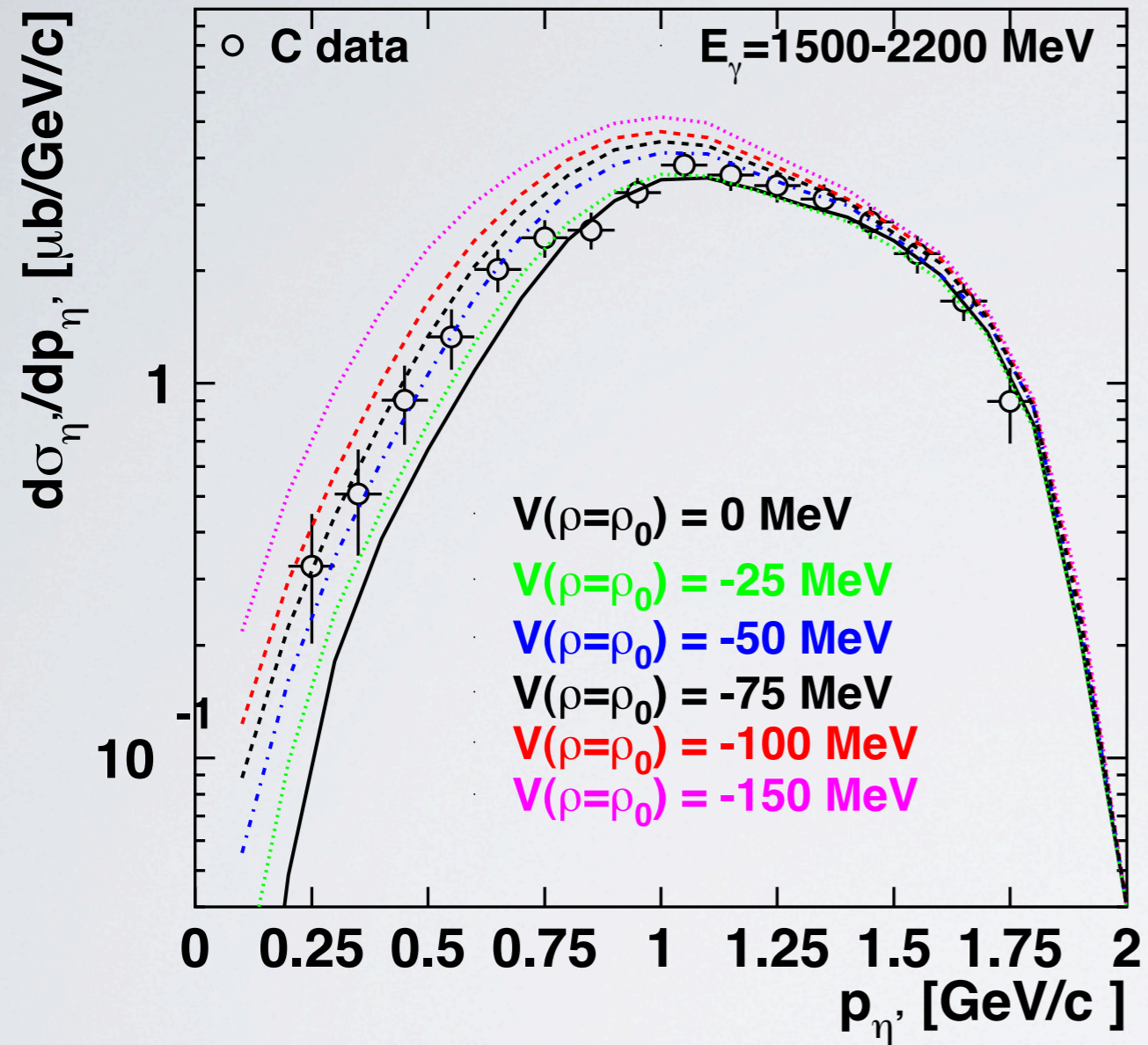
# estimation of the of $\eta'$ -nucleus potential depth from the $\eta'$ momentum distribution



# estimation of the of $\eta'$ -nucleus potential depth from the $\eta'$ momentum distribution

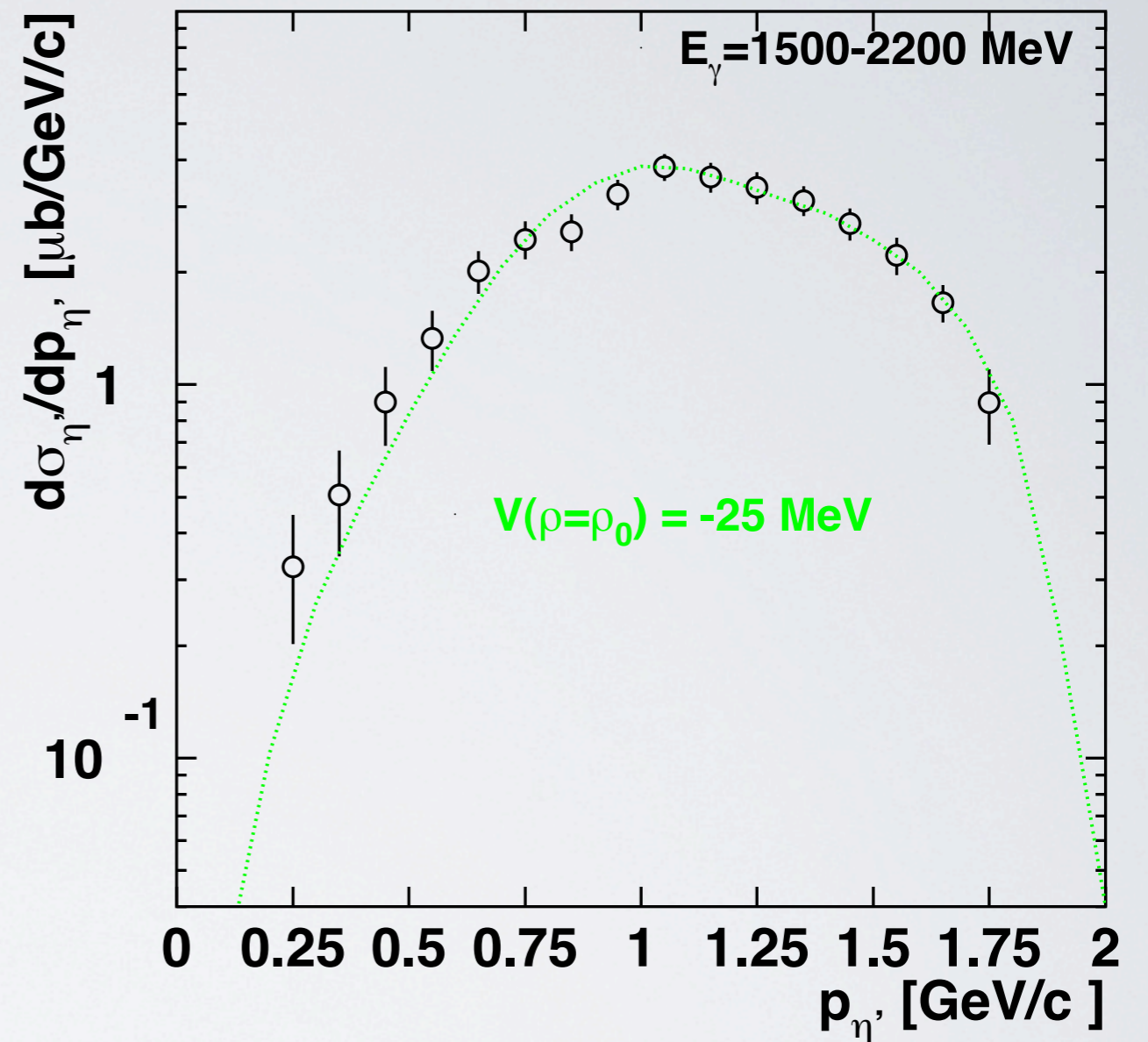
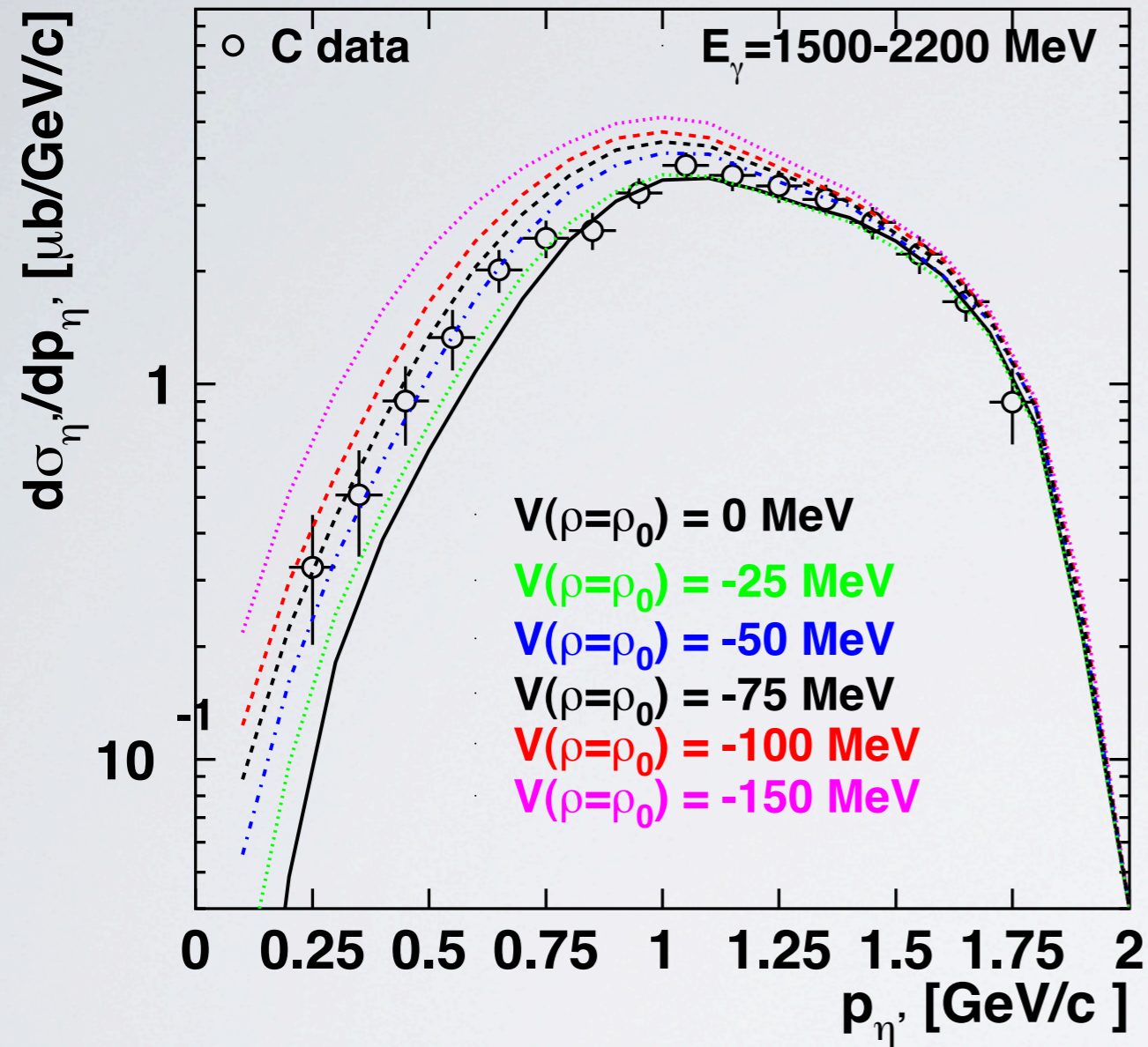


# estimation of the of $\eta'$ -nucleus potential depth from the $\eta'$ momentum distribution

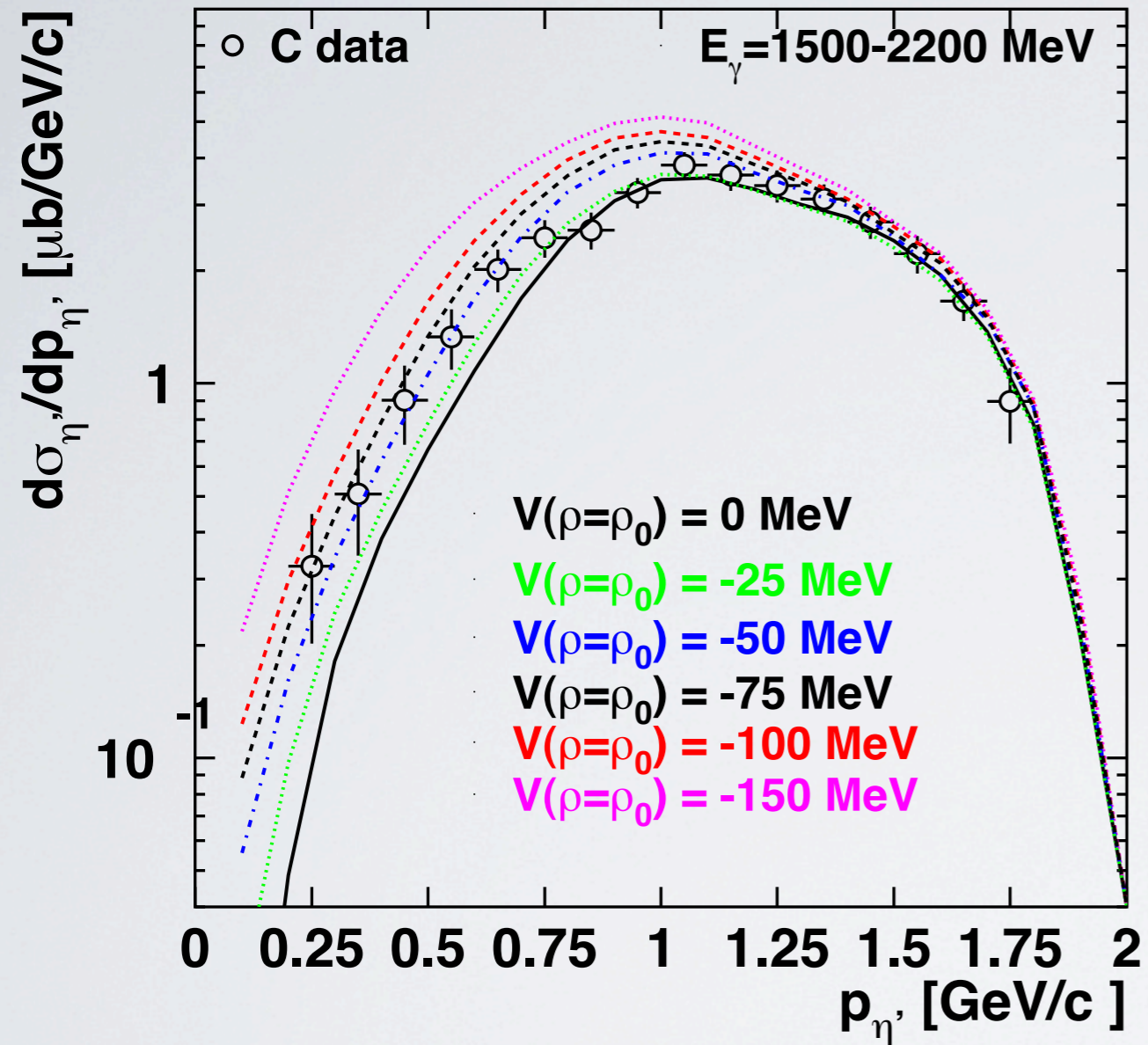




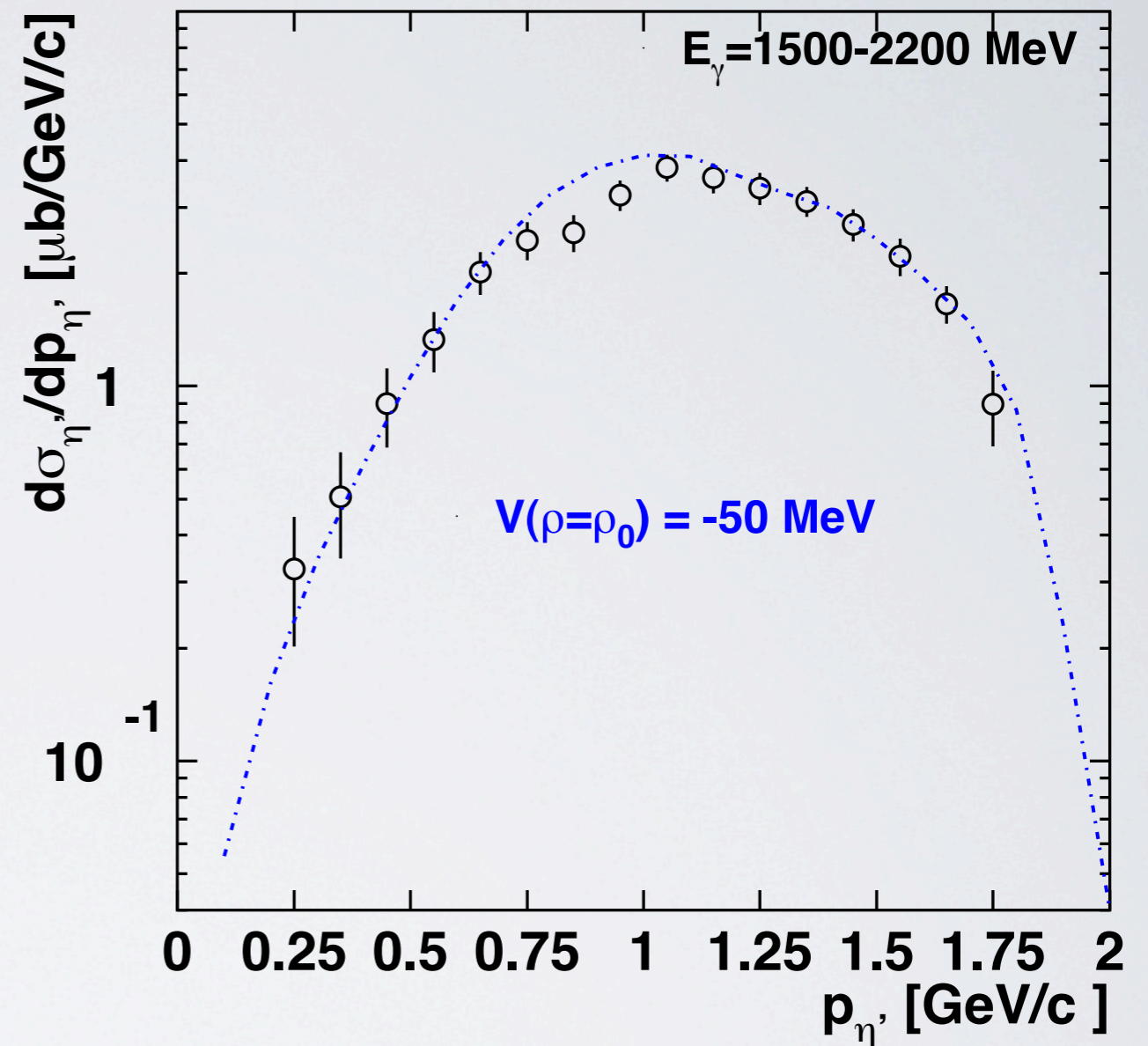
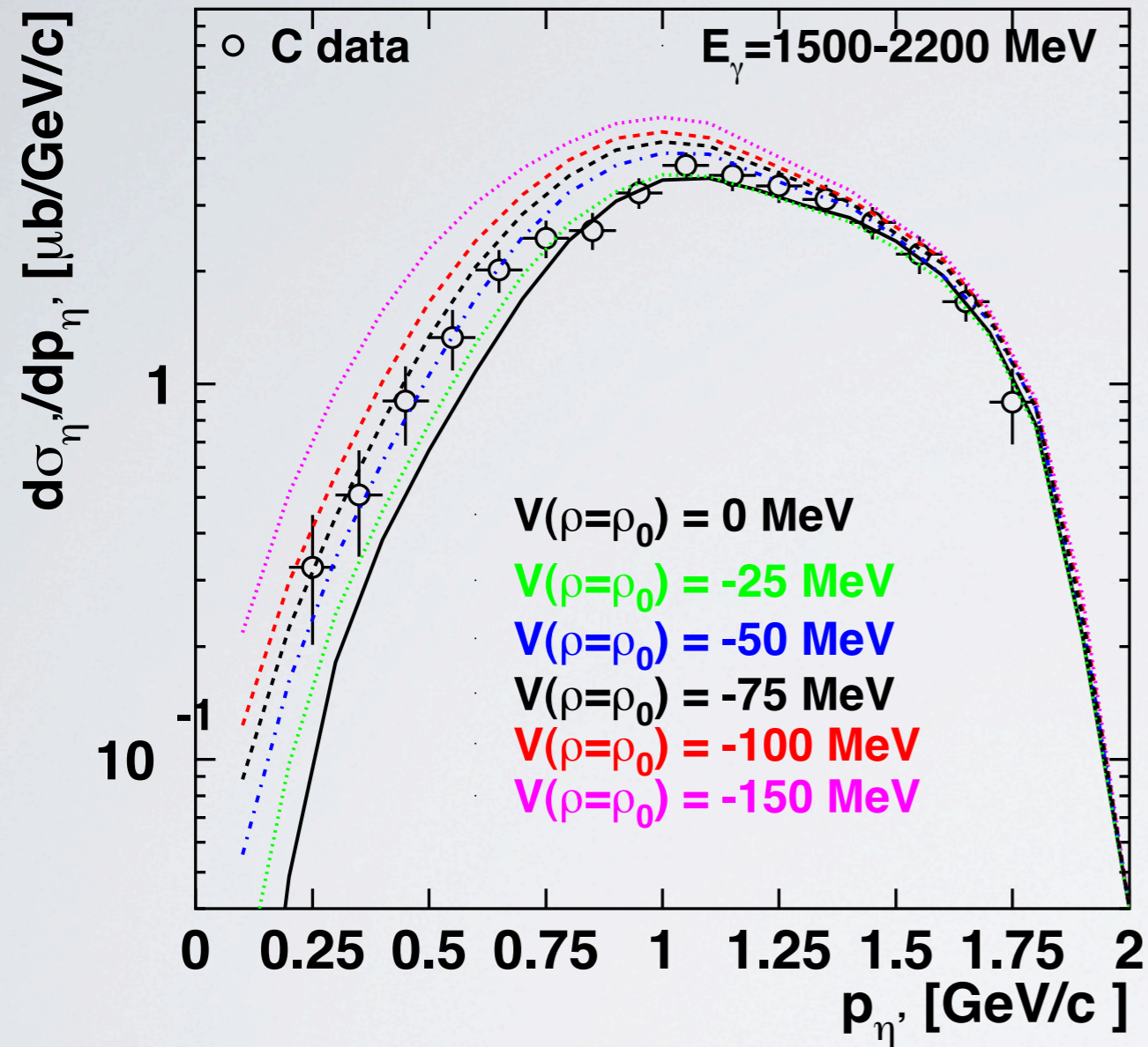
# estimation of the of $\eta'$ -nucleus potential depth from the $\eta'$ momentum distribution



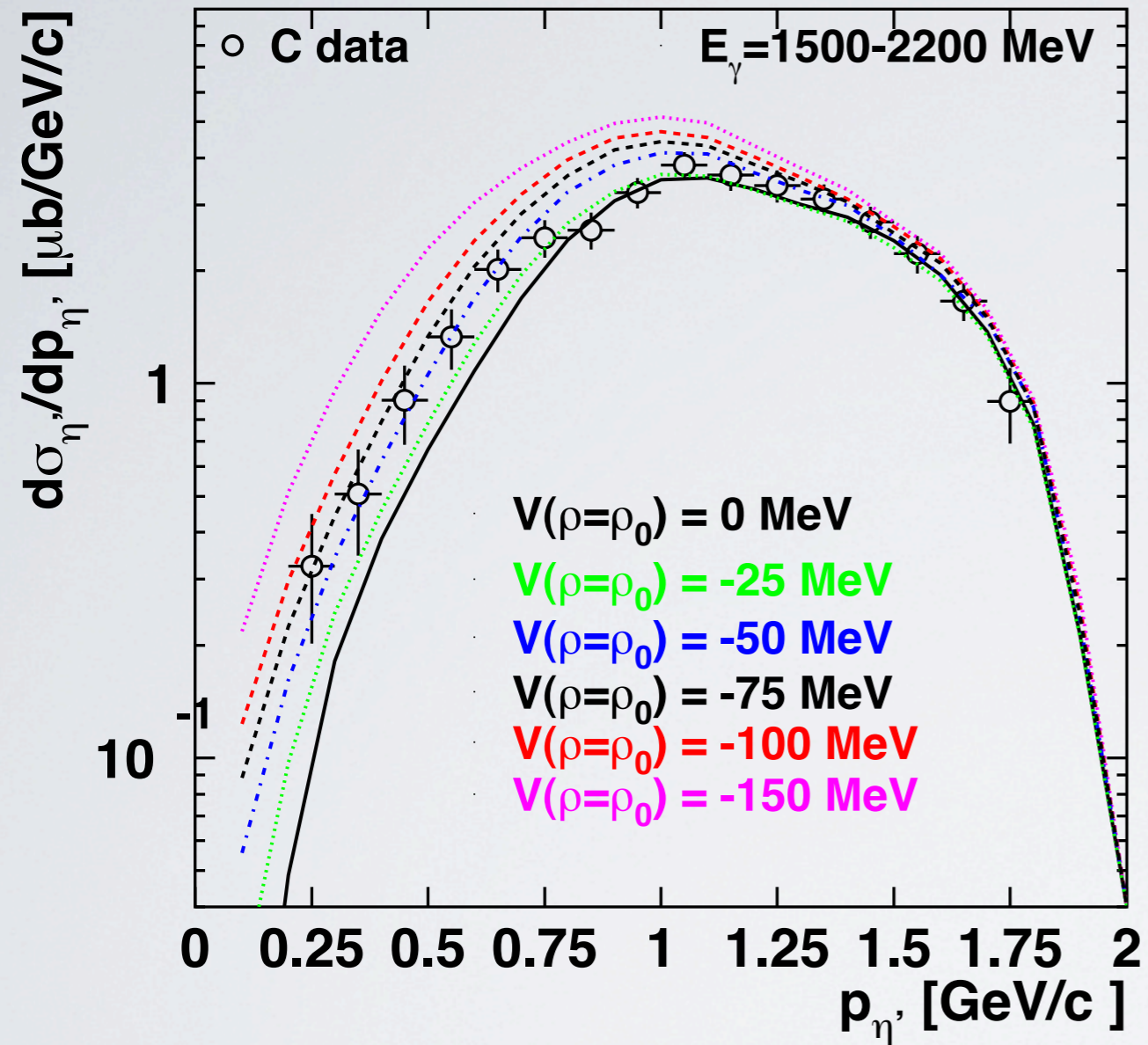
# estimation of the $\eta'$ -nucleus potential depth from the $\eta'$ momentum distribution



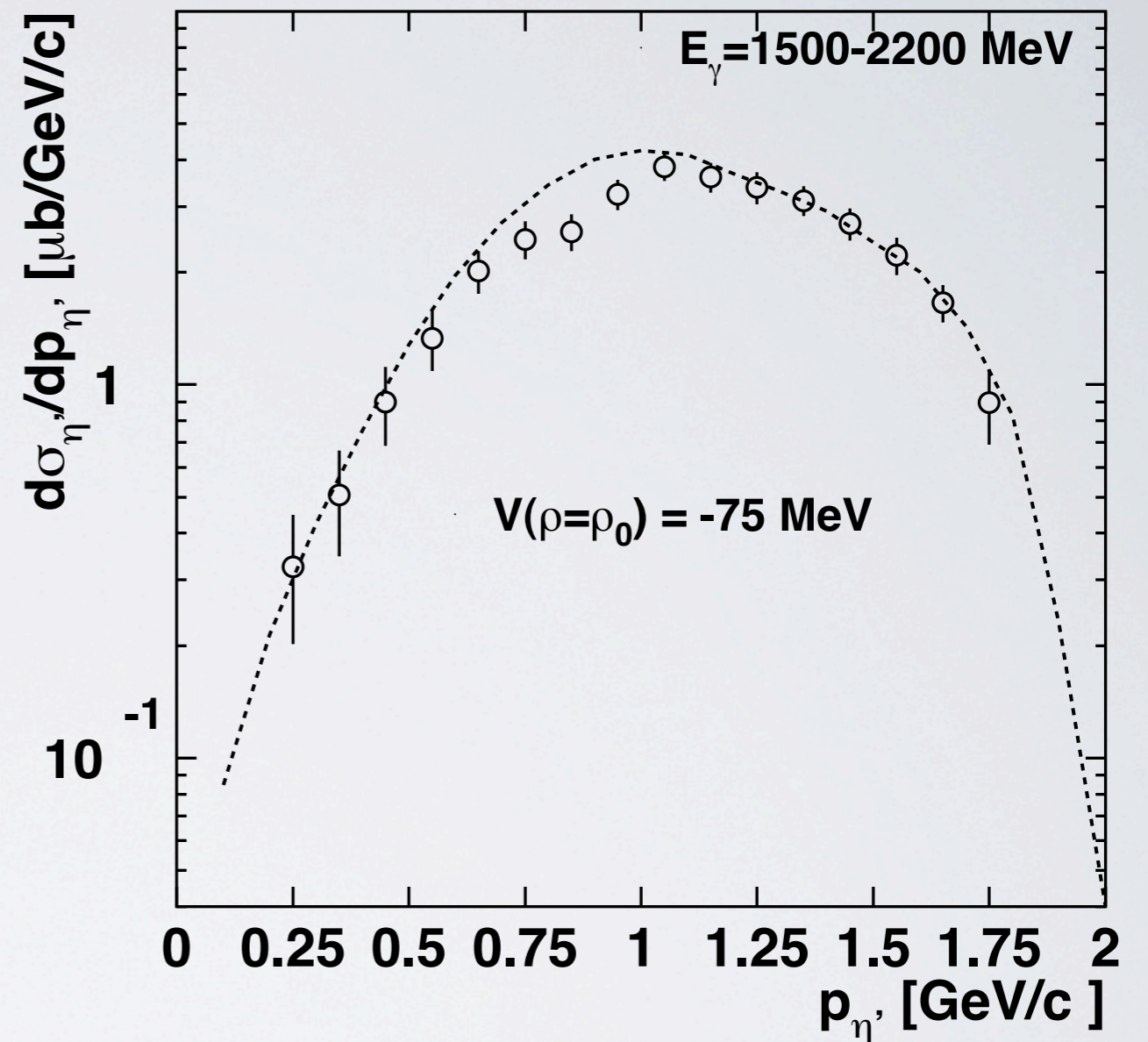
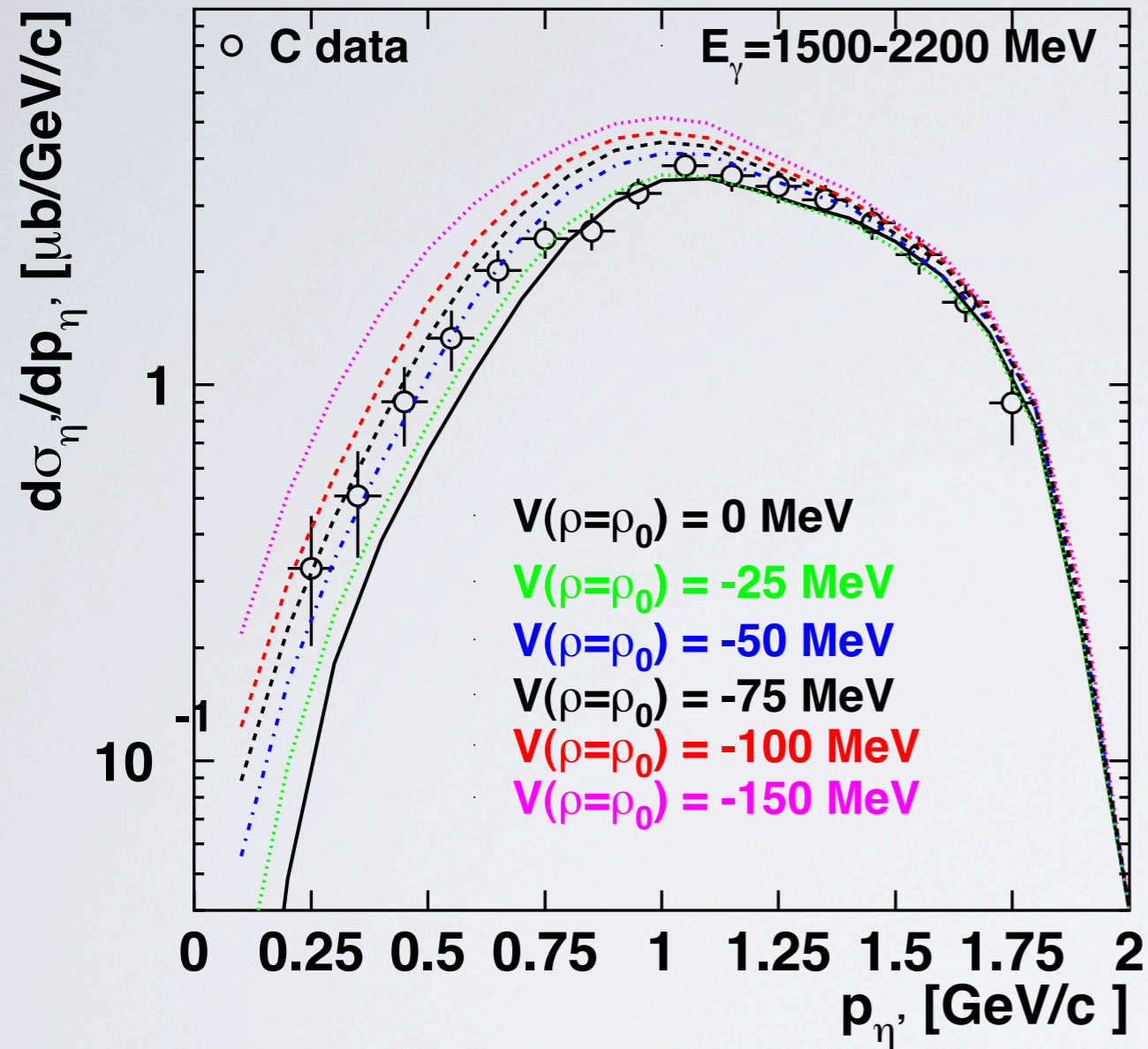
# estimation of the of $\eta'$ -nucleus potential depth from the $\eta'$ momentum distribution



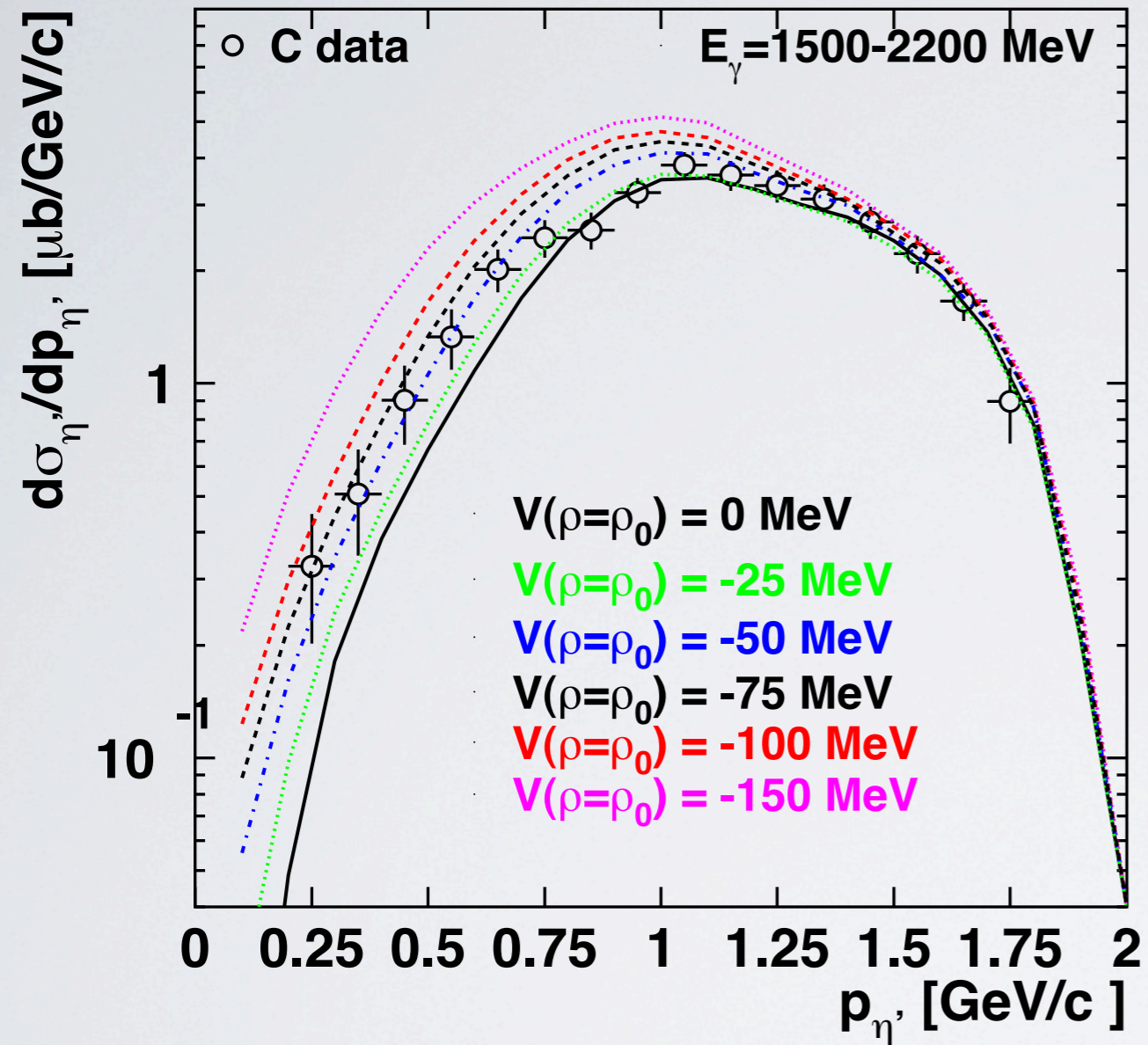
# estimation of the $\eta'$ -nucleus potential depth from the $\eta'$ momentum distribution



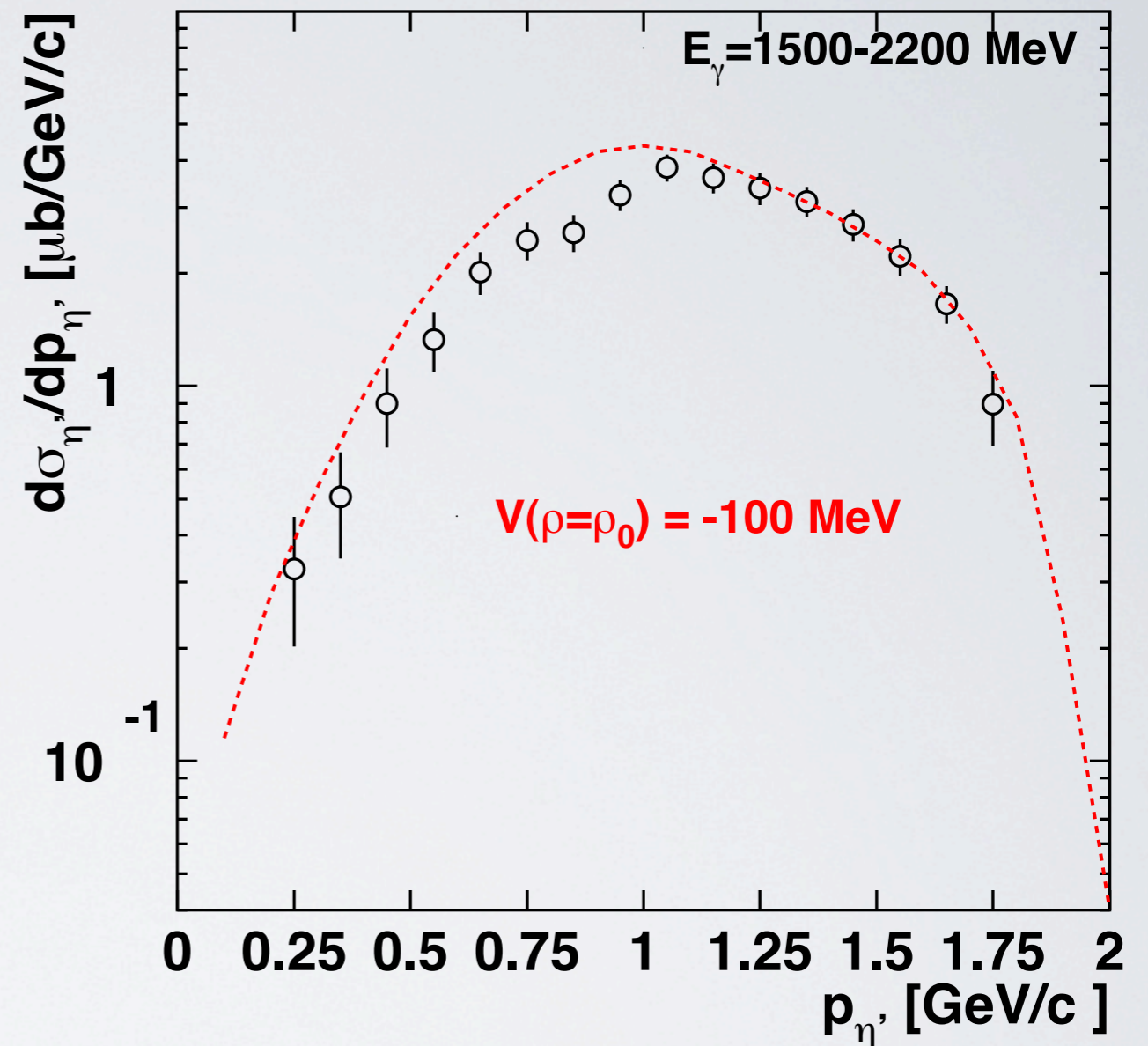
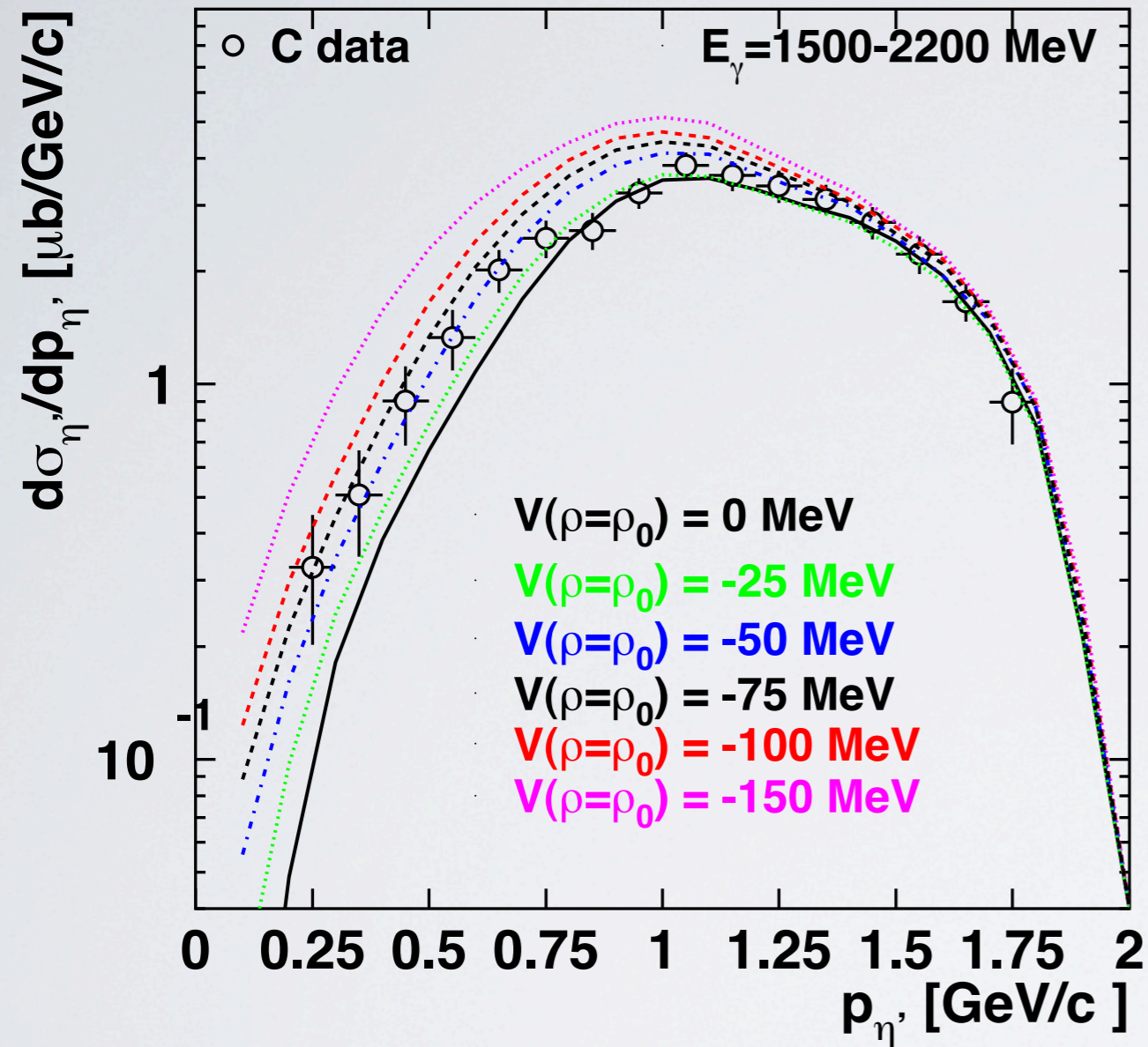
# estimation of the of $\eta'$ -nucleus potential depth from the $\eta'$ momentum distribution



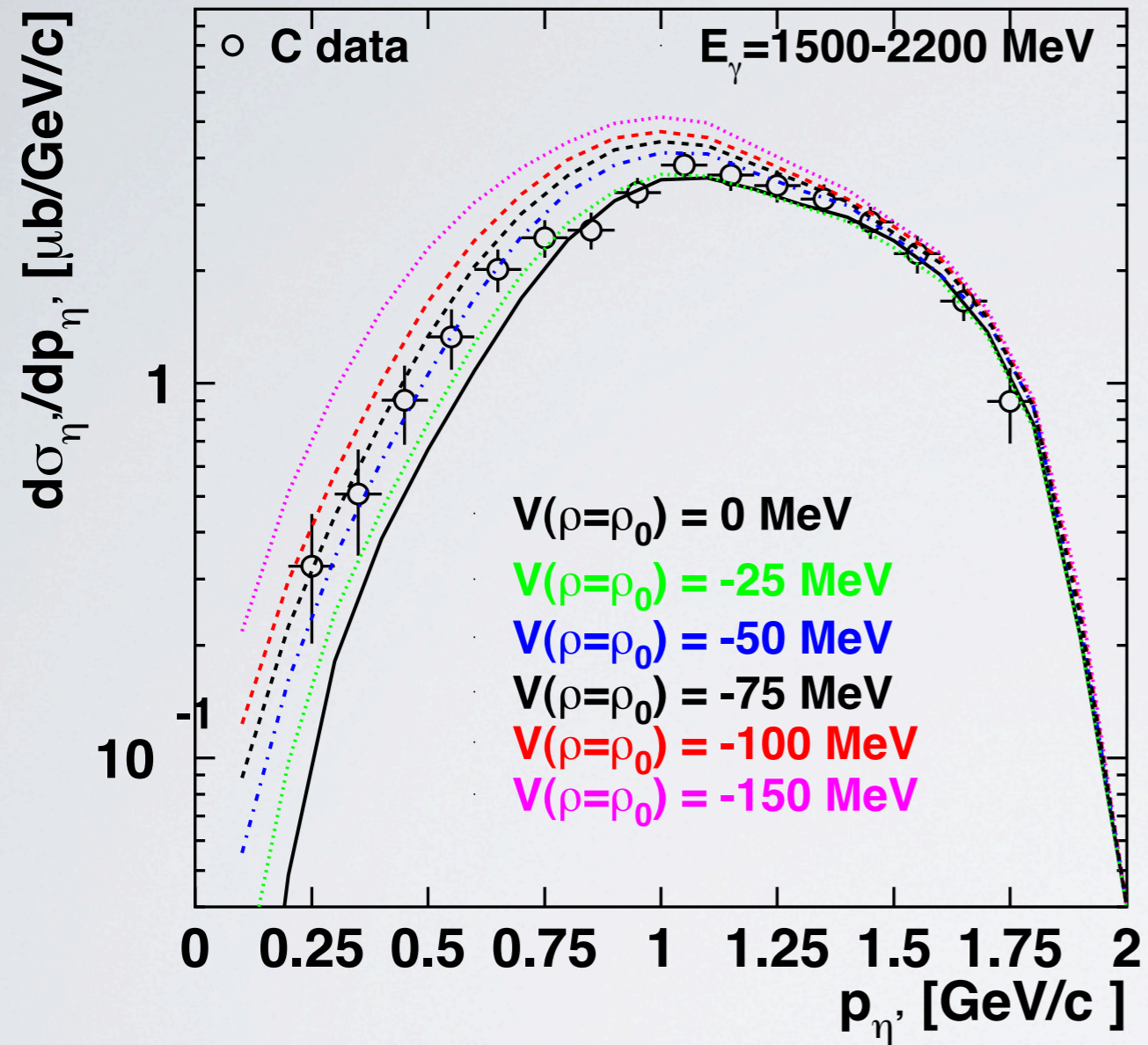
# estimation of the of $\eta'$ -nucleus potential depth from the $\eta'$ momentum distribution



# estimation of the $\eta'$ -nucleus potential depth from the $\eta'$ momentum distribution

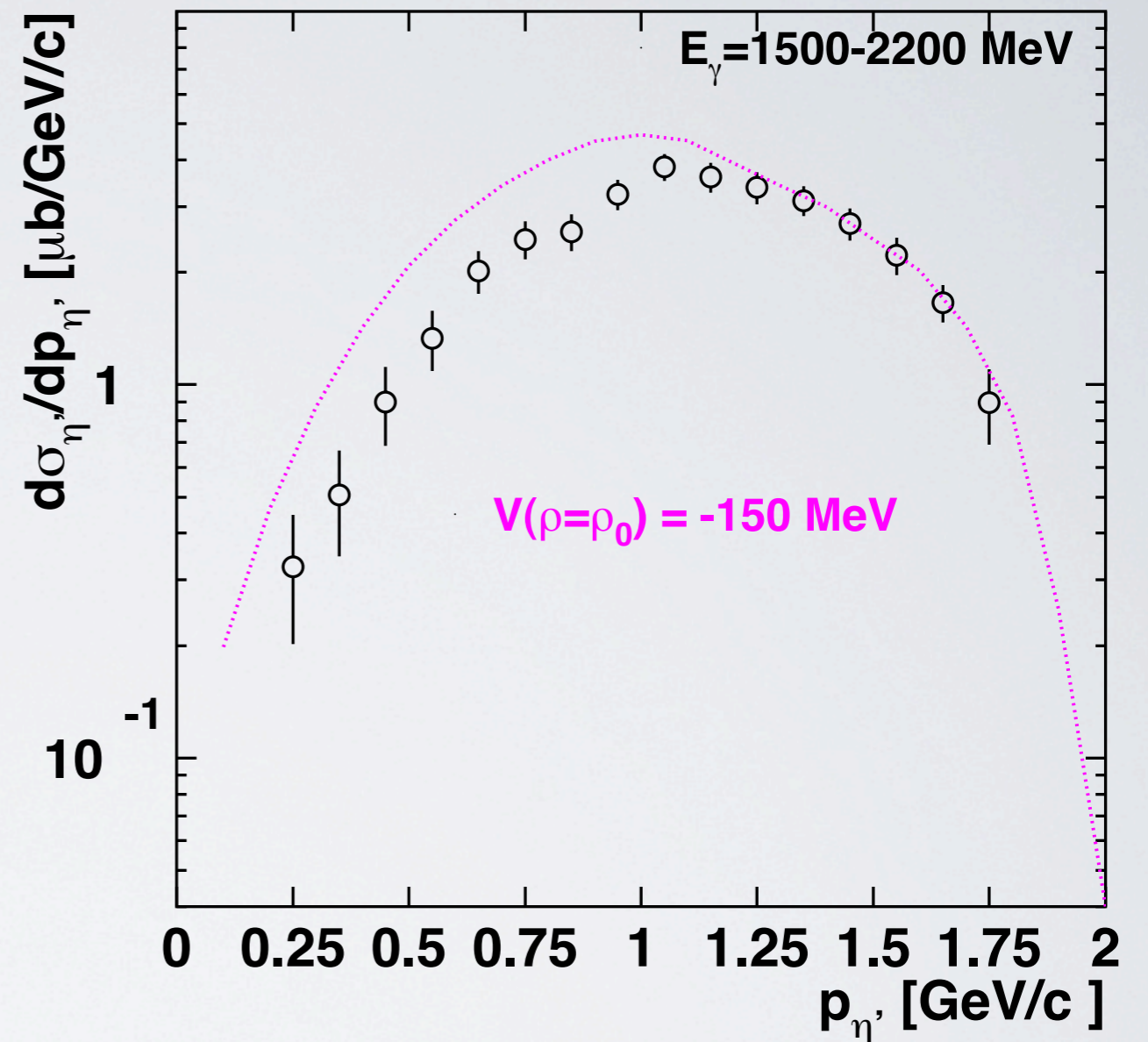
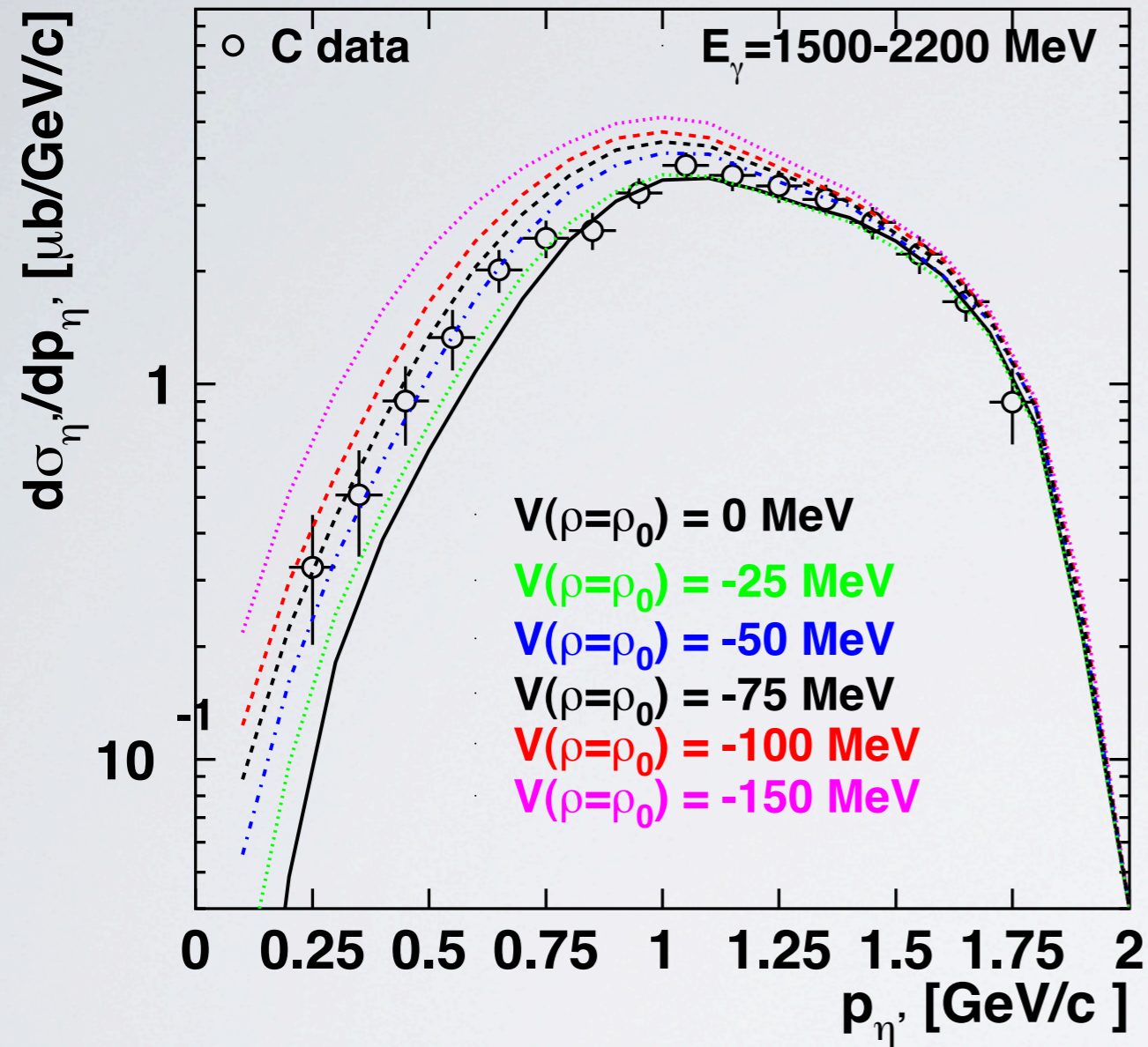


# estimation of the $\eta'$ -nucleus potential depth from the $\eta'$ momentum distribution

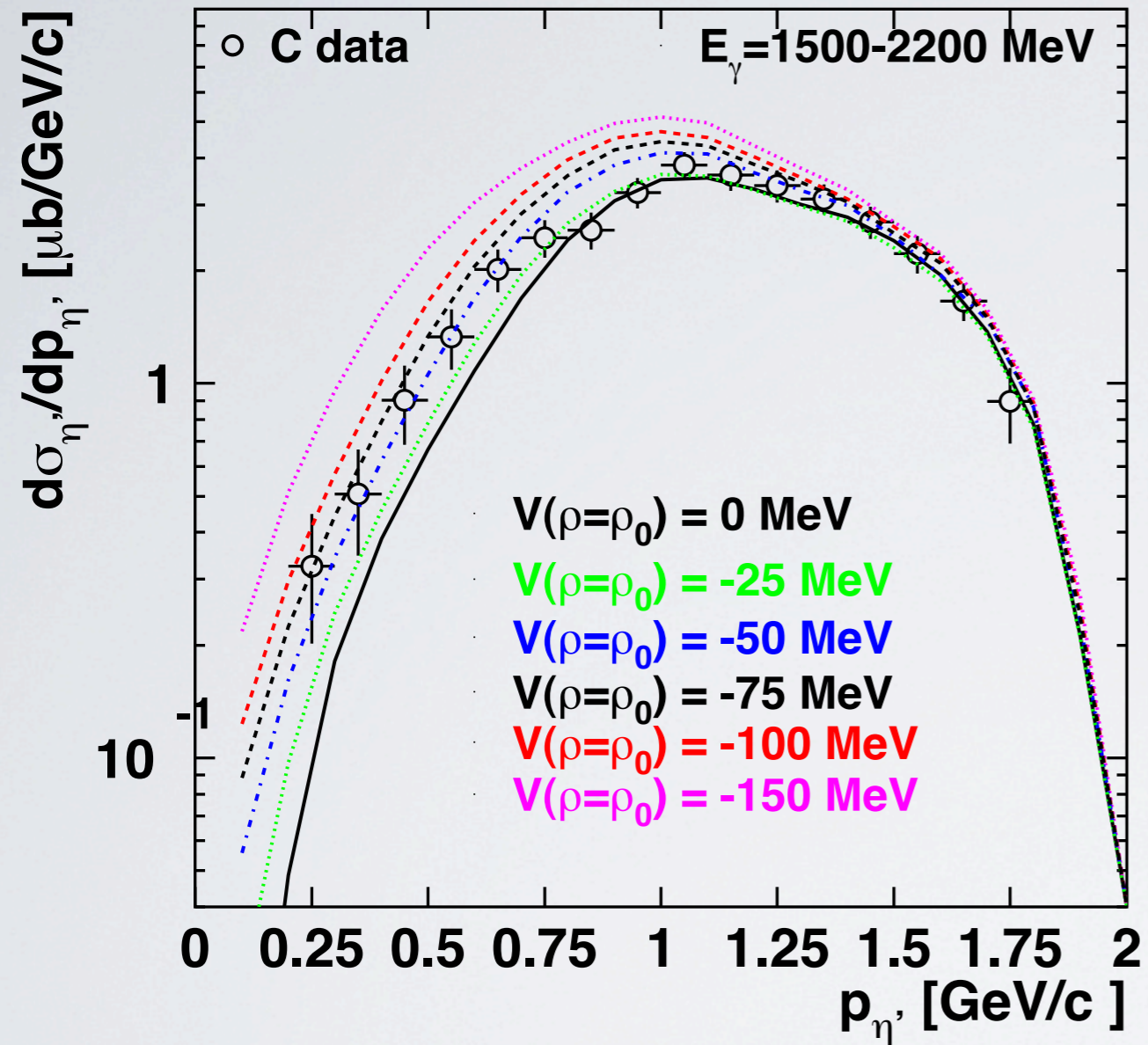




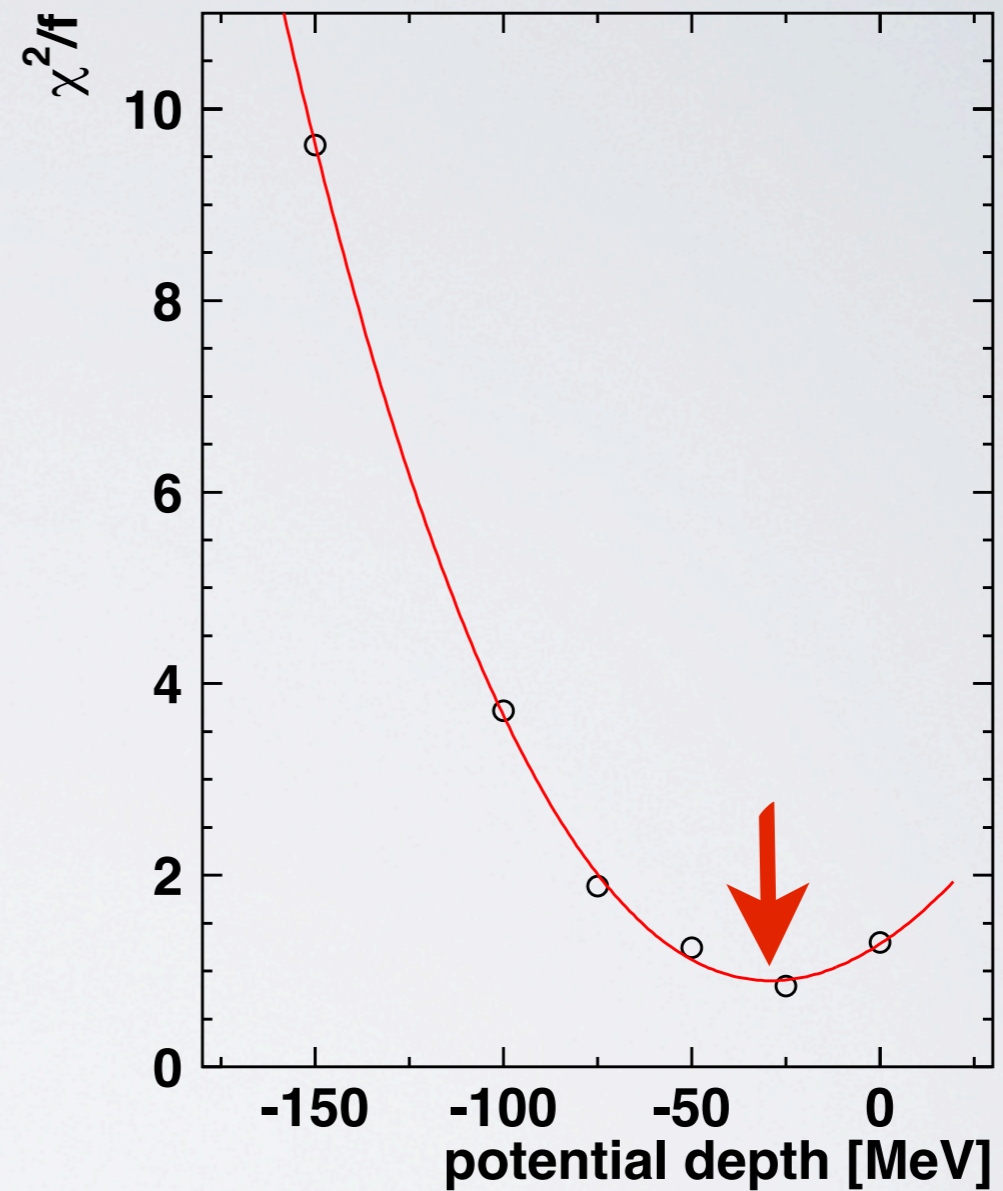
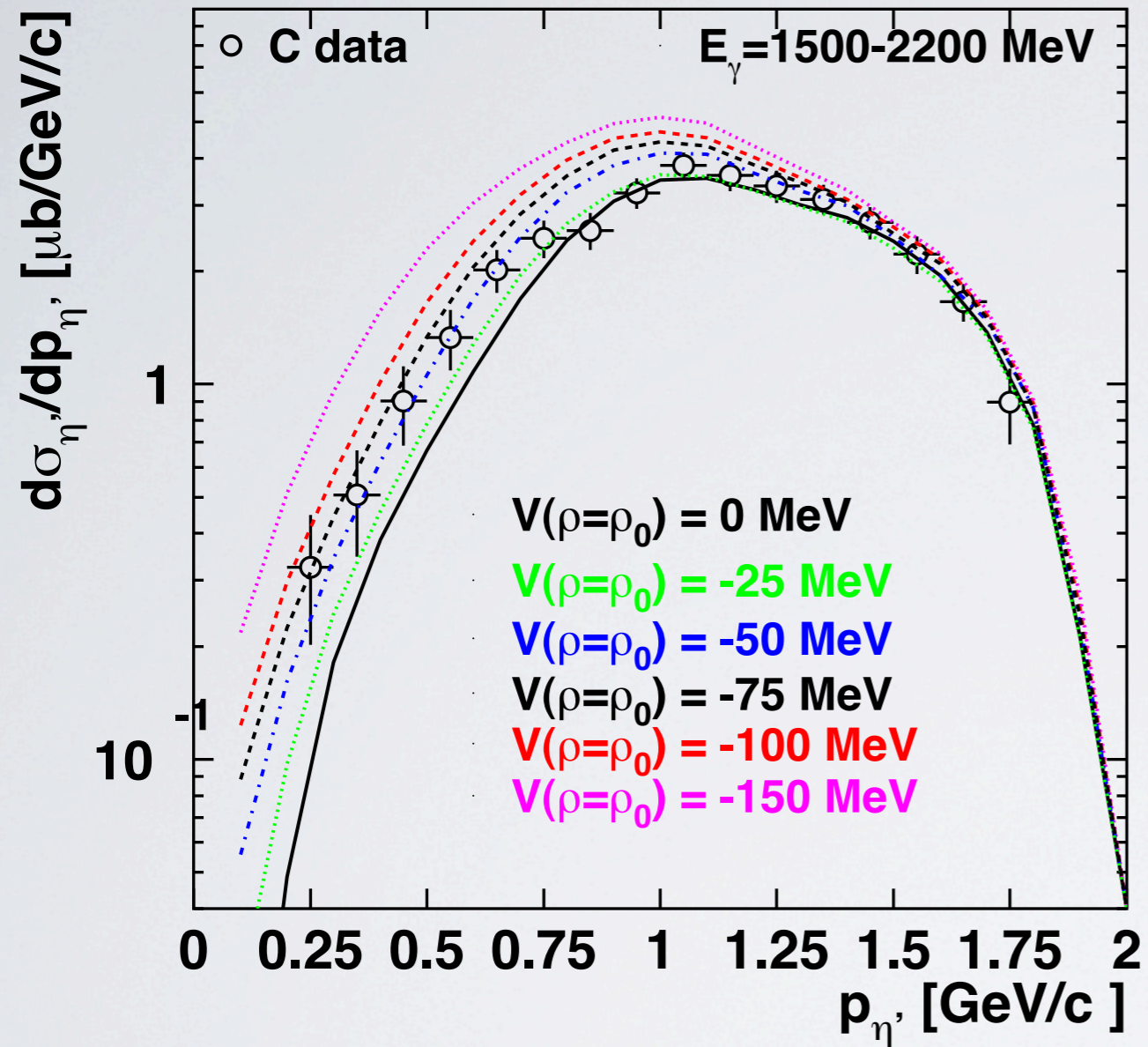
# estimation of the of $\eta'$ -nucleus potential depth from the $\eta'$ momentum distribution



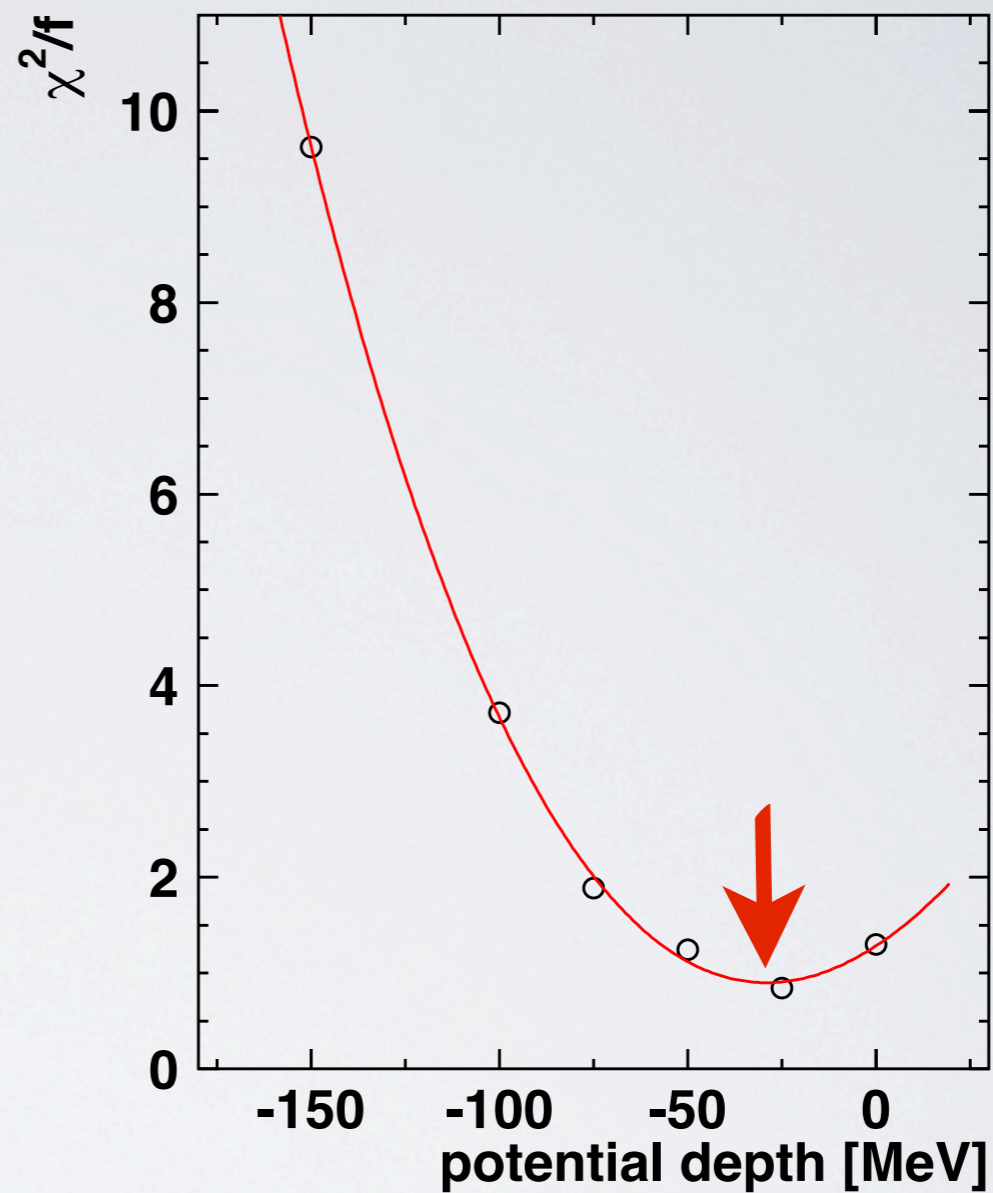
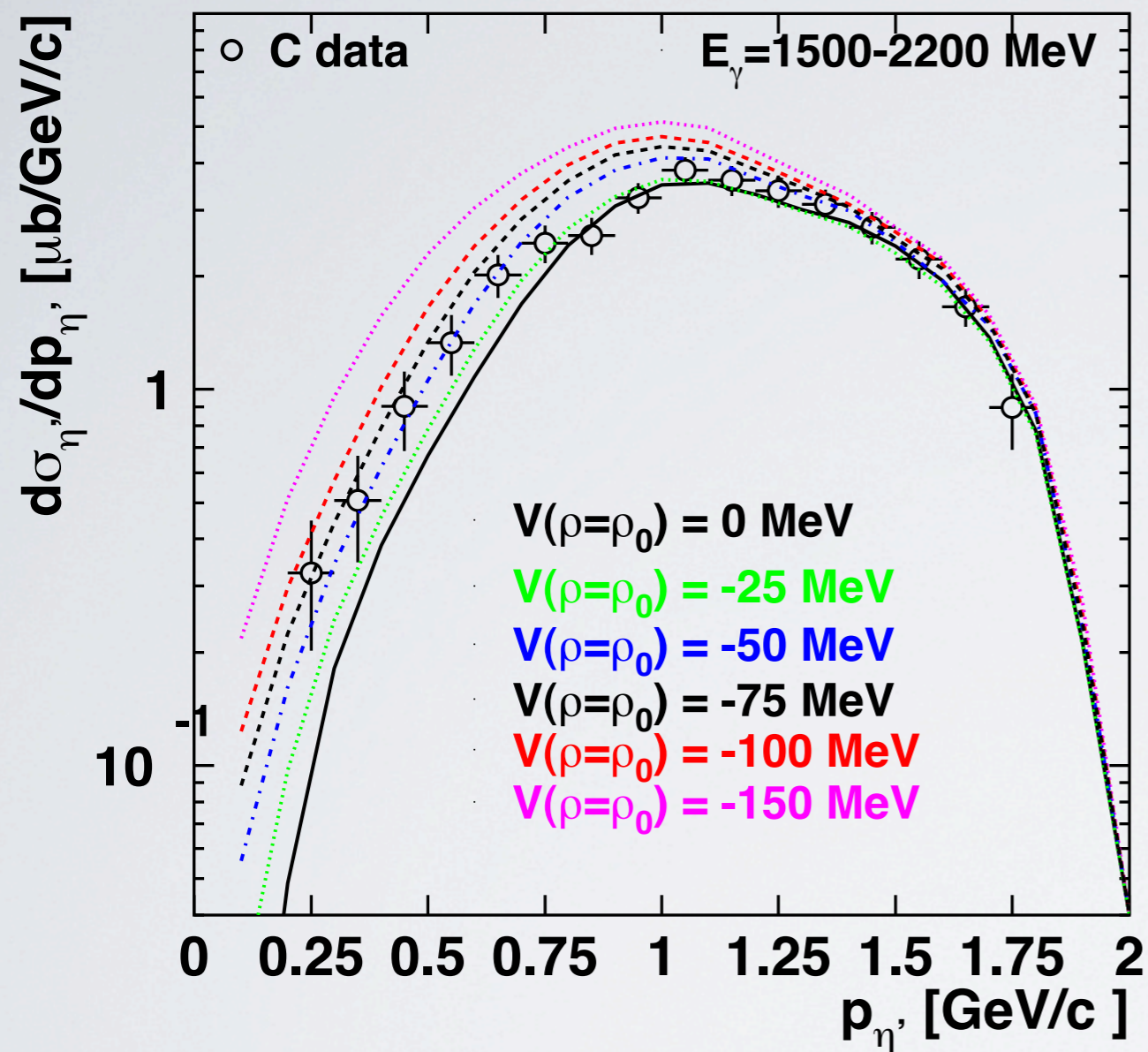
# estimation of the of $\eta'$ -nucleus potential depth from the $\eta'$ momentum distribution



# estimation of the of $\eta'$ -nucleus potential depth from the $\eta'$ momentum distribution

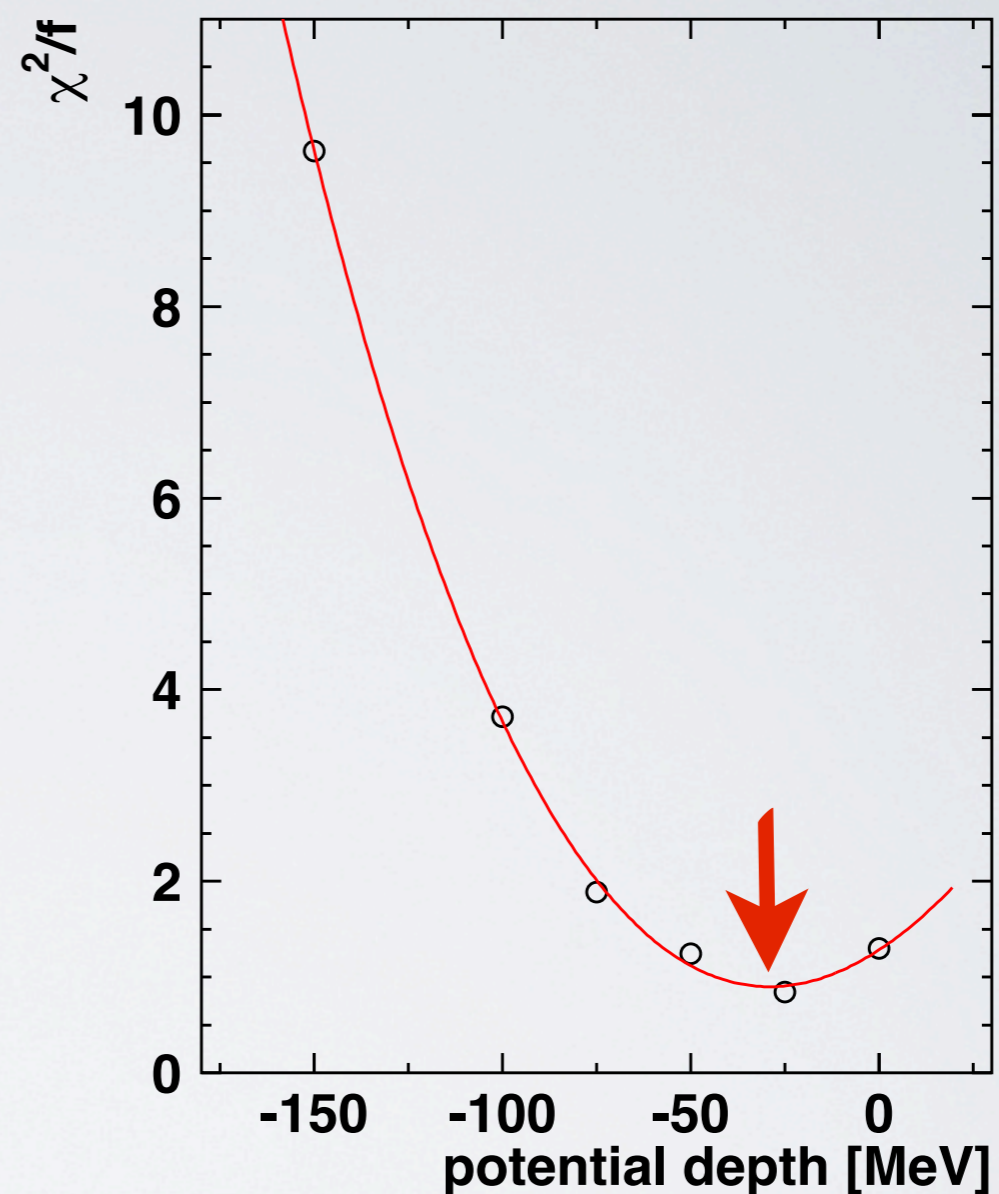
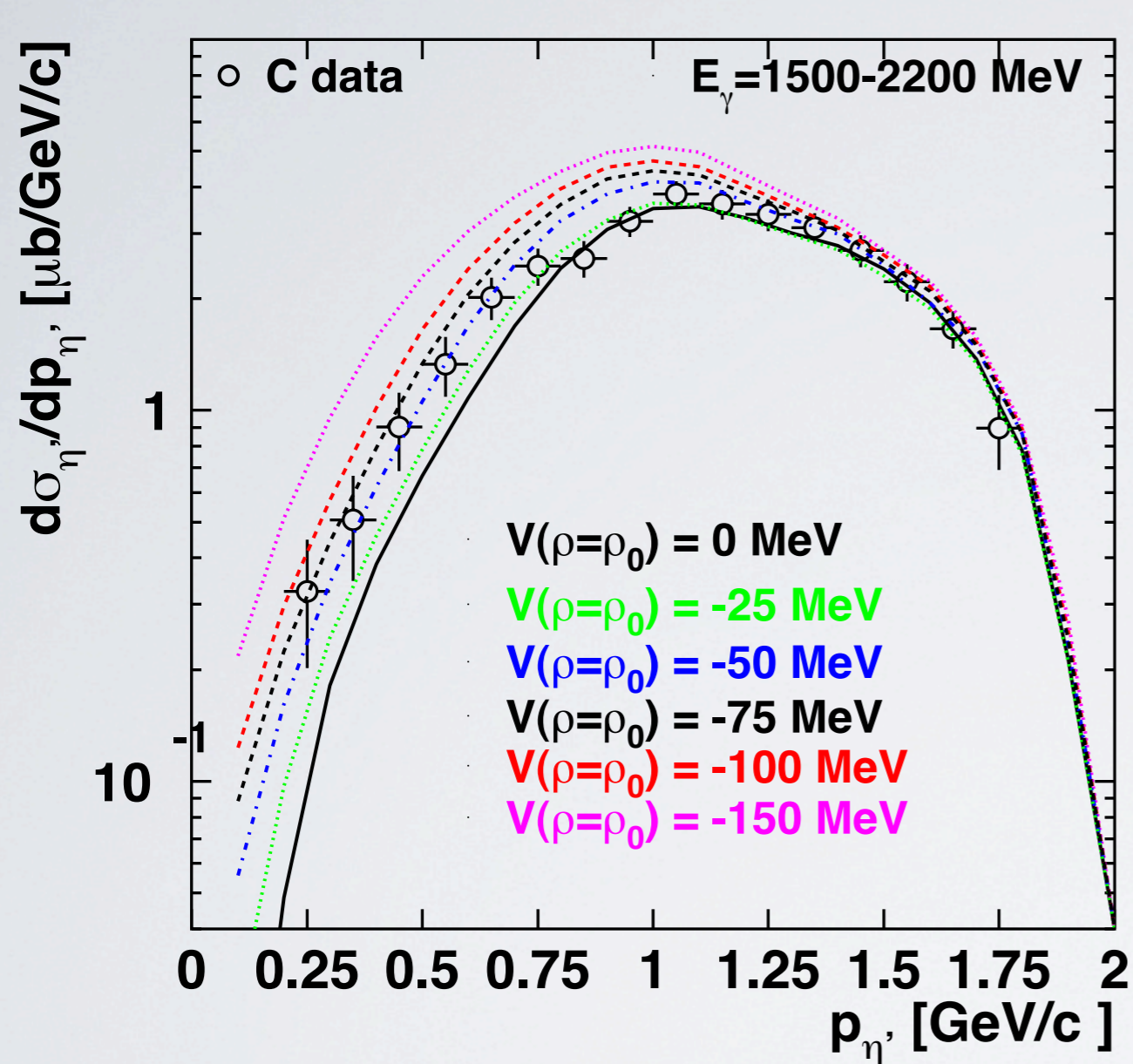


# estimation of the of $\eta'$ -nucleus potential depth from the $\eta'$ momentum distribution



$$V(\rho=\rho_0) = -32 \pm 11 \text{ MeV}$$

# estimation of the of $\eta'$ -nucleus potential depth from the $\eta'$ momentum distribution



$$V(\rho=\rho_0) = -32 \pm 11 \text{ MeV}$$

consistent with predictions by:

S. Bass and A.W.Thomas, Acta Phys. Pol. B 41 (2010) 2239

H. Nagahiro et al., PLB 709 (2012) 87.

# Summary

1. **Imaginary part** of the  $\eta'$ - nucleus optical potential determined from transparency ratio measurements:  $W(\rho=\rho_0)=-\Gamma_0/2 = -10\pm 2.5$  MeV

2. **Real part** of the  $\eta'$ - nucleus optical potential determined from:

a. measurement of the excitation function of the  $\eta'$ -meson

$$V(\rho=\rho_0) = -40\pm 6 \text{ MeV}$$

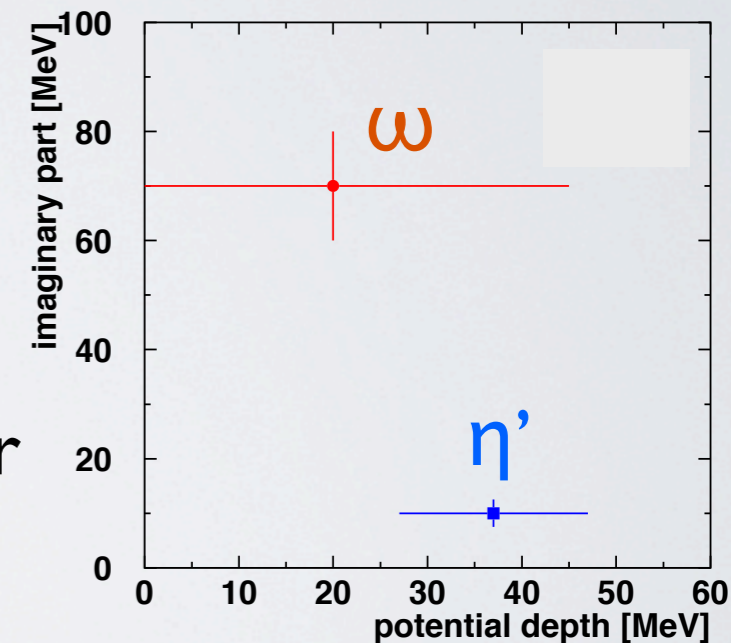
b. measurement of the momentum distribution of the  $\eta'$ -meson:

$$V(\rho=\rho_0) = -32\pm 11 \text{ MeV}$$

$$U_{\eta'A}(\rho=\rho_0) = -(37\pm 10(\text{stat}) \pm 10(\text{syst}) + i(10\pm 2.5)) \text{ MeV}$$

M. Nanova et al., arXiv:1311.0122; to be published in PLB

First (indirect) observation of a mass drop of a pseudoscalar meson in nuclear matter at normal conditions ( $\rho=\rho_0; T=0$ )



3.  $V \gg W!$   $\Rightarrow$   $\eta'$  promising candidate for mesic states

experiments searching for  $\eta'$  mesic states at FRS@GSI and BGO-OD@ELSA

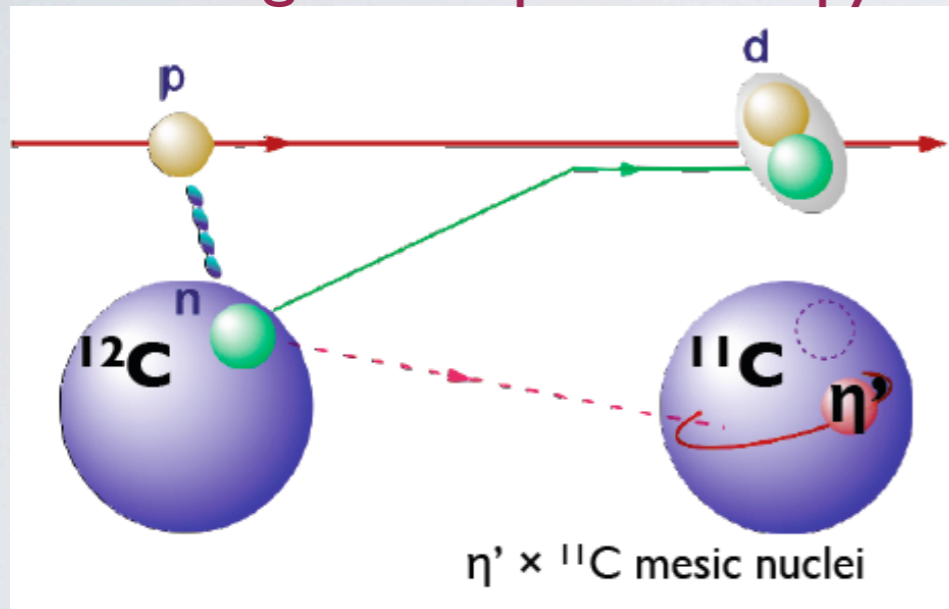
# search for $\eta'$ mesic states at FRS@GSI and BGO-OD@ELSA

**GSI**  $^{12}\text{C}(p,d) \eta'X @ 2.5 \text{ GeV}$

K. Itahashi et al.:FRS@GSI

K. Itahashi et al.,  
Prog. Theo. Phys. 128 (2012) 601

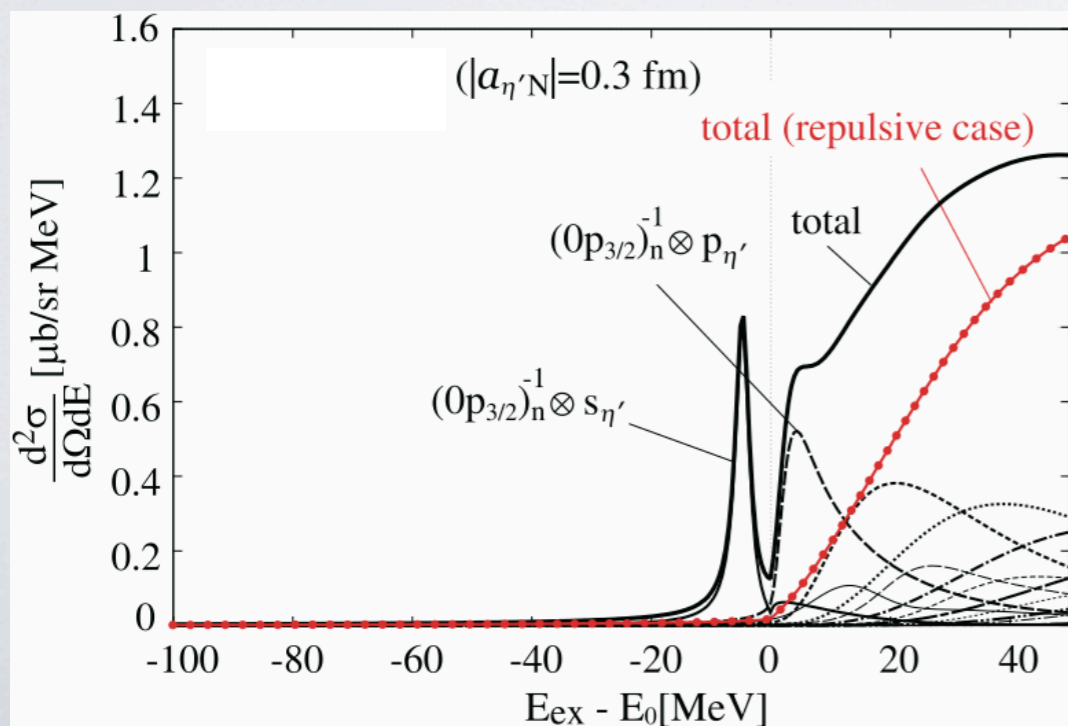
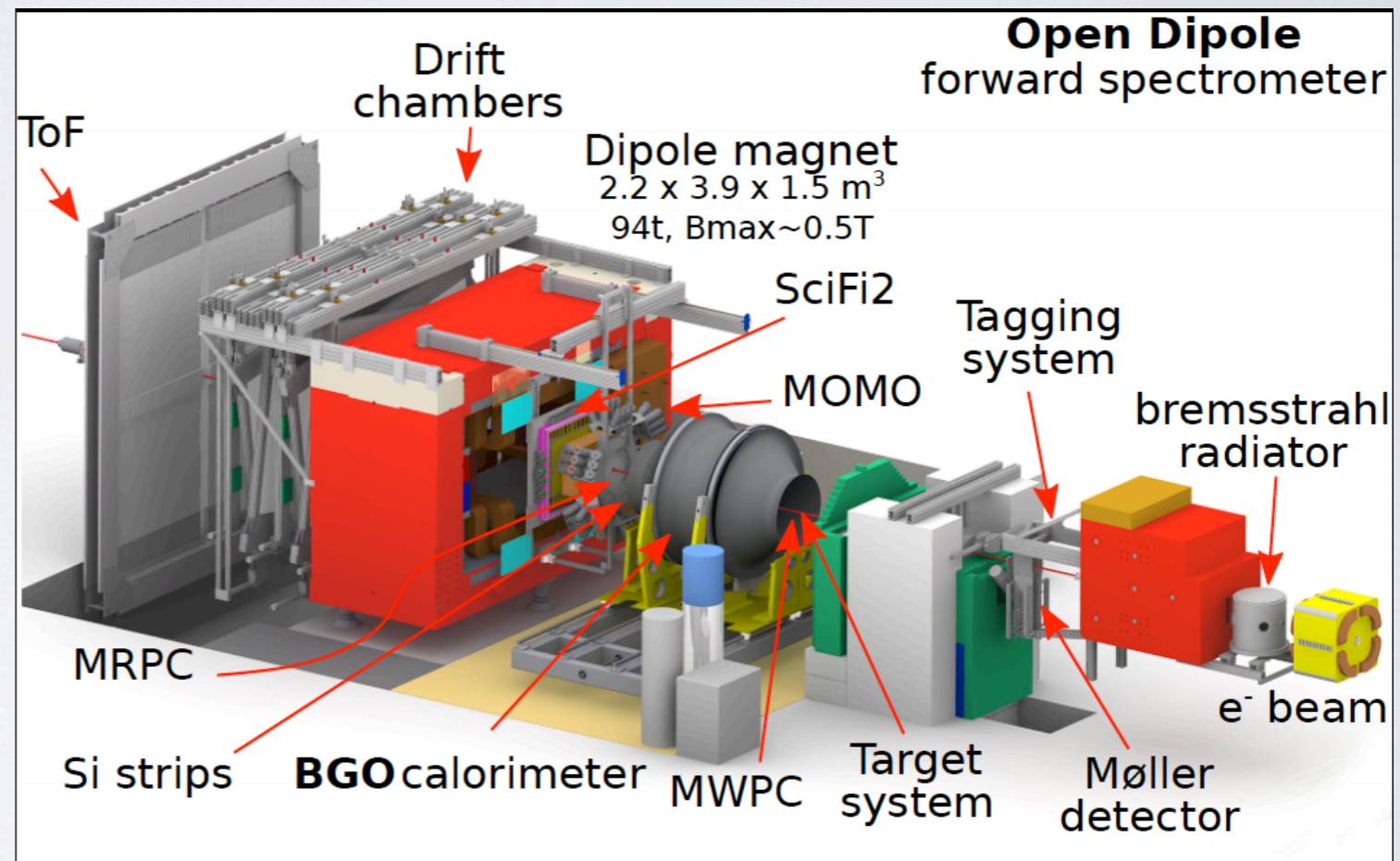
missing mass spectroscopy



$\gamma + {}^{12}\text{C} \rightarrow \eta' \otimes {}^{11}\text{B} + p @ 2.2-2.8 \text{ GeV}$  **ELSA**

semi-exclusive measurement:

coincident detection of forward going proton  
and decays of  $\eta'$  mesic states:  $\eta'N \rightarrow \eta N$





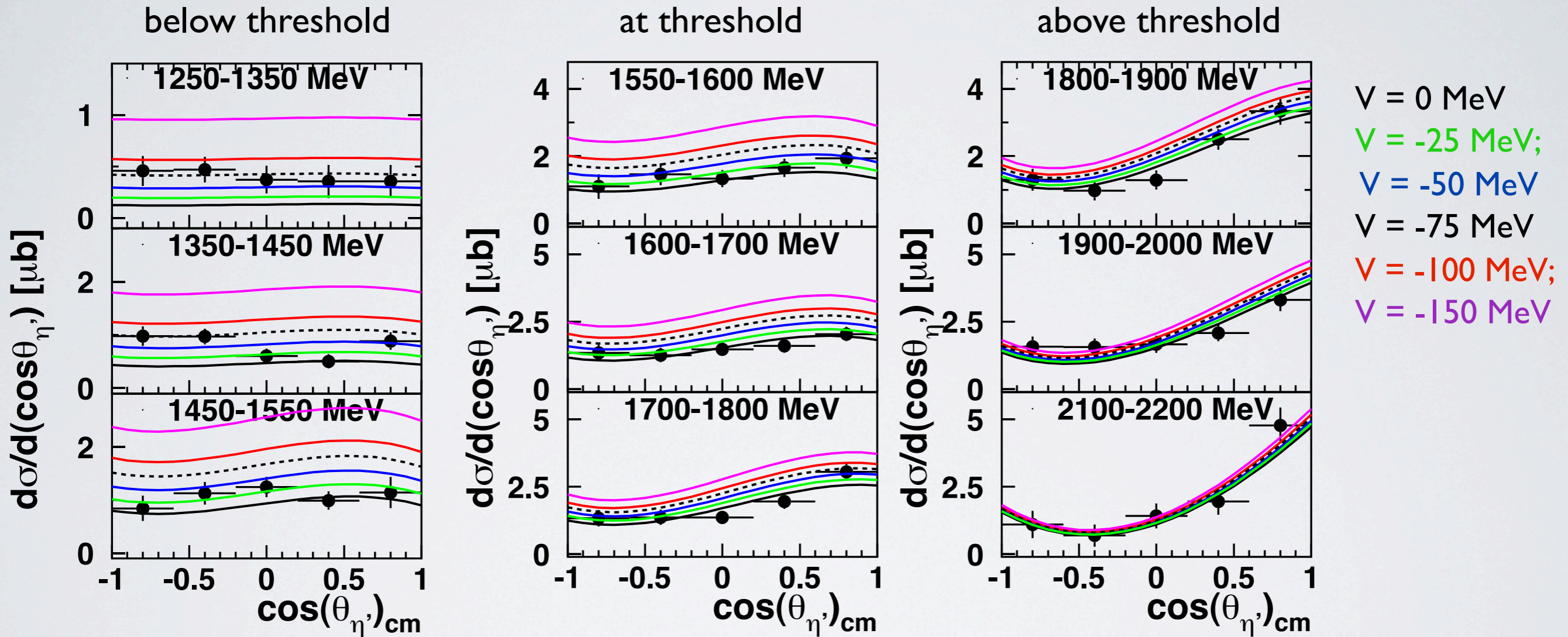


# differential cross sections for $\eta'$ photoproduction off $^{12}\text{C}$

$E_\gamma = 1250 - 2600 \text{ MeV}$        $\eta' \rightarrow \pi^0 \pi^0 \eta \rightarrow 6\gamma$       BR: 8.1%

sensitivity to different scenarios

E. Ya. Paryev, priv. communication



high sensitivity to different scenarios at threshold

strong mass shift not supported by data